

**DESENSITISATION OF THE PITUITARY  
VASOPRESSIN RECEPTOR: DEVELOPMENT OF  
A MODEL SYSTEM TO ASSESS INVOLVEMENT  
OF G PROTEIN- COUPLED RECEPTOR KINASE**

**5**

**MICHELLE GATEHOUSE**

A thesis  
submitted in partial fulfilment  
of the requirements for the Degree  
of  
Master of Science in Biochemistry

University of Canterbury

2008

# TABLE OF CONTENTS

<b>TABLE OF CONTENTS</b>	<b>I</b>
<b>ABSTRACT</b>	<b>VI</b>
<b>ABBREVIATIONS</b>	<b>VIII</b>
<b>1 INTRODUCTION</b>	<b>1</b>
<b>1.1 The hypothalamo-pituitary-adrenal axis</b>	<b>1</b>
1.1.1 The hypothalamo-pituitary-adrenal axis	1
1.1.2 Vasopressinergic control of ACTH release	3
<b>1.2 Mechanisms of AVP stimulated ACTH release by the pituitary</b>	<b>4</b>
1.2.1 Pituitary AVP receptors	4
1.2.2 Activation of the phosphoinositide signaling pathway by AVP	5
<b>1.3 Attenuation of the response to AVP: desensitisation</b>	<b>7</b>
1.3.1 Desensitisation of G protein-coupled receptors	7
1.3.2 Desensitisation of the pituitary vasopressin receptor	9
1.3.3 G protein-coupled receptor kinases	10
1.3.4 Approaches employed to assess the involvement of G protein-coupled receptor kinases in G protein-coupled receptor desensitisation	13
<b>1.4 RNA interference methodology</b>	<b>15</b>
1.4.1 An introduction to RNA interference	15
1.4.2 The evolving methodology for RNAi experiments	16
1.4.2.1 Minimising off-target effects of the siRNA	16
1.4.2.2 Minimising non-specific effects of the siRNA	16
1.4.2.3 Assessing knockdown	17
1.4.2.4 siRNA controls	17
<b>1.5 Aims of this study</b>	<b>18</b>
<b>2 STANDARD METHODS</b>	<b>19</b>
<b>2.1 Materials</b>	<b>19</b>

<b>2.2 Solutions and media</b>	<b>19</b>
<b>2.3 Cell culture</b>	<b>19</b>
2.3.1 Human Embryonic Kidney 293 cell line	19
2.3.2 Chinese Hamster Ovary cell line, stably expressing the V1b receptor	20
2.3.3 Cell culture	20
2.3.3.1 Thawing cells	21
2.3.3.2 Sub-culturing cells	21
2.3.3.3 Freezing cells	23
2.3.4 Coating cell culture plates	24
2.3.4.1 Coating plates with poly-L-lysine	25
2.3.4.2 Coating plates with poly-D-lysine	26
<b>2.4 Cell viability</b>	<b>28</b>
2.4.1 Viability assay of dispersed cells	28
2.4.2 Viability assays of adherent cells	29
2.4.2.1 Trypan Blue assay of adherent cells	30
2.4.2.2 MTT-formazan assay of adherent cells	31
<b>2.5 Purification of plasmids: prV1b-R and pAlter</b>	<b>36</b>
2.5.1 Plasmids: prV1b-R and pALTER-MAX	36
2.5.2 Elution of plasmids	36
2.5.3 Transformation of <i>E.coli</i> DH5 $\alpha$ with plasmid	37
2.5.3.1 Selection of successfully transformed <i>E. coli</i> DH5 $\alpha$	38
2.5.3.2 Culture of transformed <i>E.coli</i> DH5 $\alpha$	38
2.5.4 Analysis of plasmid DNA	39
2.5.4.1 Restriction digest	39
2.5.4.2 Gel electrophoresis	40
2.5.4.3 Spectrophotometric analysis of plasmid DNA	40
2.5.5 Alkali lysis preparation of plasmid	40
2.5.6 Large scale preparation of plasmid	42
<b>2.6 Protein quantitation</b>	<b>44</b>
2.6.1 Room temperature protocol for protein quantitation	45
2.6.2 Enhanced protocol for protein quantitation	47
<b>2.7 Transfection</b>	<b>49</b>
2.7.1 Transfection of HEK293 with plasmid DNA	50
<b>2.8 Data analysis</b>	<b>51</b>
2.8.1 Analysis of IP assay results	51
2.8.2 Analysis of qRT-PCR results	54
2.8.3 Statistical analysis	55

<b>3 DEVELOPMENT OF A MODEL SYSTEM TO OBSERVE DESENSITISATION OF THE PITUITARY VASOPRESSIN RECEPTOR: V1b-R</b>	<b>56</b>
<b>3.1 Introduction</b>	<b>56</b>
<b>3.2 Standard Methods and Materials</b>	<b>58</b>
3.2.1 Materials	58
3.2.2 Solutions and media	58
3.2.3 Steps of the inositol phosphate assay	58
3.2.4 Cell labeling with <i>myo</i> -[ <sup>3</sup> H]inositol	60
3.2.5 Stimulation of the cells with AVP	60
3.2.6 Collection of cell lysates	61
3.2.7 Separation of inositol phosphates	62
3.2.8 Scintillation counting	64
3.2.9 Data analysis	64
<b>3.3 HEK293 Transfection Protocol Development and Assessment using the Inositol Phosphate Assay</b>	<b>65</b>
3.3.1 Testing the inositol phosphate assay method using HEK293 cells transfected with the V1b-R	65
3.3.2 Optimisation of transfection	67
3.3.3 Optimisation of HEK293 cell adherence using the inositol phosphate assay	70
3.3.4 The IP response of V1b-R-transfected HEK293 cells to AVP stimulation	71
<b>3.4 Development of an assay for measuring desensitisation of the IP response to AVP</b>	<b>74</b>
3.4.1 Rationale for using CHO-V1b cells	74
3.4.2 The inositol phosphate response of CHO-V1b cells to AVP stimulation	74
3.4.2.1 The effect of AVP treatment concentration	76
3.4.2.2 The effect of AVP treatment duration	77
3.4.3 Desensitisation of the inositol phosphate response of CHO-V1b cells to AVP stimulation	78
3.4.3.1 The effect of lithium chloride	80
3.4.3.2 The effect of AVP pre-treatment duration	84
3.4.3.3 The effect of AVP pre-treatment concentration	85
<b>3.5 Desensitisation of the Inositol Phosphate Response to AVP using V1b-R transfected HEK293 cells</b>	<b>86</b>
3.5.1 Desensitisation of the inositol phosphate response to AVP using V1b-R-transfected HEK293 cells	86
3.5.1.1 The effect of AVP pre-treatment concentration	88
3.5.1.2 The effect of AVP pre-treatment duration	89
3.5.1.3 The effect of the duration of incubation with <i>myo</i> -[ <sup>3</sup> H]inositol	90
<b>3.6 The final protocol for the observation of desensitisation of the V1b-R mediated IP response in HEK293 cells</b>	<b>92</b>

<b>4 ASSESSMENT OF HUMAN G PROTEIN-COUPLED RECEPTOR KINASE 5 EXPRESSION IN HEK293 CELLS USING QUANTITATIVE RT-PCR</b>	<b>93</b>
<b>4.1 Introduction</b>	<b>93</b>
<b>4.2 Standard Methods and Materials</b>	<b>94</b>
4.2.1 Materials	94
4.2.2 Solutions and media	94
4.2.3 Avoiding RNase contamination	94
4.2.4 RNA extraction	95
4.2.4.1 Preparation of HEK293 cells for RNA extraction	95
4.2.4.2 RNA extraction	95
4.2.4.3 Analysis of RNA	97
4.2.5 Reverse transcription	97
4.2.6 Polymerase chain reaction (PCR)	98
4.2.6.1 PCR reactions	98
4.2.6.2 Agarose gel electrophoresis of PCR products	99
4.2.7 DNA sequencing	99
4.2.7.1 DNA preparation	99
4.2.7.2 DNA sequencing reactions	100
4.2.8 Quantitative reverse transcription polymerase chain reaction (qRT-PCR)	100
4.2.8.1 Reference genes	101
4.2.8.2 Analysis of qRT-PCR results	102
<b>4.3 Optimisation of RNA extraction from HEK293 cells</b>	<b>102</b>
4.3.1 Comparison of TRIreagent and column-based methods of RNA extraction	103
4.3.2 The combined method of RNA extraction	105
<b>4.4 Primer design and testing</b>	<b>107</b>
4.4.1 Design of primers for amplification of GRK5	107
4.4.1.1 Primer design using Primer3 software	108
4.4.1.2 Multiple alignment of GRK protein sequences and primer design	108
4.4.2 Primer testing using PCR	113
4.4.2.1 The positive control: 18S ribosomal RNA	113
4.4.2.2 GRK5 specific primers: GRK5F/R	114
4.4.2.3 GRK5 specific primers: GRK5F1/R1 and GRK5F2/R2	114
4.4.3 Primer testing using quantitative PCR	116
4.4.4 Sequencing of the human GRK5 PCR product	119
4.4.5 Determination of the amplification efficiency of the primer pairs used for GRK5 expression studies	121
<b>4.5 Assessment of human GRK5 expression in HEK293 cells using quantitative PCR</b>	<b>124</b>
4.5.1 Reference RNA: A positive control for GRK5 expression studies	124
4.5.1.1 GRK5 expression in the reference cDNA	126

4.5.2	Optimisation of the SYBR green reaction mix for amplification of GRK5 using qPCR	126
4.5.3	EXPERIMENT 1: Assessment of the effects of HEK293 culture age on GRK5 expression	128
4.5.3.1	Preparation of cDNA from HEK293 cells of different culture age	129
4.5.3.2	GRK5 expression in HEK293 cells of different culture age	129
4.5.4	EXPERIMENT 2: Assessment of the effects of HEK293 culture conditions on GRK5 expression	130
4.5.4.1	Preparation of cDNA from HEK293 cells subjected to different culture conditions	131
4.5.3.2	GRK5 expression in HEK293 cells in different culture conditions	131
4.5.5	EXPERIMENT 3: Comparison of GRK5 expression in different cell types	133
<b>5</b>	<b>DISCUSSION</b>	<b>135</b>
5.1	Summary	135
5.2	General Comments on the Methods used	137
5.2.1	Desensitisation of the inositol phosphate response to AVP using V1b-R-transfected HEK293 cells	137
5.2.2	Assessment of human G protein-coupled receptor kinase 5 expression in HEK293 cells using qRT-PCR	139
5.3	Suggestions for Further Research	140
	<b>ACKNOWLEDGEMENTS</b>	<b>142</b>
	<b>REFERENCES</b>	<b>143</b>
	<b>APPENDIX A: MATERIALS</b>	<b>153</b>
	<b>APPENDIX B: SOLUTIONS AND MEDIA</b>	<b>155</b>

## ABSTRACT

The hypothalamic peptide arginine vasopressin (AVP) is an important regulator of adrenocorticotropin (ACTH) release from the anterior pituitary. AVP stimulates ACTH secretion from corticotroph cells by activating the pituitary vasopressin receptor (V1b-R), a member of the G protein-coupled receptor (GPCR) family. *In vitro*, repeated stimulus of anterior pituitary cells with AVP results in rapid desensitisation. The aim of this research was to develop methods needed to use RNA interference (RNAi) to investigate the role of G protein-coupled receptor kinase 5 (GRK5) in this desensitisation process. This required the development of a model system using human embryonic kidney (HEK) 293 cells transfected with the pituitary vasopressin receptor, V1b-R. AVP binding to the V1bR activates the phosphoinositide signalling pathway, leading to production of inositol phosphates (IPs), which can be measured following radiolabelling of cells with *myo*-[<sup>3</sup>H]inositol. Stimulation of V1b-R-transfected cells for 15 min with AVP (100nM) increased IP production to  $235.5 \pm 23.4$  % (n=3, p<0.02) of that seen in un-stimulated control cells. Following a 5 minute pre-treatment with 5nM VP, the IP response to stimulation with 100nM VP for 15 min was reduced to  $62.8 \pm 9.1$  % (n=4, p<0.02) of that seen in control cells that were not pre-treated. These data indicate that AVP-desensitisation can be induced and measured in V1bR-transfected HEK293 cells following a brief pre-treatment with a physiological concentration of AVP. This model system will enable RNAi to be used to investigate the role of GRK5 in AVP-desensitisation.

When using RNAi, it is essential to establish that the effects observed are the result of small interfering RNA (siRNA) specific degradation of the target mRNA. Quantitative reverse transcription PCR (qRT-PCR) was used to measure the expression of GRK5 at the mRNA level in HEK293 cells. Human GRK5 mRNA was amplified using qRT-PCR with GRK5 specific primers, providing confirmation that GRK5 is expressed endogenously in HEK293 cells. GRK5 expression studies were carried out to evaluate whether the qRT-PCR methods developed would be suitable to measure knockdown of GRK5 mRNA using RNAi. These experiments were also designed to assess the impact of HEK293 cell culture methods on

expression of GRK5. Expression of GRK5 did not vary with passage number (2-26 passages). The GRK5 expression in HEK293 cells that were maintained in culture for 5 days (grown to a confluence of approximately 100%) was  $7.4 \pm 0.9$  fold greater ( $n=2$ ,  $p<0.05$ ) than for cells cultured for 3 days (grown to a confluence of approximately 65%). These data indicate that GRK5 expression is affected by HEK293 culture conditions. Furthermore, the results demonstrated that a significant difference in GRK5 expression could be measured in HEK293 cells using qRT-PCR. Therefore the results reported in this thesis provide the basis for future studies utilising RNAi to investigate mechanisms underlying V1b-R desensitisation.



## ABBREVIATIONS

A	adenine
ACTH	adrenocorticotropin
AMEM	alpha minimal essential medium
AVP	arginine vasopressin
$\beta_2$ AR	$\beta_2$ -adrenergic receptor
BCP	1-bromo-3-chloropropane
BLAST	Basic Local Alignment Search Tool
C	cytosine
cDNA	complementary DNA
CHO-V1b	chinese hamster ovary (CHO) stably expressing the V1b receptor
CRH	corticotropin-releasing hormone
Ct	cycle threshold
DAG	diacylglycerol
ddH <sub>2</sub> O	distilled de-ionised water
DEPC	diethylpyrocarbonate
DNA	deoxyribonucleic acid
dNTPs	deoxynucleotides
dR	baseline-corrected raw fluorescence
dsRNA	double-stranded RNA
DTT	dithiothreitol
G	guanine
GPCR(s)	G-protein coupled receptor(s)
GRK(s)	G-protein coupled receptor kinase(s)
HEK293	human embryonic kidney 293 cell line
HIHS	heat-inactivated horse serum
HPA axis	hypothalamo-pituitary-adrenal axis
IP(s)	inositol phosphate metabolite(s)
IP <sub>3</sub>	inositol 1,4,5-triphosphate
Kb	kilobase(s)
M	molar
MEM	minimal essential medium
mL	millilitre(s)
mRNA	messenger RNA
mw	molecular weight marker
ng	nanogram
nM	nanomolar
nt	nucleotide
pALTER-MAX	plasmid vector
PCR	polymerase chain reaction
PIP <sub>2</sub>	phosphatidylinositol 4,5-bisphosphate
PKC	protein kinase C

PLC	phospholipase C
prV1b-R	plasmid containing the rat V1b-R
P/S	penicillin/streptomycin
PVN	paraventricular nucleus
qPCR	quantitative PCR
qRT-PCR	quantitative reverse transcription PCR
RNA	ribonucleic acid
RNase	ribonuclease
RNAi	RNA interference
rpm	revolutions per minute
siRNA	small interfering RNA
T	thymine
TAE	Tris-acetate/Na <sub>2</sub> EDTA Electrophoresis buffer
TBE	Tris-borate/Na <sub>2</sub> EDTA Electrophoresis buffer
TE8	Tris-Na <sub>2</sub> /EDTA buffer at pH 8.0
Tm	melting temperature of primer
μL	microlitre(s)
μg	microgram(s)
μM	micromolar
V1b-R	vasopressin type 1b receptor

# 1

## INTRODUCTION

### 1.1 THE HYPOTHALAMO-PITUITARY-ADRENAL AXIS

#### 1.1.1 The hypothalamo-pituitary-adrenal axis

Higher organisms depend on their ability to maintain a constant internal environment for their survival. Homeostasis is achieved by making adaptive changes in response to external and internal stimuli. The stress response involves the coordinated action of a variety of pathways at the molecular, cellular, endocrine and behavioural levels (O'Conner et al., 2000). A key endocrine system involved in the vertebrate response to stress is the hypothalamo-pituitary-adrenal axis (HPA axis) (Figure 1.1). In response to stressful stimuli there is a rapid increase in adrenocorticotropin (ACTH) release by the corticotroph cells of the anterior pituitary. The ACTH is then carried in the systemic circulation to the adrenal cortex where it stimulates the release of glucocorticoid steroid hormones. The glucocorticoids act on multiple targets to mediate the peripheral response to stress and maintain homeostasis (Buckingham et al., 1997; Munck et al., 1984).

Successful adaptation to stressful stimuli requires the ability to regulate the response. Release of ACTH from the anterior pituitary is a multifactorial process and is subject to very fine control. The hypothalamic peptides arginine vasopressin (AVP) and corticotropin-releasing hormone (CRH) are the two most potent secretagogues (Antoni, 1993). These hormones are released into the hypophyseal portal vessels and interact

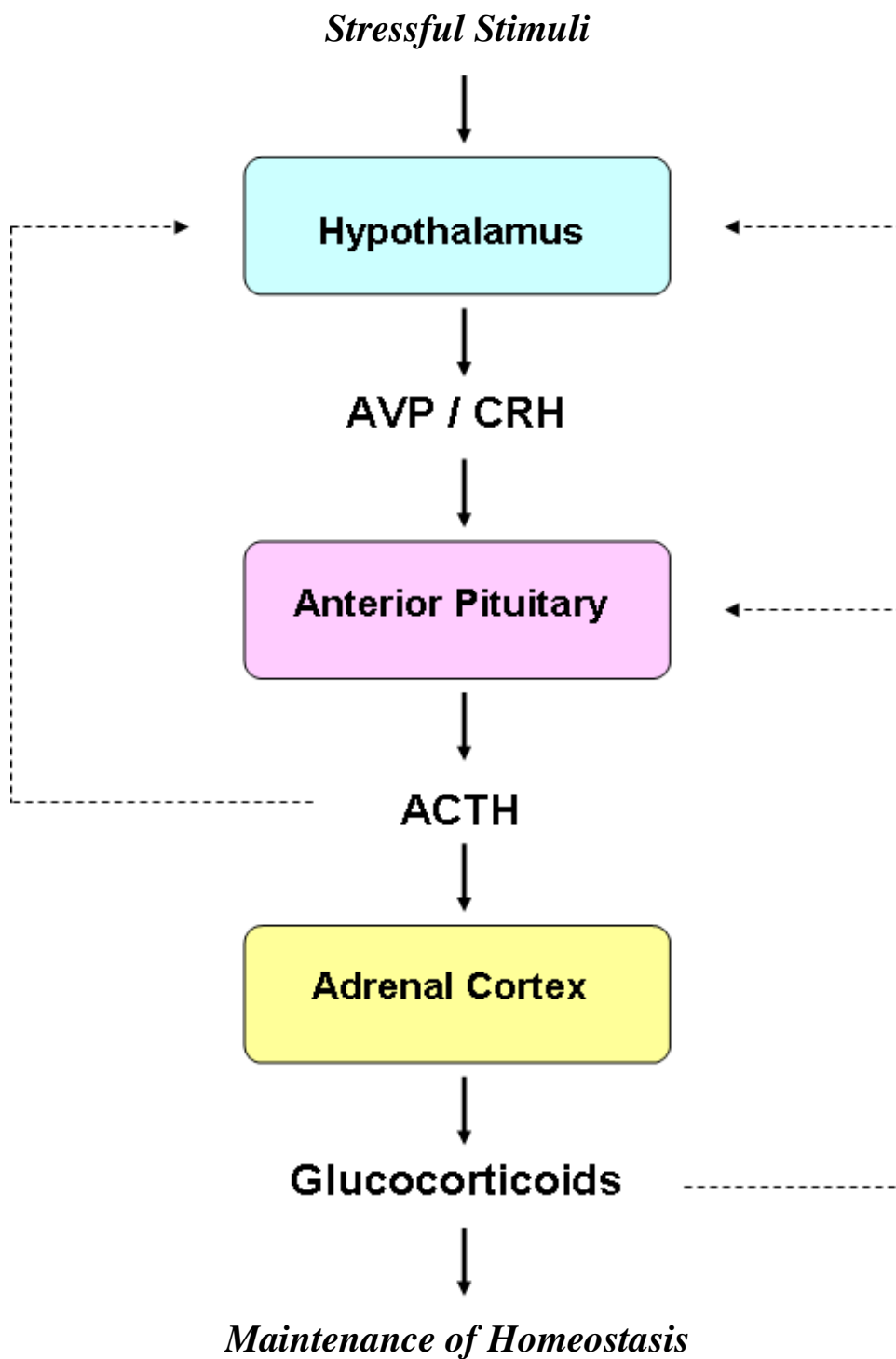


**Figure 1.1. The hypothalamo-pituitary-adrenal (HPA) axis.** Solid arrows represent positive stimulation, dashed arrows represent negative feedback. Figure adapted from a review (Buckingham et al., 1997).

with specific receptors located in the plasma membrane of the anterior pituitary corticotrophs, thereby stimulating ACTH secretion (Aguilera and Rabadan-Diehl, 2000). ACTH release is also inhibited by negative feedback from adrenal glucocorticoids (Figure 1.1).

### **1.1.2 Vasopressinergic control of ACTH release**

AVP was first implicated in the regulation of AVP release from the anterior pituitary in the 1950's (see for example Martini and Morpugo, 1955), yet it was only relatively recently that the importance of this neuropeptide in the HPA axis has become clear. Previously, most studies had focused on CRH as this was known to be a potent stimulator for ACTH release (Antoni, 1993). Although CRH is probably the main secretagogue in most animals, AVP administration also stimulates ACTH release (Scott and Dinan, 1998). In humans and rodents, AVP alone is a weak secretagogue (Aguilera et al., 2003), however in the 1980's studies using rat anterior pituitary cells confirmed that AVP significantly potentiates the effect of CRH on ACTH secretion (Gillies et al., 1982). A synergism between the two peptides is now well established with the release of ACTH being far in excess of that when either peptide is given alone (reviewed in Scott and Dinan, 1998). It has been proposed that this synergism may allow CRH to function as a permissive signal, setting the overall responsiveness of the corticotroph, while AVP is the main dynamic regulator of ACTH release (Aguilera et al., 2003; Antoni, 1993).

AVP is expressed at two sites in the hypothalamus; the parvocellular division of the paraventricular nucleus (PVN), where CRH is also expressed, and the magnocellular neurons of the supraoptic nucleus and the PVN (Scott and Dinan, 1998). It has been suggested that AVP from both origins is involved in ACTH secretion, although these two vasopressinergic systems appear to respond to different stress paradigms (Antoni, 1993). Most evidence suggests that AVP from parvocellular neurons is the source primarily responsible for the regulation of ACTH secretion during chronic stress (Aguilera, 1994).

## **1.2 MECHANISMS OF AVP STIMULATED ACTH RELEASE BY THE PITUITARY**

### **1.2.1 Pituitary AVP receptors**

In the anterior pituitary AVP interacts with specific receptors located in the plasma membrane of corticotroph cells, thereby stimulating ACTH secretion. AVP also has a number of other effects in various different tissues. In the kidney AVP has an antidiuretic effect, and in the vasculature it has a vasopressor effect (Holmes et al., 2003). The different actions of AVP are mediated by tissue-specific G protein-coupled receptors (GPCRs). These receptors are currently classified as V1 vascular, V2 renal or V3 pituitary (Holmes et al., 2003). The three receptor types share the common GPCR structure; seven transmembrane  $\alpha$ -helices joined by alternating intracellular and extracellular loops, an extracellular amino-terminal domain and a cytoplasmic carboxyl-terminal domain (Barberis et al., 1998).

The AVP receptor types have been organised into two groups on the basis of their functional differences. The V2 receptors, found in the kidney, mediate their effects via their interaction with the G-protein  $G_s$  (Birnbaumer, 2000). This leads to activation of adenylate cyclase and the subsequent production of the second messenger cyclic AMP (cAMP). In contrast, the V1 and V3 receptors mediate their effects via association with G-proteins of the  $G_{q/11}$  family, and activation of the phosphoinositide signalling pathway (Thibonnier et al., 1998). Due to their functional similarities V1 and V3 are frequently referred to as the V1a and V1b receptors. While these two receptors activate the same signalling pathway they are structurally and pharmacologically different (Holmes et al., 2003).

Due to its scarcity, the vasopressin V1b receptor (V1b-R) has only recently been characterised (Holmes et al., 2003). V1b-R receptors from the human (De Keyzer et al., 1994), rat (Lolait et al., 1995) and mouse (Ventura et al., 1999) have now been cloned. The V1b-R gene maps to chromosome region 1q32 (Rosseau-Merck et al., 1995). The 424-amino-acid sequence of the human V1b-R has homologies of 45% and 39% with the human V1a and V2 receptors respectively

(Sugimoto et al., 1994). The human V1b-R also has a high sequence homology with the V1b-R from other species, for example the human and rat V1b receptors share 82% amino acid identity (determined using cloned sequences Ventura et al., 1999). In addition, Scatchard plots indicate that the V1b-R clones isolated had a single class of binding sites with very similar dissociation constants of  $0.55 \pm 0.13\text{nm}$ ,  $0.47 \pm 0.3\text{nm}$  and  $0.63\text{nm}$  for human (De Keyzer et al., 1994), mouse (Ventura et al., 1999) and rat (Lolait et al., 1995) respectively. Despite these similarities, significant differences were found between human and mouse V1b-Rs tested in parallel using competitive binding experiments (Ventura et al., 1999). Thus the pharmacology of V1b receptors can not be transposed among different species.

### **1.2.2 Activation of the phosphoinositide signalling pathway by AVP**

Binding of AVP to the V1b-R results in activation of the phosphoinositide signalling pathway (reviewed in Mason et al., 2002) (Figure 1.2). This pathway mediates the intracellular effects of a number of extracellular signals received via GPCRs. Like other GPCRs V1b-R undergoes a conformational change upon agonist binding, facilitating the interaction of the intracellular domains of the receptor with a heterotrimeric guanine nucleotide binding protein (G protein) (reviewed in Ferguson, 2001). It is clear that the V1b-R associates with G-proteins of the  $G_{q/11}$  family (De Keyzer et al., 1994), however little is known about the molecular mechanism involved in this interaction. It is likely however that the mechanism is similar to that described for the coupling of V1a-R to  $G_{q/11}$  (reviewed in Holmes et al., 2003) due to the structural and functional similarities between the V1a and V1b. Binding of  $G_{q/11}$  causes the G protein to dissociate into its  $\alpha$  and  $\beta\gamma$  subunits. The  $\alpha$  subunit activates phospholipase C  $\beta$  (PLC  $\beta$ ), which then hydrolyses the membrane phospholipid phosphatidylinositol 4,5-bisphosphate ( $\text{PIP}_2$ ) generating two intracellular messengers; inositol 1,4,5-triphosphate ( $\text{IP}_3$ ) and diacylglycerol (DAG). Both stimulate secretion of ACTH by increasing intracellular free calcium ( $\text{Ca}^{2+}$ ) (King and Baertschi, 1990).  $\text{IP}_3$  causes the release of  $\text{Ca}^{2+}$  from intracellular stores via activation of  $\text{IP}_3$  receptors, whereas DAG increases intracellular  $\text{Ca}^{2+}$  via the activation of protein kinase C (PKC) (reviewed in Downes and Macphee, 1990).

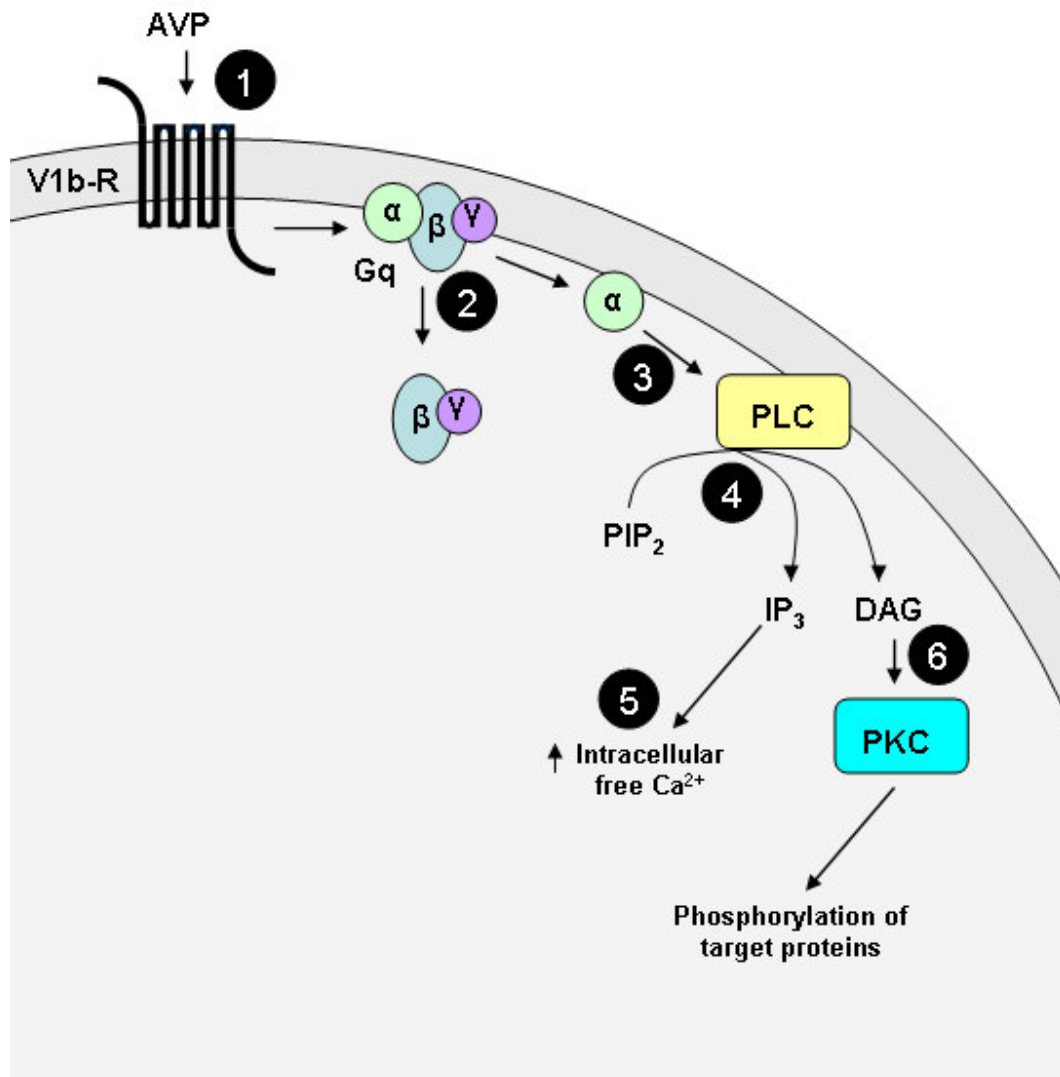


**Figure 1.2. Activation of the phosphoinositide signalling pathway by AVP.** Figure adapted from a recent review by Dautzenburg and Hauger (Dautzenburg and Hauger, 2002). Binding of AVP its specific receptor (V1b-R) (1) facilitates coupling to G<sub>q/11</sub> which results in the dissociation of the  $\alpha$  and  $\beta\gamma$  subunits of G protein (2). The  $\alpha$  activates phospholipase C (PLC) (3) which hydrolyses phospholipid phosphatidylinositol 4,5-bisphosphate (PIP<sub>2</sub>) generating inositol 1,4,5-triphosphate (IP<sub>3</sub>) and diacylglycerol (DAG) (4). IP<sub>3</sub> causes the release of Ca<sup>2+</sup> from intracellular stores (5), whereas DAG increases intracellular Ca<sup>2+</sup> via the activation of protein kinase C (PKC) (6).



### **1.3 ATTENUATION OF THE RESPONSE TO AVP: DESENSITISATION**

Activation of a GPCR by its ligand not only elicits a characteristic cellular response but also initiates the process of desensitisation (Ferguson and Caron, 1998). Desensitisation involves attenuation of the response to an agonist with repeated or sustained exposure (Mason et al., 2002). This adaptation mechanism plays an important physiological role by acting as the feedback signal limiting both acute and chronic overstimulation of a GPCR-mediated signalling pathway (Ferguson and Caron, 1998).

In the anterior pituitary desensitisation of the response to AVP results in reduced ACTH secretion. It has recently been shown that pre-exposure of sheep anterior pituitary cells to AVP at concentrations and durations that fall within endogenous ranges, results in desensitisation to subsequent AVP stimulation (Hassan, 2001; Mason et al., 2002). This suggests that this adaptation mechanism may play a key role in regulating ACTH secretion *in vivo*.

#### **1.3.1 Desensitisation of G protein-coupled receptors**

GPCR desensitisation has been most extensively studied for the adenylyl cyclase-coupled  $\beta_2$ -adrenergic receptor ( $\beta_2$ AR) (Ferguson, 2001). Although many of the mechanisms characterised for  $\beta_2$ AR are common among GPCRs, there are also some differences in the regulation of different GPCRs. This must be borne in mind when extrapolating to the V1b-R. However, the information presented here regarding the mechanisms of desensitisation is thought to be representative of all GPCRs (Ferguson, 2001; Mason et al., 2002; Tobin, 1997) including those coupled to the phosphoinositide signalling pathway (PLC-coupled GPCRs) (Tobin, 1997). Studies have shown compelling evidence that PLC-coupled receptors undergo rapid desensitisation within seconds of agonist stimulation (see Tobin, 1997 for a review). This desensitisation process is usually partial, resulting in a change in the PLC activity from a high level observed in the few seconds following

agonist stimulation to a lower, but sustained level of activity that may persist for tens of minutes (Wojcikiewicz et al., 1993).

The mechanisms of GPCR desensitisation include uncoupling of receptors from their G proteins, the internalisation (sequestration) of receptors to endosomes and down-regulation of receptors (Ferguson and Caron, 1998). Among the GPCRs, rapid and reversible desensitisation is commonly caused by the uncoupling of the receptor from its signalling pathway (Ferguson, 2001). Uncoupling of the receptor from its G protein by receptor phosphorylation is the most rapid means of attenuating GPCR responsiveness and occurs within seconds to minutes of agonist activation (Pitcher et al., 1998). Internalisation of receptors occurs too slowly to account for the desensitisation of most GPCRs. The majority of internalised receptors are already desensitised as internalisation usually follows uncoupling of the receptor (Ferguson, 2001). It is now thought that the internalisation is more important for resensitisation (recovery from desensitisation) than for desensitisation (Ferguson, 2001; Mason et al., 2002). Receptor down-regulation is a relatively slow process requiring hours-days to take effect (Lohse, 1993). This is because down-regulation involves degradation of existing receptors and/or a reduction in the rate of synthesis of new receptors (Mason et al., 2002).

Uncoupling is usually mediated by phosphorylation of the GPCR by one or more protein kinases. Research in recent years has revealed that a large number of GPCRs have phosphorylated states, and the level of phosphorylation is dramatically increased following agonist stimulation (reviewed in Tobin, 1997). It appears, therefore, that regulation via receptor phosphorylation is a mechanism employed by most GPCRs. Receptor phosphorylation either directly or indirectly inhibits the interaction between the receptor and its G protein, thereby diminishing the agonist induced response.

Two main classes of protein kinases have been shown to be involved in phosphorylation of GPCRs; second messenger-dependent protein kinases (eg. PKA and PKC) and G protein-coupled receptor kinases (GRKs) (Ferguson, 2001). While both classes of kinase contribute to the agonist-dependent (homologous) desensitisation of GPCRs, second messenger-dependent kinases can also

phosphorylate and desensitise receptors that have not been exposed to agonist (heterologous desensitisation).

### **1.3.2 Desensitisation of the pituitary vasopressin receptor**

A variety of *in vivo* studies have shown that the V1b receptor is subject to regulatory changes during stress (reviewed in Mason et al., 2002). For example, osmotic stress, such as 2% saline injections or water deprivation, results in reduced pituitary ACTH responsiveness in rats (Aguilera et al., 1994). Studies of the V1b-R *in vitro* have also shown that the ACTH response to AVP can be decreased following prolonged or repeated exposure to the peptide (reviewed in Mason et al., 2002). For example, as indicated above, it has recently been shown that treatment of perfused ovine anterior pituitary cells with AVP can cause desensitisation of the ACTH response to a subsequent stimulation with AVP (Hassan et al., 2003). This desensitisation occurred at concentrations and durations of AVP treatment that were within the ranges of AVP pulses measured in the sheep pituitary portal circulation, suggesting that the desensitisation may play an important physiological role in the regulation of ACTH secretion *in vivo*. The desensitisation was found to be rapid (reaching a maximum within 10 minutes of the onset of AVP pre-treatment) and was readily reversible.

Little is known about the mechanisms responsible for the desensitisation of the V1b-R to AVP stimulation. The characteristics, particularly the kinetics, of desensitisation of the V1b-R may provide some clues. For all GPCRs studied to date, rapid and reversible desensitisation, such as that observed for the V1b-R (Hassan et al., 2003), is commonly caused by uncoupling of the receptor from its signalling pathway. Uncoupling is typically mediated by receptor phosphorylation by one or more protein kinases (Ferguson, 2001).

A recent study investigated the mechanisms involved in desensitisation of the ACTH response of sheep anterior pituitary cells to AVP (Hassan and Mason, 2005). This looked specifically at the roles of the protein kinases PKC and casein kinase 1 $\alpha$  (CK1 $\alpha$ ), relevant protein phosphatases

(types 2A and 2B) and internalisation in the processes of desensitisation and resensitisation. The results suggest that desensitisation of the ACTH response to AVP is not mediated by either PKC-catalysed or CK1 $\alpha$ -catalysed phosphorylation. The data did indicate that desensitisation was at least partly dependent on V1b receptor internalisation, and that resensitisation is dependant on PP2B-mediated dephosphorylation. This suggests that although the kinases PKC and CK1 $\alpha$  are not involved, phosphorylation of the V1b receptor remains the most likely mechanism involved in desensitisation to AVP. This leaves GRKs as the most likely kinases to mediate the phosphorylation of the V1b-R. The V1b-R amino acid sequence contains GRK consensus motifs suggesting a possible role of GRK in mediating V1b-R desensitisation (reviewed in Mason et al., 2002).

In a recent study, the physical association of V1b-R with GRKs was investigated (Berrada et al., 2000). Following stimulation with AVP, the association of the V1b-R with GRK2, 3, 5 and 6 was investigated using fluorescence, immunoprecipitation and immunoblotting techniques. Of the GRKs studied, only GRK5 was detected in immune complexes with the V1b-R, suggesting a possible role for GRK5 in mediating V1b-R-signalling. GPCR regulation by specific GRKs probably occurs in a cell type-specific manner, meaning that regulation of a given receptor in a particular cell will be determined not only by which GRK or GRKs are expressed in that cell, but also by the relative and absolute expression levels of each GRK (Pitcher et al., 1998). Unfortunately, there is no information available regarding the levels of GRK expression in the corticotroph cells of the anterior pituitary. However, it has been shown using Northern blot analysis that GRK5 mRNA is expressed in a variety of human tissues, with the highest levels in heart, placenta and lung > skeletal muscle > brain, liver, pancreas > kidney (Kunapuli and Benovic, 1993).

### **1.3.3 G protein-coupled receptor kinases**

Phosphorylation of the receptor is the major mechanism underlying homologous desensitisation of GPCRs (Ferguson, 2001; Kelly et al., 2008). Until the mid 1980's GPCR phosphorylation by

second messenger-dependent protein kinases was originally believed to be the principal mechanism of GPCR desensitisation (Benovic et al., 1985). The identification of a novel protein kinase with the ability to phosphorylate the agonist-occupied  $\beta_2$ AR was a landmark in GPCR biology (Benovic et al., 1986). This kinase was soon found to be just one of a family of kinases, later termed the G protein-coupled receptor kinases (GRKs). However, it was found that GRK phosphorylation of GPCRs alone was insufficient to produce substantial desensitisation (Benovic et al., 1987). This led to the discovery of another family of regulatory proteins called the arrestins. The current understanding is that GRK-phosphorylation of an agonist-occupied GPCR facilitates arrestin binding to the receptor, thus uncoupling the receptor from its G protein (Ferguson, 2001; Kelly et al., 2008). The high-affinity binding of arrestins also activates the process of internalisation of the GPCR, which is usually followed by dephosphorylation and recycling of the receptor to the plasma membrane. Together these processes are referred to as the “classical model” for the homologous desensitisation of GPCRs and are generally considered applicable to most GPCRs (Ferguson, 2001; Kelly et al., 2008) (Figure 1.3). For all GRK-phosphorylated GPCRs studied to date the kinase invariably phosphorylates serine or threonine residues either on the 3rd intracellular loop or the carboxyl terminal of the receptor (Kelly et al., 2008; Yang and Xia, 2006).

To date, seven mammalian GRKs have been identified. These have been classified into three subfamilies on the basis of sequence and functional homology: 1) GRK1 (rhodopsin kinase) and GRK7 (cone opsin kinase); 2) GRK2 and GRK3 (also known as  $\beta$ -adrenergic receptor kinases 1 and 2), and the GRK4 subfamily comprising GRK4, GRK5 and GRK6 (Ferguson, 2001; Yang and Xia, 2006). GRK1 and GRK7 are expressed almost exclusively in the retina, whereas GRK4 is predominately found in the testis, and to a lesser extent in some brain regions and the kidney (Yang and Xia, 2006). GRK2, 3, 5 and 6 are expressed ubiquitously. In the absence of GPCR activation by an agonist GRK1-3 are localised in the cytosol, whereas GRK4-6 all exhibit substantial membrane localisation.

The basic structure of the non-visual GRKs (GRK2, 3, 4, 5 and 6) is similar, with a highly conserved central (263-266 amino acids) catalytic domain (Yang and Xia, 2006). The N-terminal 185-amino acid region displays considerable homology between different GRKs, leading to speculation that this region may be important in receptor recognition. GRK4-6 also possess a

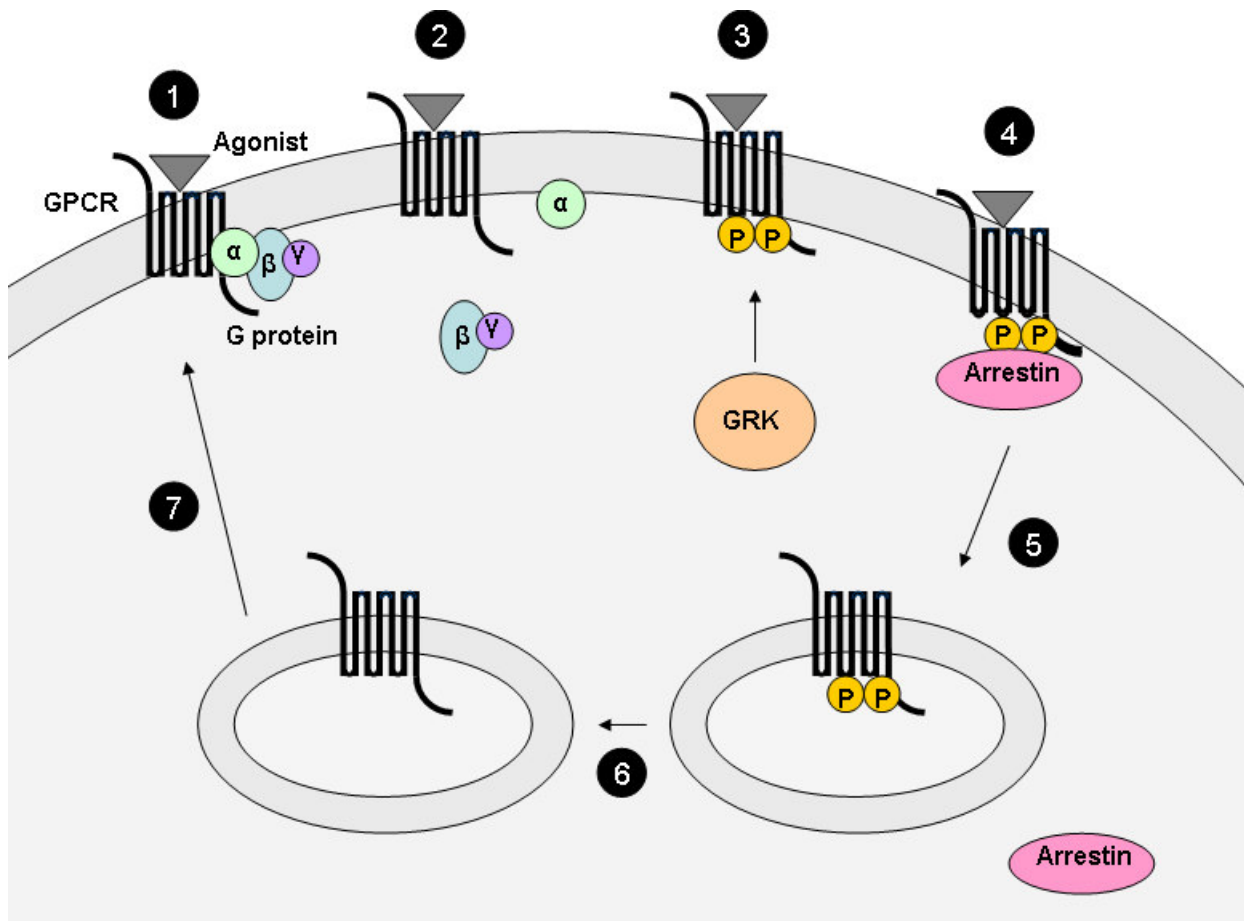


**Figure 1.3. The classical model of homologous desensitisation of GPCRs regulated by GRKs and arrestins.** Figure adapted from a recent review (Kelly et al., 2008). The GPCR is activated by an agonist leading to G protein-coupling (1) and activation of signalling by the  $\alpha$  subunit (2). The agonist-occupied GPCR is subsequently phosphorylated by a GRK (3) and arrestin then binds to the phosphorylated receptor (4). This leads to internalisation (5), dephosphorylation (6) and recycling of the GPCR to the plasma membrane (7).

highly conserved binding site (amino acids 22-29 for GRK5) for phosphatidylinositol (4,5) bisphosphate (PIP<sub>2</sub>) (Yang and Xia, 2006), which is thought to enhance catalytic activity. This provides a potential mechanism by which the GRK4-6 could also mediate GPCR signal transduction via phosphorylation-independent mechanisms. This is only one of a number of proposed mechanisms by which GRK activity and/or expression could be regulated in order to modify GPCR signalling via phosphorylation-independent mechanisms (Pitcher et al., 1998).

#### **1.3.4 Approaches employed to assess the involvement of G protein-coupled receptor kinases in G protein-coupled receptor desensitisation**

Increasingly, it seems that the vast majority of G protein-coupled receptors will prove to be substrates for GRKs (Pitcher et al., 1998). Because most mammalian cells and tissues tested thus far express more than one GRK, determining which GRKs regulate which receptors has proved daunting. With a very large number of GPCRs and relatively small number of GRKs, each GRK regulates innumerable receptors. For example, GRK2 (also referred to as  $\beta$ -adrenergic receptor kinase 1) not only phosphorylates the  $\beta$ -adrenergic receptors, but also several other G<sub>q/11</sub> coupled-GPCRs such as the Angiotensin II type 1a receptor (Kim et al., 2005) and the V2 vasopressin receptor (Ren et al., 2005). In addition, GRK2 also phosphorylates a number of distantly related G<sub>s</sub>-coupled GPCRs, such as the prostacyclin receptor (Smyth et al., 2000) and the leukotriene B<sub>4</sub> receptor (Gaudreau et al., 2002).

A number of methods are currently employed to investigate the role of GRKs in desensitisation of a GPCR (reviewed in Pitcher et al., 1998). Studies of homologous receptor desensitisation in an intact cell system have provided strong evidence for GRK-involvement in desensitisation of particular GPCRs. Because GRKs phosphorylate agonist-activated GPCRs, direct studies of receptor phosphorylation are also a robust method for identifying GRK substrates. The combination of phosphorylation and desensitisation studies is thought to be the optimal way to demonstrate the involvement of a specific GRK in the desensitisation of a certain GPCR (Pitcher et al., 1998).

Cellular signalling studies are widely used to investigate the involvement of a GRK in GPCR desensitisation (Pitcher et al., 1998). One method that has been used to assess the impact of GRKs in cellular systems is the inhibition of GRK function. For example, heparin (a non-selective GRK inhibitor) treatment of permeabilised human retinal Y-79 cells resulted in a small but significant reduction (34%) in desensitisation of CRF<sub>1</sub> receptors (Dautzenberg et al., 2001). A number of other substances have also been reported to modulate GRK activity, including Zn<sup>2+</sup> and mastoparan. However, each of these has a non-specific effect(s) that could have important consequences for studying the role of GRKs: for example, heparin is an IP<sub>3</sub> receptor agonist (Kobayashi et al., 1989), Zn<sup>2+</sup> is cytotoxic (Hasbi et al., 1998) and mastoparan activates G proteins (Higashijima et al., 1988). While heparin is currently still in use, modification of desensitisation with heparin treatment is by itself not sufficient to demonstrate the involvement of GRKs (Pitcher et al., 1998). There are currently no suitable GRK-inhibitors available.

GRK over-expression is another method employed by researchers to assess the role of a particular GRK in intact cells (for example see Gaudreau et al., 2002). Cells expressing the GPCR of interest are transfected with individual GRK cDNAs, and so the cells express levels of the GRK protein that are many-fold higher than the normal endogenous cellular levels. A reduction in agonist-induced receptor phosphorylation in cells overexpressing a GRK has been interpreted as evidence for the involvement of that GRK. However, the results may not reflect what would happen with normal endogenous levels of the GRK. In addition, negative results from GRK over-expression assays may be difficult to interpret because the receptor phosphorylation observed derives from the activity of both transfected and endogenous cellular GRKs.

Evidence for the activity of particular GRKs in GPCR desensitisation has also been obtained by “knockdown” of GRKs using specific GRK antibodies (Dhami et al., 2002), antisense oligonucleotides (Nagayama et al., 1996) or RNA interference (RNAi) (Ren et al., 2005). A general problem with antisense methodology has been the need to screen a significant number of oligonucleotides to find a selective and effective agent, and some concerns remain about the specificity of this approach. RNAi is currently the method of choice for loss-of-function studies due to its efficiency and efficacy compared to other techniques (Nature Cell Biology Editorial, 2003). Reduction (or “knockdown”) of GRK mRNA using RNA interference is the best method



currently available to assess the involvement of a particular GRK in desensitisation of cell signalling in an intact cell system.

## **1.4 RNA interference methodology**

### **1.4.1 An introduction to RNA interference**

RNA interference (RNAi) is the process of sequence-specific post-transcriptional gene silencing in animals and plants that is initiated by double-stranded RNA (dsRNA) that is homologous in sequence to the silenced gene (Dykxhoorn et al., 2003; Elbashir et al., 2001). The mediators of sequence-specific messenger RNA (mRNA) degradation are small interfering RNAs (siRNAs), usually 21-23 nucleotides in length. The siRNA duplexes are capable of specifically suppressing expression of endogenous genes in different mammalian cell lines, including the human embryonic kidney cell line (HEK293), without activating the interferon response (Elbashir et al., 2001). Therefore, since its discovery in animals (*Caenorhabditis elegans*) in 1998 (Fire et al., 1998), RNAi has rapidly become a widely used tool for studying the function of individual genes in mammalian cell systems.

There are several methods available for RNAi delivery in mammalian cells, including introducing transgenes that produce dsRNA (plasmid-based), and virus vector mediated delivery. However, transfection of mammalian cells with synthetic siRNA is the favoured method for transient silencing of a gene (<72 hours) in mammalian cells because the silencing is the efficient and potent, and the siRNA-transfection mediated effects are initiated immediately (Dykxhoorn et al., 2003). The siRNA can also be co-transfected with the receptor of interest using modern cationic lipid transfection reagents.

### **1.4.2 The evolving methodology for RNAi experiments**

The field of RNA interference (RNAi) research is rapidly evolving, with new modes of siRNA action still emerging. As we learn more about the complexity of the mechanisms of gene silencing by RNAi, it has become clear that it is crucial to design RNAi experiments with extreme care and to include adequate controls. Outlined below are the methods generally considered necessary for publication of the results of an RNAi-based experiment (Nature Cell Biology Editorial, 2003). These requirements must be fulfilled in order to use RNAi to assess the role of GRKs in V1b-R desensitisation.

#### **1.4.2.1 Minimising off-target effects of the siRNA**

The off-target effects of a siRNA are minimised by careful siRNA design. To ensure that the chosen siRNA sequence targets a single gene, a Basic Local Alignment Search Tool (BLAST) search of the selected sequences should be carried against sequence databases using the National Centre for Biotechnology Information (NCBI) website. Sequences in these databases that share partial homology with the siRNAs might be targeted for silencing by the siRNA. Potential off-target effects of the siRNA are therefore minimised by choosing a siRNA with maximum sequence divergence from the list of genes with partial sequence identity to the intended mRNA target.

#### **1.4.2.2 Minimising non-specific effects of the siRNA**

Titration of the siRNA is strongly recommended for RNAi experiments. RNAi is often extremely effective at minimal concentrations, and titration to the lowest possible levels reduces the chance of non-specific effects. For example, the siRNA can have cytotoxic effects (Ciccarone et al., 1999). These effects can be monitored using cell viability/proliferation assays (Jiang et al., 2008). In addition, siRNAs as short as 21 nucleotides can trigger innate immune responses in mammalian cell lines, particularly at high concentrations (Reynolds et al., 2006; Sledz et al., 2003). Useful controls are available to detect unintentional activation of global translational repression through the interferon response using commercial assay kits, or expression of unrelated proteins.

The siRNA should be titrated to maximise silencing while keeping the amount of siRNA required to a minimum. This is especially important because the RNAi machinery (the RISC complex in particular) is saturable, at least in some settings.

#### 1.4.2.3 Assessing knockdown

When using RNAi, it is essential to establish that the effects observed are the result of siRNA-specific degradation of the target mRNA. The “classical” mechanism of RNAi is characterised by four major steps: assembly of siRNA with the RNA-inducing silencing complex (RISC), activation of the RISC, siRNA-mediated target recognition and cleavage of target mRNA (Dykxhoorn et al., 2003). Although siRNA-mediated target mRNA degradation is by far the most likely mechanism of siRNA action, siRNAs can exert their effects through a number of surprisingly diverse mechanisms. For example, the siRNA can act via a miRNA mechanism mediating translational inhibition. Both mechanisms can result in a reduction in protein levels, and so to distinguish between them it is essential to measure knockdown of the target at both the protein and the mRNA level. If both message and protein are reduced, the response is “classical” RNAi. In contrast, if only the protein is reduced, the chances are that a miRNA-related translational mechanism is at work. Protein and mRNA levels must be assessed with quantitative techniques to allow for an accurate estimate of the level of reduction.

#### 1.4.2.4 siRNA controls

Control siRNAs must be used to demonstrate that knockdown of the target gene is mediated by the specific interaction of the target mRNA with the siRNA. There are a number of methods available for this. siRNAs that target different regions of the same gene can vary markedly in their effectiveness (Reynolds et al., 2004). However, a useful way to enhance confidence in RNAi data is to demonstrate a similar effect with two or more siRNAs targeted to different sites in the target mRNA. Mismatch or scrambled siRNAs have also been used as controls for RNAi experiments (for an example see Ren et al., 2005). These are of somewhat limited value as the scrambled

sequence is often too different from the “active” siRNA to function as a truly informative control. The best available control for any RNAi experiment is rescue expression of the target-gene in a form refractory to siRNA. This can often be achieved by utilising one or more silent third-codon point mutations within the targeted region of the mRNA, thus rendering the mRNA insensitive to siRNA-mediated degradation (for an example see Kim et al., 2005).

## **1.5 AIMS OF THIS STUDY**

The aim of this research was to develop methods needed to investigate the mechanism of desensitisation of the V1b-R mediated response to vasopressin. Several of the protein kinases that may mediate this process have now been excluded (Hassan and Mason, 2005). For example, unlike the closely related V1a receptor, evidence suggests that phosphorylation of the V1b-R is not mediated by the second messenger-dependent protein kinase C (Berrada et al., 2000; Hassan and Mason, 2005). The vast majority of GPCRs studied to date are substrates for phosphorylation by GRKs (Pitcher et al., 1998), however their involvement in the desensitisation of V1b-R mediated cell signalling has not yet been investigated. This is partly due to a lack of suitable pharmacological inhibitors of this family of kinases.

Knockdown of expression of GRK genes using RNA interference (RNAi) is one of the best techniques currently available to investigate the role of GRKs in GPCR desensitisation. The aim of this study was to develop methods needed to use RNA interference to investigate the role of GRK5 in V1b-R desensitisation. This involved the development of a model cellular system that could be used to assess the effect of GRK knockdown by RNAi. For successful RNAi experiments, a variety of methods are required to demonstrate that observations are target-specific, ie. mediated by the target gene. This research involved the development and evaluation of methods needed to:

1. Measure AVP-induced V1b-R desensitisation
2. Assess transfection-mediated cytotoxicity
3. Demonstrate GRK5 mRNA knockdown using quantitative PCR.

## **2**

# **STANDARD METHODS**

## **2.1 MATERIALS**

For the sources of all materials used in this study, refer to Appendix A.

## **2.2 SOLUTIONS AND MEDIA**

For the details of all solutions and media used in this study, refer to Appendix B.

## **2.3 CELL CULTURE**

### **2.3.1 Human Embryonic Kidney Cell Line**

For this study a human embryonic kidney cell line (HEK293) obtained from ATCC was used as a model system. These cells were transiently transfected with the vasopressin V1b receptor (V1b-R) as required for experiments.

The HEK293 cells were cultured in Eagle's Minimal Essential Medium (MEM) containing Earle's salts, L-glutamine, and nonessential amino acids, with sodium bicarbonate added. For routine maintenance of the culture the medium was supplemented with 10% heat-inactivated horse serum (HIHS), 1% sodium pyruvate and 1% penicillin/streptomycin (P/S), and this complete culture medium will herein be referred to as MEM+.

### **2.3.2 Chinese Hamster Ovary Cell Line**

Chinese hamster ovary (CHO) cells stably expressing the V1bR (CHO-V1b) were used in initial experiments to investigate whether desensitisation of the V1b-mediated response to AVP could be detected using the inositol phosphate assay. Several parameters influencing the desensitisation response were investigated using CHO-V1b as seen in chapter 3.

The CHO-V1b cells were cultured in Minimal Essential Alpha Medium (AMEM) containing Earle's salts, L-glutamine, and nonessential amino acids, with sodium bicarbonate added. For routine maintenance of CHO-V1b cells the AMEM was supplemented with 10% foetal bovine serum (FBS) and 1% penicillin/streptomycin, and this complete culture medium will herein be referred to as AMEM+. Neomycin was added to AMEM+ to give a final concentration of 100 $\mu$ g/mL for maintenance of the culture, and approximately once each month the cells were treated with 200 $\mu$ g/mL for selection.

### **2.3.3 Cell Culture**

The method of culturing CHO-V1b and HEK293 cells are very similar apart from their different medium requirements as indicated above. Both cell lines were cultured in 20mL of the appropriate medium in 75cm<sup>2</sup> culture flasks, and incubated at 37°C in a humid atmosphere of 95% air: 5% CO<sub>2</sub> for routine maintenance of the culture.

For all cell culture procedures the cells were handled in a biological safety cabinet and aseptic conditions were maintained throughout. All glassware used for cell culture was sterilized either by autoclave (20 minutes, 121°C, 20 lb/in<sup>2</sup>) or heat sterilized in an oven (2 hours, ≥170°C). All solutions used were either autoclaved as above or filter sterilized (see appendix B for details). All plasticware used was also sterile.

#### 2.3.3.1 Thawing Cells

Stocks of HEK293 and CHO-V1b cells were stored in a liquid nitrogen canister in cryotubes containing approximately 1mL of cells in cell freezing medium. A tube of the required cells was removed from the liquid nitrogen canister and immediately placed in a 37°C water bath. The tube was gently agitated to allow rapid thawing and then using a 5mL pipette with a wide tip the contents of the tube were transferred to a 75cm<sup>2</sup> culture flask containing 19mL of the appropriate medium pre-warmed to 37°C. The culture was then incubated for approximately 24 hours at 37°C in a humid atmosphere of 5% CO<sub>2</sub> in air. This allowed the cells to adhere to the culture flask. The medium was then aspirated to remove the cell freezing medium and replaced with 20mL of fresh pre-warmed medium.

#### 2.3.3.2 Sub-culturing Cells

HEK293 and CHO-V1b cells were regularly sub-cultured (ie. passaged) before confluence was reached in order to maintain healthy cells. Cell cultures were split at approximately 80-90% confluence for HEK293 cells, and 90-100% confluence for CHO-V1b cells.

A solution of 0.25% (1x) Trypsin with EDTA (T/E) was used to detach the cells from the culture flask. The growth medium was aspirated from the 75cm<sup>2</sup> culture flask containing the cells and then 2mL of T/E solution at 37°C was added. The flask was then immediately tilted to cover the cells with the T/E.

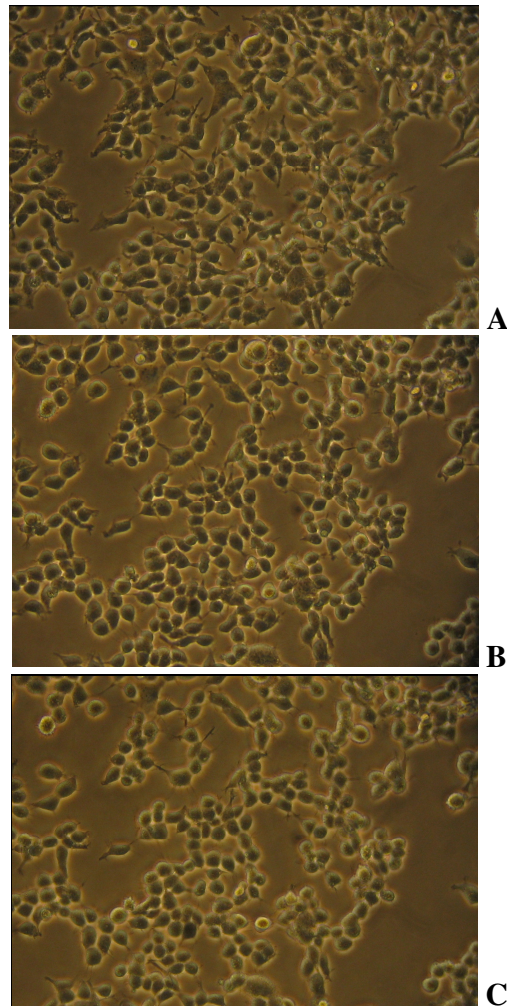


**Figure 2.1. Phase contrast micrograph of HEK293 cells taken during trypsinisation in a 75cm<sup>2</sup> culture flask at 40X magnification.** After 1 minute in the presence of T/E the cells started to retract (A) and after 5 minutes the cells were almost completely rounded (B). At approximately 12 minutes (C) the cells were round and detaching, as evidenced by their tendency to form clumps.

For CHO-V1b cells the flask was immediately placed into a 37°C incubator for 2 minutes, and following this the flask was firmly banged 2-3 times to dislodge the cells. For HEK293 cells the flask was incubated at room temperature (approximately 22°C). The cells were observed under an inverted microscope during trypsinisation. Almost immediately the HEK293 cells start to retract and after approximately 12 minutes the cells were round and detaching, as shown by their tendency to form clumps (see Figure 2.1). At this stage the flask is gently tilted 3-4 times to dislodge the cells.



Following cell dispersion 8mL of the appropriate pre-warmed growth medium for each cell type was used to gently wash the cells off the surface of the culture flask. The cell suspension was gently re-pipetted 4 times to disperse the cells in the medium, and was then used to seed a new flask. For CHO-V1b cells 0.5mL of cell suspension was added to 19.5mL of AMEM+, and for HEK293 cells 2.5mL of cell suspension was added to 17.5mL of MEM+. At these subcultivation ratios both cell types required sub-culturing approximately every 3 days. Approximately 24 hours after sub-culture the growth medium was aspirated and replaced with fresh medium to remove the T/E as this could inhibit growth.

There is evidence that the properties of some cells change over time with continuous cell culture, particularly at high passage number. For example, there is evidence that after many passages the transfection efficiency when using Lipofectamine 2000 reagent can change (Hawley-Nelson and Shih, 1995). For this reason all assays were performed using early passage (<10) cells (unless otherwise stated).

### 2.3.3.3 Freezing Cells

Frozen cell stocks were made from the cell suspension at the time of sub-culturing. The cell suspension was transferred to a 50mL centrifuge tube and spun at 900rpm for 8 minutes to pellet the cells. The supernatant was then aspirated and the tube was tapped to loosen the cell pellet before an appropriate volume of cell freezing medium was added. For 8-10mL of cell suspension 4mL of cell freezing medium was used. For HEK293 cells this gave approximately  $2 \times 10^6$  cells per mL of cell freezing medium.

After gently resuspending the cells by repipetting, 1mL aliquots were transferred to cryotubes. These tubes were then put into a Nalgene cell freezer containing isopropyl alcohol to facilitate slow freezing of the cells. The cells were kept at -80°C for approximately 24 hours before being transferred to liquid nitrogen for long term storage.

### **2.3.4 Coating Cell Culture Plates**

One of the challenges when using HEK293 cells is that these cells are a weakly adherent cell type (Robbins and Horlick, 1998). The plastic surface of cell culture plates provides a negatively charged surface which most cells adhere to. However, HEK293 cells do not produce enough positively charged extracellular matrix proteins to adhere strongly to the surface (Vancha et al., 2004).

In optimal conditions HEK293 cells adhere to a culture plate within a couple of hours, however if left at temperatures less than 37°C for any length of time the cells begin to lift from the plastic surface. Several of the methods used in this study require that the cells are incubated at temperatures lower than 37°C and/or the medium on the cells needs to be changed rapidly which also causes the cells to lift. Pre-coating of the plastic surface with attachment promoting factors was required to improve the adherence of the cells and minimise cell loss.

Pre-coating of the plastic surface with an extracellular matrix protein such as collagen is often used to promote attachment for weakly adherent cell types. For HEK293 cells however, collagen has a very minimal effect and pre-coating with a synthetic polymer results in much stronger cell adherence and resistance to cell loss during washes (Vancha et al., 2004). The synthetic polymer poly-lysine is commonly used as a coating substrate for cell culture plates and has been shown to be effective for HEK293 cells (Pichet and Ciccarone, 1999b; Vancha et al., 2004) and so was used for this study.

Poly-lysine is a synthetic polycation which binds to DNA and any negatively charged protein. It works by enhancing electrostatic interactions between negatively charged ions of the cell membrane and the culture surface. When adsorbed to the surface of a culture plate, poly-lysine increases the number of positively charged sites available for cell binding and hence improves the adherence of the cells to the surface.

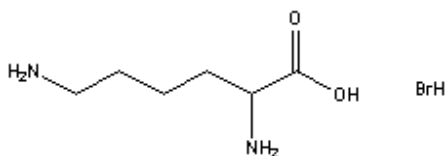


**Figure 2.2. The molecular structure of L-lysine.** The hydrobromide group is required for solubility in water. Molecular Formula:  $C_6H_{15}BrN_2O_2$

Both the D- and L- form of the poly-lysine can be used as a coating solution since poly-lysine is a nonspecific attachment factor for cells. However, certain cells can digest poly-lysine. In this case, poly-D-lysine should be used as the attachment factor so that the cells are not disrupted by excessive uptake of L-lysine. For this study both poly-L-lysine and poly-D-lysine were tested experimentally to achieve the best possible HEK293 cell adherence.

#### 2.3.4.1 Coating Plates with Poly-L-lysine

Poly-L-lysine solution was purchased as a 0.1% (w/v) solution. For adhesion of tissue sections to glass slides, the supplier recommends diluting this 1:10 with distilled de-ionized water (ddH<sub>2</sub>O) for use. However, for coating tissue culture plates a more dilute solution (eg. 1:100) is generally used. To determine the optimum dilution for use in this poly-L-lysine dilutions 1:10, 1:50 and 1:100 were tested. These dilutions were used to treat wells of Nunclon 24-well culture plates, using the following protocol.

A 200 $\mu$ L aliquot of poly-L-lysine diluted with ddH<sub>2</sub>O was added to each well. The plate was then incubated at room temperature for 30 minutes before the solution was aspirated from the well. The plate was left with the lid off in a laminar flow hood for approximately 45 minutes to allow the plate to dry. HEK293 cells in MEM+ were then plated into the dry wells at a density of  $1.5 \times 10^5$  cells/mL.

After culturing for approximately 24 hours at 37°C in a CO<sub>2</sub> incubator, there was no visible difference between the cells in untreated wells and those in wells treated with 1:50 or 1:100

dilutions of poly-L-lysine, when observed under an inverted microscope. Cells plated into wells treated with a 1:10 dilution of poly-L-lysine however, appeared to have quite a different morphology. The cells were more rounded and had formed clumps, which are both indicators of poor health. This suggests a possible toxic effect of the poly-L-lysine on the cells at a 1:10 dilution, and may be the result of excessive lysine uptake by the cells.

To test the effects of poly-L-lysine on cell lifting and loss during media removal/addition the cells were subjected to a rapid medium change. Aspiration of the medium did not appear to result in any significant cell loss in either coated or uncoated wells. The addition of new medium is commonly the time when cells tend to lift and get washed from the culture plate surface. After addition of new medium in this experiment there was a much greater degree of cell lifting and loss in uncoated wells. Also, in the untreated wells the cells that remained attached tended to clump as a result of the medium change, but this was reduced in all poly-L-lysine treated wells.

It was noted that the HEK293 cells tended to lift and be washed from the culture plate surface more easily when the confluence was high. At or close to confluence cell loss after a medium change could be very dramatic as the cells tended to remain attached to other cells and so would lift from the plastic in “sheets” from the edges of the wells. The effect of poly-L-lysine on this was tested at five different cell densities. HEK293 cells were plated at densities of  $0.5 \times 10^5$ ,  $1.0 \times 10^5$ ,  $1.5 \times 10^5$ ,  $2.0 \times 10^5$  and  $2.5 \times 10^5$  cells/mL into a 24-well plate treated with 1:10, 1:50 and 1:100 dilutions of the stock poly-L-lysine solution. The cells were approximately 35%, 55%, 70%, 80% and 90% confluent after 24 hours incubation. In wells where the cells were 35-80% confluent poly-L-lysine treatment effectively reduced the cell loss caused by a medium change compared to untreated wells. In contrast, in wells where the confluence was high (80-100%) cell loss occurred even in poly-L-lysine treated wells due to the cells lifting in “sheets”.

#### 2.3.4.2 Coating Plates with Poly-D-lysine

Poly-D-lysine is the stereo-isomer of poly-L-lysine. L-lysine is the biologically active isomer and some cells can digest this, whereas D-lysine cannot be used by cells and poly-D-lysine cannot be

broken down into L-lysine. The use of Poly-D-lysine eliminates the risk of excessive uptake of the amino acid which could disrupt normal cellular function.

Poly-D-lysine was purchased from the supplier as a lyophilized powder. According to the manufacturer's instructions 2.5-5 $\mu$ g of poly-D-lysine per cm<sup>2</sup> of plate area should be adequate for coating. Approximately 10mg of this powder was weighed, and dissolved in an appropriate volume of ddH<sub>2</sub>O to create a 1% solution. For coating culture plates the 1% (w/v) solution was then diluted with MEM to give the desired amount of poly-D-lysine per cm<sup>2</sup> of plate area (see Table 1). For example, for a 24-well plate 300 $\mu$ L of 33.3 $\mu$ g/ $\mu$ L poly-D-lysine was added to each well to achieve a coating concentration of 5 $\mu$ g per cm<sup>2</sup> (see Table 2.1). After incubation for 1 hour at room temperature the poly-D-lysine solution was aspirated from the wells and each well was washed 3 times with MEM to remove any excess poly-D-lysine (see Table 1 for the wash volumes used). The plate was left with the lid off in a laminar flow hood for approximately 45 minutes to allow the plate to dry.

To test the optimal coating concentration for HEK293 cells poly-D-lysine wells of a 24-well plate were coated with either 2.5 or 5 $\mu$ g of poly-D-lysine per cm<sup>2</sup>. HEK293 cells were then plated into the poly-D-lysine coated wells, and some cells were plated into uncoated wells for comparison. After 24 hours the cells were observed under an inverted microscope. Those cells plated into poly-D-lysine coated wells had noticeably more cell extensions/outgrowths and appear more flattened, indicating better cell attachment to the culture plate. Also, following a medium change the cell loss in poly-D-lysine coated wells was minimal compared to uncoated wells. There was no apparent difference between wells coated with 2.5 versus 5 $\mu$ g of poly-D-lysine per cm<sup>2</sup>. The efficacy of coating with poly-D-lysine at these concentrations was then confirmed by testing the vasopressin responsiveness of cells in various coated and un-coated wells, using the inositol phosphate assay (see Chapter 3).

**Table 2.1. The protocols for coating of 6-, 12- and 24-well plates with poly-D-lysine.** The surface area of the wells, the concentration and volume of poly-D-lysine solution required, as well as the volumes of MEM used for washing are given.

Culture Plate	Surface area of the base of the well	Poly-D-lysine quantity per unit area	Poly-D-lysine Coating Solution		Volume of MEM per wash*
			Concentration	Volume	
24-well plate	2cm <sup>2</sup>	5µg per cm <sup>2</sup>	33.3µg/mL	300µL	1.5mL
		2.5µg per cm <sup>2</sup>	16.6µg/mL	300µL	1.5mL
12-well plate	4cm <sup>2</sup>	5µg per cm <sup>2</sup>	33.3µg/mL	600µL	3mL
		2.5µg per cm <sup>2</sup>	16.6µg/mL	600µL	3mL
6-well plate	10cm <sup>2</sup>	5µg per cm <sup>2</sup>	33.3µg/mL	1500µL	4mL
		2.5µg per cm <sup>2</sup>	16.6µg/mL	1500µL	4mL

\* Each well washed 3 times

For the relatively small number of experiments where HEK293 cells were cultured in 6- or 12-well plates these plates were coated, as described above with 5µg of poly-D-lysine per cm<sup>2</sup> (unless otherwise indicated). Most experiments requiring tight cell adhesion were carried out in 24-well plates. Since manual poly-D-lysine coating uses a considerable amount of MEM and is time consuming, pre-coated 24-well plates were purchased from Becton Dickinson Biosciences for these experiments.

## 2.4 CELL VIABILITY

### 2.4.1 Viability Assay of Dispersed Cells

To determine the viability of cells in suspension the trypan blue assay was used. Trypan blue is a vital dye which is negatively charged and cannot enter cells unless the membrane is damaged

(Freshney, 1987). Therefore, after a 2 minute exposure to trypan blue cells which exclude the dye were assumed to be viable while dead cells stain blue.

A 50 $\mu$ L aliquot of the cell suspension from sub-culturing was combined with 50 $\mu$ L of a working solution of trypan blue (see appendix B for details). This was incubated at room temperature for 2 minutes. The cells were then counted using a haemocytometer and the number of viable cells per mL was calculated. This information was then used to accurately dilute the cell suspension for plating of the desired density of viable cells. The viability of HEK293 cells was typically 98-99%.

#### **2.4.2 Viability Assays of Adherent Cells**

The aim of this research was to develop the methods needed to use RNAi technology to investigate the role of a GRK, specifically GRK5, in the V1bR mediated response to AVP. The delivery of reagents used for RNAi, or the delivery method itself, can give rise to cytotoxicity in gene silencing experiments (Ciccarone et al., 1999). Cytotoxic effects might be difficult to distinguish from a phenotype resulting from GRK knockdown. It is therefore important to minimise the transfection-mediated cytotoxicity for proper interpretation of an RNAi experiment. Cell viability/proliferation assays such as the MTT assay are widely used to assess the cytotoxic effects of siRNA transfection (for an example see Jiang et al., 2008). Both the trypan blue exclusion method and the MTT assay were used to assess the cytotoxic effects of a treatment on HEK293 cells.

For these viability assays HEK293 cells were plated at a density of  $3.5 \times 10^5$  cells/mL into either 24-well plates or 12-well plates so that they reached approximately 80% confluence 18 hours after plating. A 100 $\mu$ L aliquot of the desired treatment solution was then added to the wells containing both cells and medium. For all experiments 100 $\mu$ L of MEM without phenol red was added to control wells. The plate was then incubated for 5-6 hours at 37°C prior to performing the viability assay.

#### 2.4.2.1 Trypan Blue Assay of Adherent Cells

The trypan blue assay was performed after 5 hours incubation of the cells with the treatment solution. First, the medium was aspirated from the wells and replaced with 300 $\mu$ L (12-well plate) or 150 $\mu$ L (24-well plate) of MEM- (MEM without serum). An equal volume of trypan blue working solution was added to each well. Following incubation at room temperature for 2 minutes the dye solution was aspirated and 1xPBS was added to each well (300 $\mu$ L/well for a 12-well plate, or 150 $\mu$ L/well for a 24-well plate). A cell count was then performed using an inverted microscope to view the cells at 20 x magnification. The total cells and dead cells (stained blue) were counted within two different fields of view for each well, so a total of approximately 800-1000 cells were counted per well. As for the trypan blue assay of dispersed cells the viability was typically 98-99% for control cells.

The trypan blue assay as described here was used to assess cell viability in conjunction with each of the MTT assays performed (see section 2.4.2.2 below). The results were reasonably consistent with those obtained using the MTT assay method but manual counting of the cells using an inverted microscope meant that this method was somewhat time consuming, and also subject to human error. Despite this, the method provides a useful visual estimation of actual viability of cells, whereas the MTT-formazan assay can only be used to assess differences in viability relative to a control. Table 2.2 below shows some typical results for assessment of cell viability using the trypan blue assay. For this experiment, increasing concentrations of sodium chloride (NaCl) were used to osmotic disruption of cells and hence cell death.

The cell viability was calculated using the equation:

$$\text{Cell viability (\%)} = \frac{(\text{mean total number of cells}) - (\text{mean number of dead cells})}{\text{mean total number of cells}} \times 100\%.$$



**Table 2.2. Assessment of adherent cell viability using the trypan blue assay.** The assay was performed following exposure of HEK293 cells to increasing concentrations of NaCl for 5 hours. Blanks were treated with normal medium containing 6.9g/L NaCl. The mean total and dead cells counted in two fields of view at 20x magnification (n=2) and the calculated cell viability are shown.

Treatment	Mean total number of cells	Mean number of dead cells	Cell Viability (%)
18.5g/L NaCl *	842.0	4.5	94.9
30.1g/L NaCl *	302.0	112	62.9
54.5g/L NaCl *	60	45	25.0
Blank	826	4.5	99.5

\* Normal MEM has 6.9g/L NaCl

#### 2.4.2.2 MTT-formazan Assay of Adherent Cells

The MTT-formazan assay (also referred to as the MTT assay) is widely accepted as a reliable way to determine cell viability and factor-mediated cytotoxicity. This method has recently been employed to assess cytotoxic effects of siRNA delivery (Jiang et al., 2008) and plasmid transfection (Basarkar et al., 2007; Mao et al., 2007) for HEK923 cells. The MTT assay works on the basis that the yellow tetrazolium salt MTT (3-(4, 5-dimethylthiazoyl-2)-2, 5-diphenyltetrazolium bromide) is reduced by metabolically active cells (live cells), in part by the action of dehydrogenase enzymes (van de Loosdrecht, 1994). The reduction of MTT results in the formation of purple-coloured formazan which can then be solubilised and quantified using a spectrophotometer.

MTT assays were performed after 6 hours of incubation with treatment solutions. The medium was aspirated from the wells, and then each well was washed three times with PBS using 0.5mL (24-well plate) or 1mL (12-well plate) per wash. The wash was to remove the phenol red-containing MEM as phenol red interferes with the MTT, giving false colour readings. An aliquot of 0.5mg/mL MTT in 0.5mL MEM without phenol red (or 1mg/mL MTT in 1mL MEM without phenol red for a 12-well plate) was then added to each well. The MTT solution was also added to 3 empty wells (without cells) for blanks. After MTT addition, each plate was briefly viewed under an inverted microscope to assess cell loss due to the washes, which was generally minimal. The

plate was then incubated at 37°C for 1.5 hours (unless otherwise specified). All medium added to the cells were pre-warmed to 37°C before use.

0.5mL (24-well) or 1mL (12-well) of 10% SDS was added to each well after incubation with MTT. The plate was returned to the 37°C incubator for 5 minutes to allow the formazan crystals to dissolve. Each sample was then vigorously repipetted and transferred to a cuvette. The absorbance of each sample at 570nm was measured immediately using a Shimadzu UV-1601PC spectrophotometer. Distilled water was used to blank the spectrophotometer.

For accurate results the absorbance of the samples at 570nm should ideally be between 0.5 and 1.0. The absorbance represents the amount of purple-coloured formazan produced, which depends primarily upon the cell type, the cell density and the period of incubation with the MTT. Incubation periods reported for HEK293 vary from 2-4hrs (Basarkar et al., 2007; Li et al., 2005; Mao et al., 2007). To optimise the performance of the MTT assay a suitable period of incubation for this setup was determined experimentally. HEK293 cells were plated at a density of  $3.5 \times 10^5$  cells/well into a 12-well plate, and  $1.75 \times 10^5$  cells/well into a 24-well plate. The cells were then cultured for 18 hours prior to the assay. After washing with PBS, MTT solution was added to each well as described above. The formation of purple crystals was visible after 30 minutes incubation with the MTT. The absorbance of half of the samples was read at 80 minutes after the addition of MTT, and the remaining samples were measured 1 hour later (ie. 140 minutes after the addition of MTT). The resulting absorbance values are shown in Table 2.3.

The average absorbance of the blanks ranged from 0.069-0.077. This shows that a small amount of formazan was produced in the absence of cells, which is usual for the MTT assay. To correct for this, the average absorbance of the blanks was subtracted from the average absorbance of the samples to give the corrected absorbance. The corrected absorbance values for this experiment were between 0.459 and 0.524, which was at the bottom end, or slightly lower than the ideal absorbance range of 0.5-1.0. However, the absorbance did not increase between 80 and 140 minutes incubation indicating that the maximum absorbance for this experimental setup was reached within 80 minutes. For further MTT assays an incubation period of 90 minutes was used.

**Table 2.3. Testing incubation times for the assessment of adherent cell viability using the MTT assay.** The MTT assay was performed in 12- and 24-well plates and cells were incubated for either 80 minutes or 140 minutes with MTT. The mean absorbance of samples at 570nm  $\pm$  SEM (n=3) and the calculated corrected absorbance are shown.

Plate type	Period of Incubation (minutes)	Sample ID	Mean absorbance at 570nm	Corrected absorbance
12 well plate	80	Blank 1 Sample 1	0.076 $\pm$ 0.003 0.535 $\pm$ 0.012	0.459
24 well plate	80	Blank 2 Sample 2	0.069 $\pm$ 0.001 0.516 $\pm$ 0.002	0.447
12 well plate	140	Blank 3 Sample 3	0.077 $\pm$ 0.003 0.527 $\pm$ 0.021	0.45
24 well plate	140	Blank 4 Sample 4	0.069 $\pm$ 0.001 0.593 $\pm$ 0.008	0.524

There was no significant difference between 12- and 24-well plates, so 24-well plates were used for further experiments.

The transfection reagent Lipofectamine 2000 (LF2000) was used for transfection of HEK293 cells with the plasmid prV1b-R. The MTT assay was used to assess the cytotoxicity of the LF2000 and other reagents used for transfection so that the transfection procedure could be optimised. HEK293 cells were plated into 24-well plates at a density of  $1.75 \times 10^5$  cells/well and cultured for 18 hours. The cells were then incubated with the transfection mixture for 6 hours prior to the viability assay. As described in section 2.7, transfection of HEK293 with the plasmid is carried out by adding plasmid DNA and LF2000 in OptiMEM to each well. The MTT assay was performed using cells that had been treated with 100 $\mu$ L of transfection mixture containing: LF2000, plasmid and OptiMEM; LF2000 and OptiMEM; or OptiMEM at the concentrations regularly used for plasmid transfection (see section 3.8). An equal volume of MEM was used for positive controls, or 1M NaCl for negative controls. The results of the assay are shown in Table 2.4.

The cell viability (%) was calculated using the following equation:

$$\text{Cell viability (\%)} = \frac{(\text{mean absorbance at 570nm of sample})}{(\text{mean absorbance at 570nm of control})} \times 100\%.$$

**Table 2.4. Assessment of the cytotoxicity of transfection reagents using the MTT assay.** The MTT assay was performed following exposure of HEK293 cells to a transfection mixture for 6 hours. The mean absorbance of samples at 570nm  $\pm$  SEM (n=3) and the cell viability (%) compared to control are shown.

Treatment solution	Mean absorbance at 570nm	Corrected absorbance	Cell Viability (% of positive control)
LF2000, plasmid and OptiMEM	0.513 $\pm$ 0.030	0.454	102.75
LF2000 and OptiMEM	0.517 $\pm$ 0.011	0.458	101.18
OptiMEM	0.517 $\pm$ 0.027	0.459	101.33
MEM (positive control)	0.511 $\pm$ 0.012	0.453	100
NaCl * (negative control)	0.488 $\pm$ 0.019	0.43	94.92
Blank	0.059 $\pm$ 0.002		

\* 100 $\mu$ L of 1M NaCl was added to the wells containing cells and medium to give a final conc 16.25g/L NaCl.

Normal MEM has 6.9g/L NaCl

The cell viability (%) is therefore an expression of viability relative to the positive control, where the positive controls had 100 $\mu$ L of MEM (normal growth medium) added per well. This differs from the trypan blue assay of adherent cells where an actual cell count is taken and the actual % viability is calculated. The cell viability (%) did not appear to differ between the treatments. Therefore, the LF2000, plasmid DNA and OptiMEM appear to have no cytotoxic effect at the concentrations used for plasmid transfection.

A solution of sodium chloride (NaCl) was used as a negative control for the assay shown in Table 2.4. The addition of 100 $\mu$ L of 1M NaCl increased the NaCl concentration of the growth medium from 6.9g/L to 16.25g/L. Increasing the concentration of NaCl in the medium raises the osmotic pressure and can lead to cell death if sufficiently high (Burg et al., 2007). However, the results show that at a concentration of 16.25g/L, NaCl did not cause a significant reduction in cell viability. To determine whether the MTT assay method described would accurately measure a significant reduction in cell viability other treatments expected to cause cell death were tested. HEK293 cells were plated into 24-well plates, cultured for 18hours and then 100 $\mu$ L of the treatment solutions were added to each well. The cells were treated with varying concentrations of the detergent Triton-X or NaCl as shown (Table 2.5).

Treatment of the cells with increasing concentrations of NaCl further decreased the cell viability (%) (Table 2.5). At a concentration of 18.5g/L NaCl the cell viability was reduced to 79% of control. This suggests that a reduction in cell viability compared to control can be measured using

**Table 2.5. Assessment of the cytotoxicity of NaCl and Triton-X using the MTT assay.** The MTT assay was performed following exposure of HEK293 cells to a treatment solution for 6 hours. The mean absorbance of samples at 570nm  $\pm$  SEM (n=3) and the cell viability (%) compared to control are shown.

Treatment solution	Mean absorbance at 570nm	Corrected absorbance	Cell Viability (% of positive control)
18.5g/L NaCl *	0.682 $\pm$ 0.051	0.672	79.14
30.1g/L NaCl *	0.235 $\pm$ 0.033	0.224	26.42
54.5g/L NaCl *	0.017 $\pm$ 0.002	0.006	0.73
0.1% Triton-X	0.013 $\pm$ 0.003	0.003	0.33
0.5% Triton-X	0.013 $\pm$ 0.001	0.002	0.26
Blank	0.011 $\pm$ 0.001		

\* Normal MEM has 6.9g/L NaCl

this method, which is essential if the MTT assay is to be used for optimisation of transfection with siRNA.

At a concentration of 30.1g/L NaCl the cell viability was reduced to 26% of control (Table 2.5). The same NaCl concentration was assessed using the trypan blue assay of adherent cells and the cell viability was found to be 62.9% (Table 2.2). This was 63.2% of the control (which was 99.5% viable). There is therefore a considerable difference between the results of the two assays, which is most likely caused by the error associated with manual counting of the cells for the trypan blue assay. The MTT assay is the more accurate method for determining viability compared to a control, however the trypan blue assay still provides a useful estimate of the actual % viability.

Reduction of the cell viability to 26% (MTT assay) or 63% (trypan blue assay) of control represents a significant reduction, yet cell death is not complete and so 30.1g/L NaCl is well suited for use as a negative control for future viability assays. For cells treated with 54.5g/L NaCl, 0.1% or 0.5% Triton-X the viability was reduced to <1% of control, meaning almost complete cell death had occurred.

The LF2000 reagent is recommended for co-transfection with both a plasmid and siRNA at the same time. Co-transfection requires careful optimisation to minimise the cytotoxic effects of the reagents, including the siRNA itself. The MTT assay described here can be used to assess any reduction in cell viability caused by co-transfection.

## 2.5 PLASMID PURIFICATION

### 2.5.1 Plasmids: prV1b-R and pALTER-MAX

HEK293 cells were transfected with the plasmid prV1b-R so that they expressed the V1b-R. The rat V1b-R full clone (2.7kb) as described by Lolait and colleagues (Lolait et al., 1995) was inserted into the pALTER-MAX-MAX vector (5.5kb) (Figure 2.3) to give prV1b-R (8.2kb). The pALTER-MAX-MAX plasmid was originally from Promega, whereas the prV1b-R was originally made by Bioserve – Biotechnologies, MD, USA. Both plasmids were kindly supplied as a gift from Dr. Greti Aquilera of the NIH. The pALTER-MAX-MAX vector (shown in Figure 2.3), and the prV1b-R, includes a selection marker that confers resistance to the antibiotic chloramphenicol ( $\text{Cm}^r$ ).

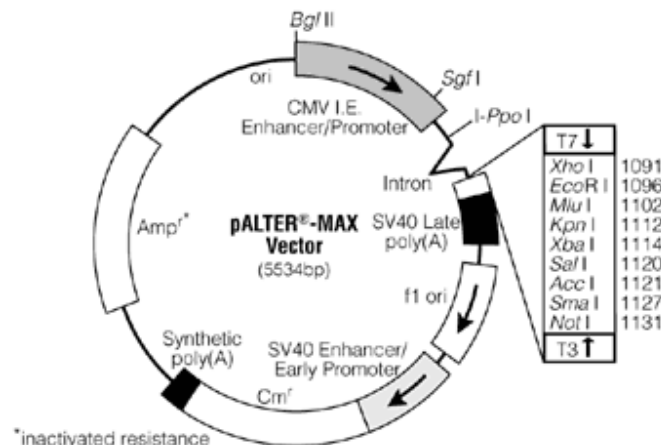


Figure 2.3. Map of the pALTER-MAX-MAX vector (5.5kb) showing restriction sites.

### 2.5.2 Elution of Plasmids

The plasmids were received on dry filter paper. To elute the plasmid the area of filter paper spotted with plasmid was cut out using sterile scissors and put into a 1.5mL tube. A 100 $\mu$ L aliquot of TE8

was added to the tube and then incubated at room temperature for 10 minutes. The tube was then briefly spun and the supernatant removed. A second elution was then carried out to ensure a good yield of plasmid was recovered from the filter paper. To do this the filter paper was transferred to a support construct inside a second 1.5mL tube. A 100 $\mu$ L aliquot of TE8 was added to the filter paper and it was incubated at room temperature for 10 minutes. The tube was then spun briefly and the supernatant was collected. The supernatants from the two elutions were combined and then aliquoted into several tubes for storage at -20°C.

Native DNA gel electrophoresis of the eluted samples on a 0.8% agarose confirmed the presence of plasmid DNA (as described in section 2.5.4). As expected the undigested plasmid gave two bands on a gel, representing the relaxed and supercoiled forms of the plasmid (as seen in Figure 2.4). The concentration of the DNA was determined using a Nanodrop spectrophotometer (as described in section 2.5.4). The DNA concentrations were 22.9ng/ $\mu$ l for prV1b-R and 15.1ng/ $\mu$ L for pALTER-MAX-MAX.

### **2.5.3 Transformation of *E.coli* DH5 $\alpha$**

The desired plasmid, prV1bR (or the control plasmid pALTER-MAX-MAX), was used to transform *E. coli* DH5 $\alpha$  competent cells. To determine the transformation efficiency a control plasmid, pUC19 was used. The pUC19 plasmid confers ampicillin resistance. As an additional control, untransformed cells were included.

Each of the plasmid solutions (prV1b-R, pALTER-MAX and pUC19) were diluted to 4ng/ $\mu$ L with TE8. A single tube of *E. coli* DH5 $\alpha$  competent cells was thawed on ice and 50 $\mu$ L of the cells was transferred to a single tube for each transformation. A 2.5 $\mu$ L aliquot of the plasmid solution (containing 10ng of DNA) was then added to the cells in the tube. The tubes were incubated on ice for 30 minutes, heated to 42°C for 30 seconds, and then returned to the ice for 2 minutes. LB broth (950 $\mu$ L) was added to each tube, and then the tubes were incubated at 37°C with shaking (225rpm in an orbital shaker) for 1 hour.

### 2.5.3.1 Selection of successfully transformed *E. coli* DH5 $\alpha$

Selective agar plates were used to isolate successfully transformed *E. coli* DH5 $\alpha$  colonies. prV1b-R-, pALTER-MAX- and un-transformed cells were plated onto LB agar plates containing chlormaphenicol at 20 $\mu$ g/mL of agar. pUC19-transformed cells were plated onto plates containing ampicillin at 100 $\mu$ g/ml of agar. Aliquots of 20 $\mu$ L, 100 $\mu$ L and 200 $\mu$ L of the cells were transferred to the appropriate agar plates and then spread using a flamed sterile glass spreader. The plates were incubated at 37°C for approximately 16 hours.

The efficiency of transformation of the *E. coli* DH5 $\alpha$  competent cells was calculated using the following formula as suggested by the supplier of the pUC19 plasmid (Invitrogen):

$$\frac{\text{\# colonies on the pUC19 plate}}{250\text{pg DNA used for transformation}} \times \frac{1000\mu\text{L}}{100\mu\text{L plated into selective plates}} \times 10^6 \text{ pg}/\mu\text{g}$$

A total of approximately 42 colonies were counted on a single selective plate for pUC19 giving a transformation efficiency of  $1.7 \times 10^6$  transformants per  $\mu$ g of pUC19 DNA. This exceeds the acceptable transformation efficiency (ie.  $1 \times 10^6$  transformants per  $\mu$ g of pUC19 DNA) given by the supplier of the *E. coli* DH5 $\alpha$  competent cells (Invitrogen).

### 2.5.3.2 Culture of transformed *E. coli* DH5 $\alpha$

A single colony of successfully transformed cells was collected from a selective plate using a sterile loop. This was used to inoculate 3mL of LB broth. This starter liquid culture was incubated at 37°C for approximately 18 hours with shaking (250rpm in an orbital shaker). For large scale preparation of the plasmids a bulk culture of the transformed *E. coli* DH5 $\alpha$  was then generated. A 200 $\mu$ L aliquot from a starter liquid culture was used to inoculate 100mL of LB broth. This was incubated at 37°C for approximately 16 hours with vigorous shaking (300rpm in an orbital shaker).

A 200 $\mu$ L aliquot of the starter or bulk culture was used to make glycerol stocks of the transformed *E. coli* DH5 $\alpha$ . The procedure used to make glycerol stocks was based on methods described by Sambrook, Fritch and Maniatis (Sambrook et al., 1989). The cell suspension was diluted 5-fold



with glycerol and the mixture was frozen immediately in a dry ice/ethanol bath. The glycerol stocks were stored at -80°C and used as required for further plasmid preparations. To do this, a flamed loop was used to scrape the surface of the culture while still frozen. The collected cells were then used to streak a new selective plate in a zig zag manner so that individual colonies could be collected to start a new culture.

For all bacterial culture procedures aseptic conditions were maintained. All glassware used was sterilized either by autoclave (20 minutes, 121°C, 20 lb/in<sup>2</sup>) or in a dry oven (2 hours, ≥170°C). All plasticware used was also sterile. All solutions used were either autoclaved as above or filter sterilized (see appendix B for details). Culture media, such as selective agar plates and LB broth, were also pre-warmed to 37°C prior to use.

## **2.5.4 Analysis of Plasmid DNA**

### **2.5.4.1 Restriction digest**

The plasmid DNA solutions were analysed by carrying out a restriction digest using the restriction enzyme Xho1, followed by gel electrophoresis. As shown in Figure 2.3 Xho1 has a single restriction site in the vector pALTER-MAX. There are no restriction sites for Xho1 in the rat V1b-R sequence (determined using the web-based software NEB cutter). Therefore the enzyme Xho1 was a “single cutter” of the plasmids pALTER-MAX and prV1b-R, and restriction digest of the circular plasmid with this enzyme resulted in a single fragment of linear DNA. This allowed the identification of the plasmid based on its size which was estimated by comparison with a DNA ladder (lambda DNA cut with Eco RI and HinDIII) (Figure 2.4).

Restriction digests contained 2µL Xho1 enzyme, 1µL of restriction enzyme-specific buffer (1x), 2-5µL of plasmid DNA solution, made up to 10µL with sterile ddH<sub>2</sub>O. The tube was then centrifuged briefly to combine the reagents, and incubated at 37°C overnight (approximately 18 hours).

#### 2.5.4.2 Gel electrophoresis

Restriction digestion products and un-digested DNA were separated by electrophoresis through a 0.8% agarose/1xTBE gel (see Appendix B for details) using an EASY-CAST gel tank (Owl Scientific, Inc.) and a Gibco BRL electrophoresis power supply (Life Technologies). A 10 $\mu$ L aliquot of the DNA sample was combined with 2 $\mu$ L of gel loading dye (see Appendix B for details) then loaded onto the gel. The gel was run at 80V (approximately 45mA) for 80 minutes in Tris Borate EDTA running buffer (see Appendix B for details). The gels were stained with ethidium bromide (0.5g/mL in ddH<sub>2</sub>O) for 20 minutes and the DNA was visualized by UV illumination at 300nm and photographed (UltraLum gel documentation system, SciTech).

#### 2.5.4.3 Spectrophotometric analysis of plasmid DNA

The plasmid DNA concentration was estimated using a ND1000 NanoDrop spectrophotometer. TE8 was used to zero the spectrophotometer prior to reading each sample, and 1 $\mu$ L of the DNA sample was then used to read the concentration of DNA (ng/ $\mu$ L). The absorbance ratios 260/280 and 360/230 were also recorded for each DNA sample, as these values indicate the purity of the DNA.

#### 2.5.5 Alkali lysis preparation of plasmid

From the starter liquid culture a small scale preparation of the plasmid was carried out using the alkali lysis method. This method provided a quick and simple way to ensure that the plasmid of interest had been purified before carrying out a large scale preparation of plasmid DNA. The alkali lysis procedure used was based on the method described by Sambrook, Fritch and Maniatis (Sambrook et al., 1989).

For plasmid preparation 1.5mL of culture was removed from a liquid starter culture of transformed *E. coli* DH5 $\alpha$  and transferred to a new tube. This was then centrifuged at 12,000 g for 30 seconds

at 4°C. The supernatant was removed by aspiration. The cell pellet was then suspended in 100µL of ice-cold “solution I” (see appendix B for details) by vigorous vortexing. A 200µL aliquot of “solution II” was then added and the tube was inverted to mix until a clear solution was achieved. 150µL of “solution III” was then added and the mixture was gently vortexed to mix. The mixture was incubated on ice for 5 minutes, and then centrifuged at 12,000 g for 2 minutes at 4°C. The DNA was then precipitated from the supernatant by the addition of 2 volumes of 100% ethanol. This was incubated at room temperature for 2 minutes, and then centrifuged at 12,000 g for 5 minutes at 4°C. The pellet was washed with 1mL of 70% ethanol, and centrifuged as before. Following removal of the supernatant the pellet was allowed to air dry for 5 minutes and then dissolved in 50µL of TE8 (with RNAase at 20µg/mL).

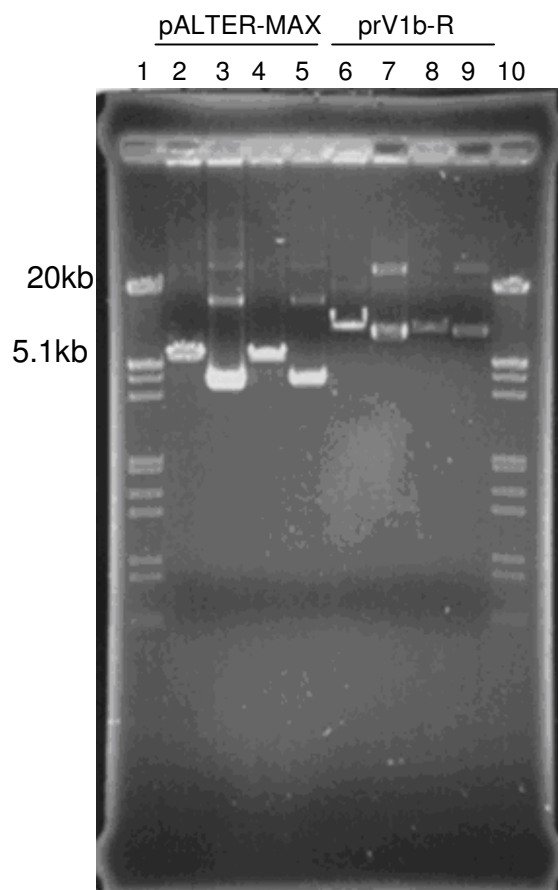


**Figure 2.4. Gel electrophoresis of prV1b-R (lanes 2-5) and pALTER-MAX (lanes 6-9) plasmid DNA.** The plasmid DNA was purified using the alkali lysis method. DNA samples in even numbered lanes (2, 4, 6 and 8) have been digested with the restriction enzyme Xho1. DNA samples in odd numbered lanes (3, 5, 7 and 9) were undigested. The ladder (lanes 1 and 10) is lambda DNA cut with Eco RI and HindIII.

Plasmid DNA solutions from this preparation were analysed by carrying out a restriction digest followed by electrophoretic separation on a 0.8% agarose gel (as described in section 2.5.4) (Figure 2.4). As expected, electrophoretic separation of the undigested plasmid (lanes 3, 5, 7, and 9 of Figure 2.4) gave two bands on a gel, representing the relaxed and supercoiled forms of the circular plasmid. In lanes 3 and 5 a third faint band (closest to the origin) is visible. It is most likely that this band is degraded DNA. DNA samples that had been digested by the enzyme XhoI gave a single band on the gel (lanes 2, 4, 6 and 8). The positions of these bands in relation to the ladder (lambda DNA cut with Eco RI and HindIII) gives some indication of the size of the vector and plasmid. This ladder is not ideal as the resolution is poor for DNA greater than 5kb. However, the gel confirmed the presence of a plasmid close to the expected size for both prV1b-R (8.2kb) and pALTER-MAX (5.5kb). The DNA concentration obtained from the alkali lysis preparation was  $61.2 \pm 0.2 \text{ ng}/\mu\text{L}$  for pALTER-MAX (n=2) and  $189.4 \pm 36.1 \text{ ng}/\mu\text{L}$  (n=4) for prV1b-R.

### **2.5.6 Large scale preparation of plasmid**

An entire bulk liquid culture (100mL) was used to carry out a large scale preparation of the plasmids prV1b-R and pALTER-MAX using a Qiagen Plasmid Maxi kit. This method of preparation gives highly purified plasmid DNA for use in transfection. The protocol recommended by Qiagen was used for this procedure. The Qiagen plasmid DNA extraction protocols are based on a modified alkali lysis procedure, followed by purification of the DNA using Qiagen anion-exchange resin.

First the cells were pelleted by centrifugation at 6000rpm (Sorvell centrifuge using a GSA rotor) for 15 minutes at 4°C. The DNA was then extracted by the sequential addition of 10mL each of the following kit solutions: P1 (resuspension buffer), P2 (lysis buffer) and P3 (neutralisation buffer). The solutions are similar in composition to those used for the alkali lysis preparation (see section 2.5.5 above and Appendix B for details). The lysate was incubated on ice for 20 minutes, and then centrifuged at 13000rpm (Sorvell centrifuge using an SS-34 rotor) for 30 minutes at 4°C. The supernatant was transferred to a fresh pre-equilibrated (using 10mL of kit solution QBT) Qiagen anion-exchange column. The column was washed twice with 30mL of kit solution QC (wash

buffer), and then 15mL of kit solution QF (elution buffer) was used to elute the DNA. The DNA was precipitated from the solution using 5mL of 70% ethanol and pelleted by centrifugation at 13,000rpm (Sorvell centrifuge using an SS-34 rotor) for 10 minutes at 4°C. The pellet was allowed to air dry for approximately 10 minutes, and DNA was then resuspended in 1mL of TE8.

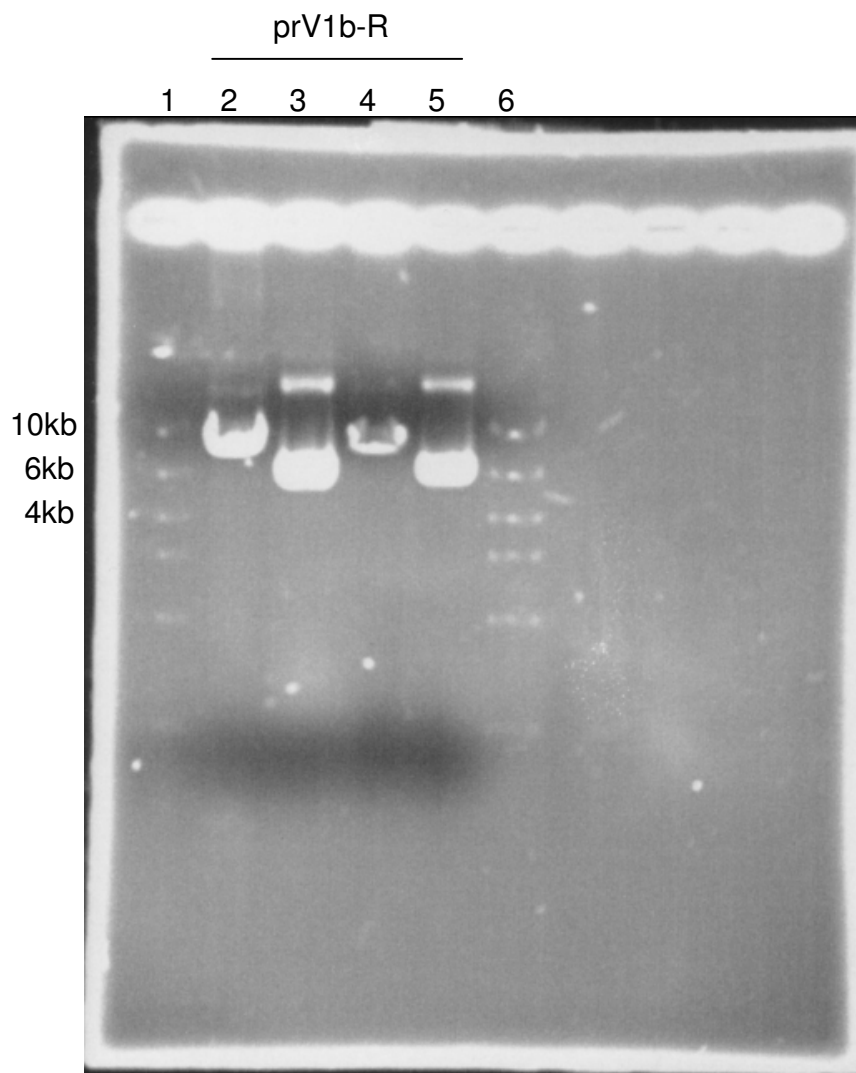


**Figure 2.5. Gel electrophoresis of prV1b-R (lanes 2-3) plasmid DNA from a large scale preparation using the Qiagen Plasmid Maxi kit.** DNA samples in even numbered lanes (2 and 4) have been digested with the restriction enzyme Xho1. DNA samples in odd numbered lanes (3 and 5) were un-digested. The ladder (lanes 1 and 6) is a High Mass DNA ladder (Gibco).

The resulting plasmid DNA solutions were analysed by carrying out a restriction digest using Xho1, followed by gel electrophoresis (Figure 2.5 shows the results for a single preparation of prV1b-R). From the gel, the size of the digested plasmid (lanes 2 and 4) was estimated by comparison with a suitable DNA ladder (High Mass DNA ladder from Gibco). The ladder appears faint in the image below (Figure 2.5) due to the high DNA concentration in the samples. The bands for prV1b-R (8.2kb) (Figure 2.5) and pALTER-MAX (5.5kb) (results not shown) appeared to be approximately the expected size indicating that the desired plasmid was present. The DNA concentration was 297.9ng/μL for pALTER-MAX and 333.9ng/μL for prV1b-R. The 260/280 and 260/230 readings for these samples were above 1.8, which indicates that a good level of purity was achieved (ie. protein and/or carbohydrate contamination of the samples was very low).

## 2.6 PROTEIN QUANTITATION

The Pierce® BCA protein assay kit was used for the colorimetric detection and quantitation of total cellular protein. This method combines reduction of  $\text{Cu}^{2+}$  to  $\text{Cu}^{1+}$  by protein in an alkaline medium (the biuret reaction) with detection of  $\text{Cu}^{1+}$  using a unique reagent called bicinchoninic acid (BCA) (Smith et al., 1985). A purple-coloured reaction product that exhibits a strong absorbance at 562nm is formed. The change in absorbance is nearly linear with increasing protein concentrations over the range of 20-2000μg/mL. The protein concentrations determined using this kit were reported with reference to a standard protein, bovine serum albumin (BSA). A series of dilutions of known BSA concentration were prepared and assayed alongside unknowns and the concentration of each unknown was determined based on the standard curve.

The BCA protein quantitation assay will be used to determine the total cellular protein of cells wherever data needs to be normalised by expressing relative to an indicator of cell number. In this way, variables can be expressed per mg of total cellular protein. HEK293 cells were plated at a density of  $1.75 \times 10^5$  cells/well into a 24-well plate so that a confluence of 80-90% confluence was

reached approximately 20 hours after plating. Cells were then lysed with 0.1M NaOH. The lysate was frozen at -20°C for up to 2 months prior to protein quantitation. The Pierce® BCA protein quantitation assay was carried out according to the supplier's instructions. Two procedures were tested: the "room temperature protocol" and the "enhanced protocol".

### **2.6.1 Room temperature protocol for protein quantitation**

In initial experiments, the total cellular protein was determined using the "room temperature" method. BSA protein standards were prepared by diluting the stock BSA (2000µg/mL) with lysis buffer (0.1M NaOH) to give the following concentrations: 2000, 1500, 1000, 750, 500, 250, 125, 25 and 0µg/mL. For each reaction, 0.1mL of the standard or unknown sample was mixed with 2mL of the working reagent (WR, see Appendix B for details). Each unknown was assayed both undiluted and diluted 1/10 with lysis buffer, and each assay was prepared in duplicate (n=2). For the room temperature method the samples were incubated at room temperature (approximately 22°C) for 2 hours. The absorbance of each standard and sample at 562nm was measured using a Shimadzu UV-1601PC spectrophotometer (distilled water was used as the blank).

To analyse the results of the assay a standard curve for BSA was generated. Firstly, the absorbance at 562nm of the blank standard (0µg/mL BSA) was subtracted from the absorbance of all standards. This blank-corrected absorbance was then plotted against the concentration of BSA in the standards (Figure 2.6). According to the instructions that were supplied with the kit a best-curve fit provides more accurate results than a linear fit. GraphPad Prism® graphing software was used to plot the graph, and draw the curve of best fit. The standard curve was then used to estimate the protein concentration for two unknowns (Table 2.6) as follows.

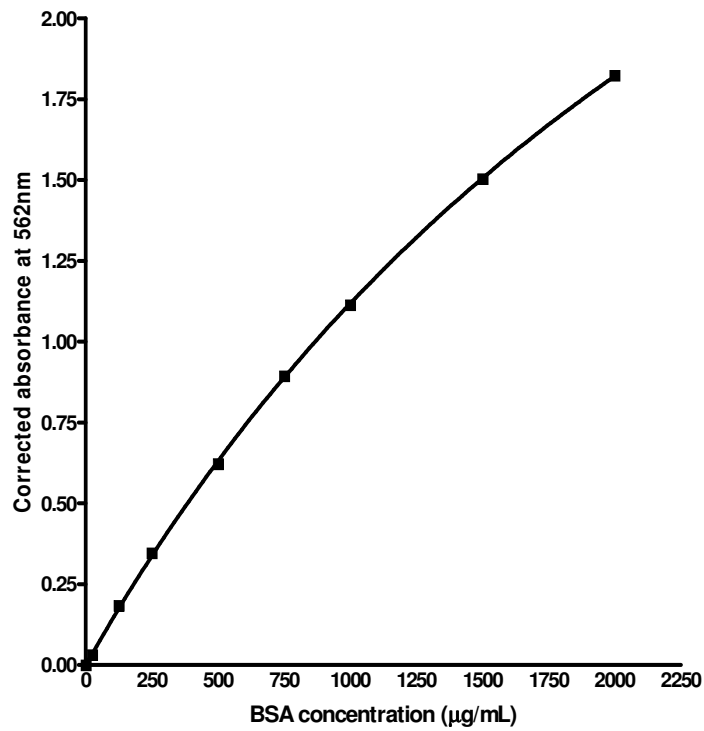


Figure 2.6. BSA standard curve generated using the “room temperature” method for the determination of protein concentration in unknown samples.

**Table 2.6. Quantitation of total cellular protein for two cell lysates (unknowns 1 and 2) using the BCA protein assay “room temperature” protocol.** The assay was performed with either undiluted or 1/10 diluted sample (n=2 for each assay). Using the average corrected absorbance of the samples the protein concentration was estimated from the BSA standard curve (Figure 2.6).

Sample ID	Sample dilution factor	Average corrected absorbance $\pm$ SEM	Protein concentration ( $\mu\text{g/mL}$ )
Unknown 1	Undiluted	$0.218 \pm 0.002$	218.2
Unknown 1	1/10	$0.0215 \pm 0.003$	24.2
Unknown 2	Undiluted	$0.225 \pm 0.001$	227.7
Unknown 2	1/10	$0.021 \pm 0.001$	24.2



The absorbance at 562nm of the blank standard (0µg/mL BSA) was subtracted from the absorbance of each individual unknown sample replicate, giving the corrected absorbance. The average corrected absorbance was then calculated and GraphPad Prism® software was used to determine the protein concentration from the BSA standard curve (Figure 2.6). Using the room temperature protocol for the BCA assay the protein concentrations of the undiluted samples were 218.2µg/mL for unknown 1, and 227.7µg/mL for unknown 2. These values are low compared to the majority of the BSA standard concentrations. In this situation a different protocol, referred to as the “enhanced protocol”, can be used to improve the accuracy of protein quantitation at low concentrations (<250µg/mL).

### **2.6.2 Enhanced protocol for protein quantitation**

The “enhanced protocol” was carried out according to the protocol provided with the kit. BSA protein standards were prepared by diluting the stock BSA (2000µg/mL) with lysis buffer (0.1M NaOH) to give the following concentrations: 250, 125, 50, 25, 5 and 0µg/mL. The BCA assay was then setup as described above for the room temperature protocol and the same two unknowns were used. Each unknown was assayed using samples diluted with lysis buffer (0.1M NaOH) as follows: undiluted, 1:2 and 1:5. For the enhanced temperature method the samples were incubated for 30 minutes at 60°C with gentle shaking in an Eppendorf Thermomixer. The tubes were then transferred to ice and the absorbance of each standard and sample at 562nm was measured immediately. A standard curve was generated (Figure 2.7) and the protein concentration of the unknowns was determined from the curve (Table 2.7) using the methods described above (section 2.6.1).

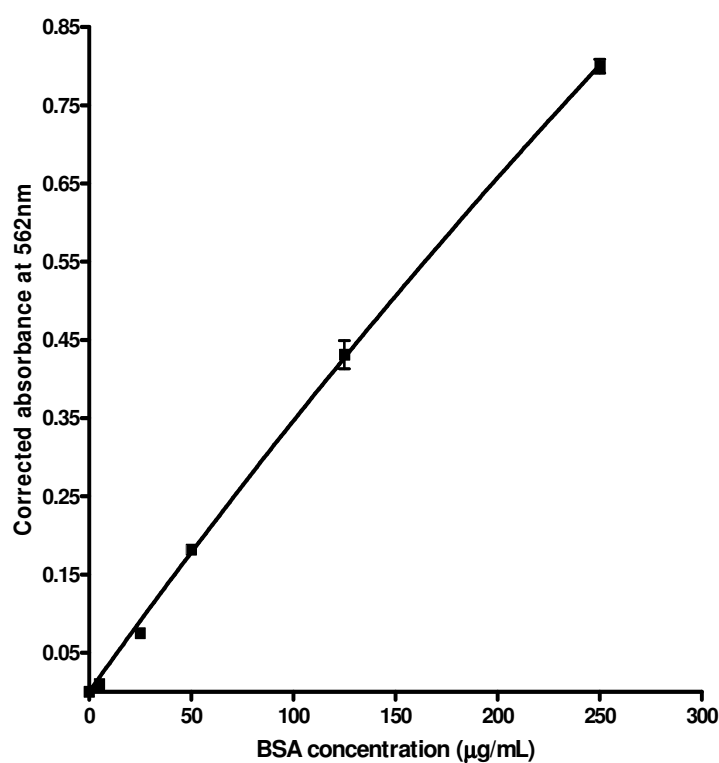


**Figure 2.7** BSA standard curve generated using the “enhanced” protocol for the determination of the protein concentration in unknown samples.

**Table 2.7** Quantitation of total cellular protein for two cell lysates (unknowns 1 and 2) using the BCA protein assay “enhanced protocol”. The assay was performed with undiluted, 1/2 and 1/5 diluted sample (n=2 for each assay). Using the average corrected absorbance of the samples the protein concentration was estimated from the BSA standard curve (Figure 2.7).

Sample ID	Sample dilution	Average corrected absorbance $\pm$ SEM	Protein concentration ( $\mu\text{g/mL}$ )
Unknown 1	Undiluted	$0.555 \pm 0.002$	171.4
Unknown 1	1/2	$0.317 \pm 0.005$	97.9
Unknown 1	1/5	$0.123 \pm 0.001$	39.0
Unknown 2	Undiluted	$0.563 \pm 0.013$	174.0
Unknown 2	1/2	$0.314 \pm 0.009$	96.0
Unknown 2	1/5	$0.114 \pm 0.005$	34.5

Comparison of the room temperature method (Table 2.6) and the enhanced temperature method (Table 2.7) revealed that by increasing the temperature of the incubation, the net absorbance of the two unknowns was increased. This decreased both the minimum detection level and also the working range of the assay (ie. 0-250 $\mu$ g/mL for the “enhanced” protocol vs. 0-2000 $\mu$ g/mL for the “room temperature” protocol). Therefore, protein concentrations <250 $\mu$ g/mL were more accurately determined using the enhanced protocol. Using the enhanced temperature method the protein concentrations of the undiluted samples were 171.4 $\mu$ g/mL for unknown 1 and 174.0 $\mu$ g/mL for unknown 2.

The protein concentrations of the diluted samples were as follows: 1/2 diluted samples were 97.9 $\mu$ g/mL for unknown 1 and 96.0 $\mu$ g/mL for unknown 2; 1/5 diluted samples were 39.0 $\mu$ g/mL for unknown 1 and 34.5 $\mu$ g/mL for unknown 2. After correction for the dilution, these values gave protein concentrations of 195.0 $\mu$ g/mL or 195.8 $\mu$ g/mL for unknown 1, and 172.5 $\mu$ g/mL or 192.0 $\mu$ g/mL for unknown 2. In general, these values are slightly higher than those determined using undiluted samples. Despite this, the diluted samples are a useful way to check the reproducibility of the results across a range of protein concentrations and should be included for future assays. The method described here can be used to accurately quantify the total cellular protein of HEK293 cells.

## **2.7 TRANSFECTION**

HEK293 cells were transfected with the purified plasmid prV1b-R (described in section 2.5.1) so that they expressed the V1b-R. For transient expression of the receptor (<7 days) in fast growing adherent cell lines, such as HEK293, transfection with a lipid-based transfection reagent is recommended (Cupo, 1999). Transiently transfected HEK 293 cells have previously been used by the Lefkowitz group to look at the involvement of GRKs in signalling by the angiotensin II receptor (Kim et al., 2005; Wei et al., 2003) and the V2 vasopressin receptor (Ren et al., 2005). In

each of these papers HEK293 cells were transiently co-transfected with the both the receptor of interest, and siRNA, using the transfection reagent GeneSilencer. For this study a similar lipid-based transfection reagent, Lipofectamine<sup>TM</sup> 2000 (LF2000) from Invitrogen, was used. LF2000 is widely used for the transfection of DNA and RNA, and transfects HEK293 cells with high efficiency in both 96-well (Pichet and Ciccarone, 1999a) and 24-well plate format (Roy et al., 1999) resulting in high levels of recombinant protein expression.

LF2000 was used for this study because plasmid and siRNA co-transfection is also possible with this reagent. Co-transfections have been tested by the manufacturer (Invitrogen) using LF2000 with GripTite (HEK293 derived) cells plated at  $1.8 \times 10^5$  cells/well in a 24-well plate (0.5mL medium per well). They co-transfected 200ng of two different reporter plasmids with 10pmol of siRNA, using 2 $\mu$ L LF2000 per well (Invitrogen LF2000 transfection reagent, product notes). The total volume of the transfection mixes was 100 $\mu$ L, and was added to medium in the wells.

The plasmid transfection procedure used for the study reported here (see section 3.8.1 below) was based on the co-transfection procedure described above. Use of LF2000 and similar transfection procedures at this stage for plasmid-only transfection should facilitate the development of a co-transfection protocol (ie. plasmid plus siRNA) when RNAi experiments are carried out in future.

### **2.7.1 Transfection of HEK293 with plasmid DNA**

For transfection, HEK293 cells in MEM + HIHS (no P/S) were plated at a density of  $1.25 \times 10^5$  cells/0.5mL/well in a 24-well plate and cultured for 20 hours in 95% air: 5% CO<sub>2</sub> at 37°C. The cell confluence was typically 60-80% at the time of transfection. The transfection mixture was prepared using the instructions provided by the supplier (Invitrogen). Table 1 shows the volumes of LF2000, plasmid DNA (prV1b-R or pAlter) and OptiMEM (reduced serum medium) used for the transfection of a single well of a 24-well plate. These volumes were selected based on results of transfection optimisation using the inositol phosphate assay (see chapter 3) and were used for all transfections unless otherwise specified.

**Table 2.8. Volumes of reagents used for plasmid (prV1b-R or pAlter) transfection of HEK293 cells.** The volumes of OptiMEM (reduced serum medium), Lipofectamine 2000 (LF2000) and plasmid DNA shown are for the transfection of a single well of a 24-well plate. For the plasmids prV1b-R and pAlter, the appropriate volume of plasmid solution was added to give 0.8µg of DNA.

Transfection	OptiMEM	LF2000	prV1b-R DNA (334ng/µL)	pAlter DNA (298ng/µL)
prV1b-R	100µL	1.6µL	2.4µL	-
pAlter	100µL	1.6µL	-	2.7µL

For one well, 2µL of LF2000 reagent was diluted with 50µL of the OptiMEM, and the mix was incubated at room temperature for 5 minutes. During this time the volume of plasmid solution required to give 0.8µg of DNA (see Table 2.8) was diluted with 50µL OptiMEM in a separate tube. At the end of the 5 minute incubation, the contents of the two tubes were combined and the mixture was incubated at room temperature to allow formation of transfection complexes. 104µL of the transfection mix was then added to each well containing the cells and medium. The cells were incubated in a CO<sub>2</sub> incubator at 37°C for 5-6 hours before removal of the medium. Any experimental procedures involving characterisation of the V1b-R, such as the inositol phosphate assay, were carried out >18 hours after the transfection reagents were added.

## 2.8 DATA ANALYSIS

### 2.8.1 Analysis of IP assay results

The IP response of cells to agonist stimulation can be expressed in a number of ways; as an absolute value by comparison with [<sup>3</sup>H]IP<sub>3</sub> standards (Neill et al., 1998), or expressed relative to control as either a percentage (Freedman et al., 1997; Gaudreau et al., 2002) or fold increase (Liu and Wess, 1996). For this study the [<sup>3</sup>H]IP production was expressed as a percentage of control. The CPM value of each sample determined by scintillation counting was used for calculations. For an example of how the IP response was calculated see Table 2.9 below.

**Table 2.9. Data analysis for two representative experiments (n=2), with each treatment performed in duplicate.** Cells were treated with either 100nM or 0nM AVP (un-stimulated control) for 15 minutes in the presence of 10mM LiCl.

	AVP treatment (nM)	CPM <sub>1</sub>	CPM <sub>2</sub>	Mean CPM	% <sub>1</sub>	% <sub>2</sub>	Mean %
<b>Experiment A</b>	0	596.7	578.1	587.40	101.6	98.4	100.0
	100	1042.2	1573.7	1307.95	177.4	267.9	222.7
<b>Experiment B</b>	0	337.1	262.7	299.90	112.4	87.6	100.0
	100	769.1	879.2	824.15	256.5	293.2	274.8

	AVP treatment (nM)	Overall Mean %	SEM (%)
<b>Experiments A and B</b>	0	100.0	5.1
	100	248.7	25.0

Microsoft Excel was used for data analysis. “CPM<sub>1</sub>” and “CPM<sub>2</sub>” represent the CPM value from two wells (equivalent treatments) determined using scintillation counting. Each CPM result was normalised to the control (0nM AVP treatment) using the following equation:

$$\text{percentage response (eg. \%}_1\text{)} = \frac{\text{each CPM value (eg. CPM}_1\text{)}}{\text{mean CPM for the control}}$$

The results from the two experiments, A and B (performed on different days), were then combined. The “overall mean %” represents the IP response relative to the control (defined as 100%). The standard error of the mean (SEM) was determined using the %<sub>1</sub> and %<sub>2</sub> values. The IP response (% of control) was then displayed histogram (for examples see Gaudreau et al., 2002; for examples see Gaudreau et al., 1998) where appropriate.

For desensitisation experiments cells were exposed to an AVP pre-treatment, and the IP response of the cells to a subsequent AVP treatment (“test” treatment) was determined. For an example of data analysis for this type of experiment see Table 2.10 below. The stimulated increase (ie. stimulated increase<sub>1</sub> and stimulated increase<sub>2</sub>) relative to the control (0nM AVP<sub>test</sub> treatment) was calculated using the following equation:

$$\text{Stimulated increase (eg. stimulated increase}_1\text{)} = \text{mean CPM for the control} - \text{each CPM value (eg. CPM}_1\text{)}$$

The “mean stimulated increase” was calculated for the control (pre-treated with 0nM AVP) and pre-treated (pre-treated with 5nM AVP). The percentage response ( $\%_1$  and  $\%_2$ ) was then calculated using the following equation:

$$\text{percentage response (eg. } \%_1) = \frac{\text{each stimulated increase value (eg. stimulated increase}_1)}{\text{mean stimulated increase for the control}}$$

The “overall mean %” and SEM were calculated as described above. The “overall mean %” represents the IP response below basal (pre-treated with 0nM AVP) and is relative to the control (defined as 100%).

**Table 2.10. Data analysis for two representative desensitisation experiments (n=2), with each treatment performed in duplicate.** Cells were pre-treated with 5nM or 0nM AVP for 5 minutes (no LiCl), and then exposed to a subsequent treatment (test) with 100nM or 0nM AVP (un-stimulated control) for 15 minutes in the presence of 10mM LiCl.

	Protocol	AVP <sub>pre-treatment</sub> (nM)	AVP <sub>test</sub> (nM)	CPM <sub>1</sub>	CPM <sub>2</sub>	Mean CPM
<b>Experiment A</b>	Control	0	0	449.0	562.5	505.8
		0	100	1060.4	940.5	1000.5
	Pre-treated	5	0	602.5	468.5	535.5
		5	100	990.4	708.4	849.4
<b>Experiment B</b>	Control	0	0	250.0	241.0	250.0
		0	100	774.0	860.0	817.0
	Pre-treated	5	0	280.2	357.9	319.1
		5	100	783.3	673.4	728.4

	Protocol	Stimulated increase <sub>1</sub>	Stimulated increase <sub>2</sub>	Mean stim. increase	$\%_1$	$\%_2$	Mean %
<b>Experiment A</b>	Control	554.6	434.7	494.7	112.1	87.9	100.0
	Pre-treated	454.9	172.9	313.9	92.0	35.0	63.5
<b>Experiment B</b>	Control	525.8	614.5	570.2	92.2	107.8	100.0
	Pre-treated	464.2	354.3	409.3	81.4	62.1	71.8

	Protocol	Overall Av. %	SEM (%)
<b>Experiments A and B</b>	Control	100.0	5.9
	Pre-treated	67.6	12.5

## 2.8.2 Analysis of qRT-PCR results

Results were analysed using the software provided with the Stratagene Mx3005P<sup>TM</sup> real time PCR system and Microsoft Office Excel. The Mx3005P<sup>TM</sup> software readout includes an amplification curve and dissociation curve for each sample assayed. The PCR amplification curve charts the accumulation of fluorescent emission (expressed as dR, baseline-corrected raw fluorescence) at each reaction cycle. The curve can be broken into four different phases; the linear ground, early exponential, log-linear, and plateau phases. Data gathered during these phases enabled calculation of the cycle threshold (Ct) and amplification efficiency which were later used to calculate the relative GRK5 expression in different complementary (cDNA) samples.

The Ct represents the cycle number at which the fluorescence rises above a “chosen” threshold. An appropriate threshold was calculated by the PCR instrument depending upon the baseline fluorescence (default settings were not altered). To get accurate results this threshold must intersect the exponential phase of the individual amplification plots (Bustin and Nolan, 2004). If the Ct values were very high (>35), the fluorescence (dR) was often very low which resulted in a poorly defined exponential phase. Therefore, only Ct values <35 were used for analysis.

The relative expression of GRK5 was determined using the comparative Ct method. This mathematical model is a form of relative quantitation used to calculate changes in gene expression as a relative fold difference from a reference sample (Wong and Medrano, 2005). This method uses the Ct value for each sample and includes a correction for the amplification efficiency (Livak and Schmittgen, 2001). The amplification efficiency for each primer pair was determined by generating a standard curve using serial dilutions of the template cDNA. From the standard curve the amplification efficiency was calculated automatically by the Mx3005P<sup>TM</sup> software using the following formula (Rasmussen, 2001):

$$\text{Amplification efficiency} = [10^{(1-\text{slope})}] - 1$$

For a single qPCR run each cDNA sample was assayed using primers specific for GRK5, and the two reference genes  $\beta$ -actin and 18S ribosomal RNA (rRNA). Each reaction was performed in duplicate and the mean Ct of the duplicates (referred to simply as Ct in subsequent sections of this



report) was used for all further calculations. To account for differences in the amount and quality of total cDNA added to the reaction, the data for GRK5 was normalised to the reference genes  $\beta$ -actin and 18S rRNA. The change in Ct (dCt) for each cDNA sample was calculated by subtracting the mean Ct from each individual Ct value (data for each reference gene was calculated separately). The mean dCt of the two reference genes was then calculated for each cDNA. The GRK5 data was normalised by adding the mean dCt of the reference genes to the Ct for GRK5 (for each cDNA).

The following equation was then used to correct the GRK5 data based on the amplification efficiency of the GRK5 primer pair:

$$\text{GRK5 expression} = (\text{Amplification efficiency})^{\text{Ct}}$$

The GRK5 expression in different cDNA samples was expressed as a fold difference. Expression data from different qPCR runs were combined and plotted on a histogram (Metaye et al., 2002).

The qRT-PCR products were also analysed by gel electrophoresis to confirm the presence of a single band of the expected size for each primer pair. PCR products were separated through a 1% agarose/1 x TAE gel as described (section 4.2.6.2).

### **2.8.3 Statistical analysis**

Microsoft Excel and GraphPad Prism 4 were used for statistical analysis. For IP response data statistical significance of values expressed as percentages of control/un-stimulated release were determined by constructing confidence intervals (CI) for each experimental mean as described previously (LeBeau, 1998; Mason et al., 1994). A particular value was determined as being significant, at the level stated, if the value representing control (100%) did not fall within the CI. Significance of comparisons between experimental means was determined by the Student's *t*-test or one-way ANOVA. P values less than 0.05 ( $P < 0.05$ ) were considered significant.

### 3

## **DEVELOPMENT OF A MODEL SYSTEM TO OBSERVE DESENSITISATION OF THE PITUITARY VASOPRESSIN RECEPTOR: V1b-R**

### **3.1 INTRODUCTION**

Ligand binding to the V1b-R activates the phosphoinositide signalling pathway, resulting in the cleavage of phosphatidylinositol 4,5-bisphosphate (PIP<sub>2</sub>) to generate the second messengers inositol 1,4,5-triphosphate (IP<sub>3</sub>) and diacylglycerol (DAG). Desensitisation can therefore be detected as a reduction in IP<sub>3</sub> production in response to AVP, following prior exposure to AVP. The IP<sub>3</sub> production can be measured using the inositol phosphate assay (IP assay, also referred to as the phosphoinositide hydrolysis assay) (Tobin, 1997). Following its synthesis IP<sub>3</sub> is sequentially de-phosphorylated generating inositol 1,4-bisphosphate (IP<sub>2</sub>), inositol 1-phosphate (IP<sub>1</sub>), and finally free inositol (Berridge et al., 1983). Free inositol rejoins DAG and ultimately PIP<sub>2</sub> is regenerated. Lithium (Li<sup>+</sup>) blocks the action of inositol monophosphatase so that IP<sub>1</sub> cannot be converted into inositol. Thus, in the presence of Li<sup>+</sup> the inositol phosphate metabolites (IPs, ie. IP<sub>3</sub>, IP<sub>2</sub> and IP<sub>1</sub>) accumulate in the cell (Berridge et al., 1982). The IPs can then be separated from water soluble cell extracts using anion-exchange chromatography as described previously (Downes and Michell, 1981). Prior labelling of the cells with *myo*-[<sup>3</sup>H]inositol, allows the labeled inositol phosphate metabolites ([<sup>3</sup>H]-IPs) to be counted using a scintillation counter (Berridge et al., 1983).

The IP assay can be used to assess desensitisation of any PLC-coupled GPCR signaling in an intact cell system. For example, this method has recently been used to investigate desensitisation of the

human serotonin receptors (Berg et al., 2001), the rat neurotensin receptor (Hermans and Maloteaux, 1996) and the type 1A Angiotensin II receptor (Franca et al., 2003; Tang et al., 1998) using intact CHO cells as a model system. This method has also been used to study desensitisation of the endothelin receptors (Freedman et al., 1997) and the type 1A Angiotensin II receptor (Oppermann et al., 1996) using intact HEK293 cells. The IP assay can also be used to assess the role of GRKs in mediating GPCR desensitisation (Pitcher, 1998). For example, analysis of metabotropic glutamate 1A receptor signaling using the IP assay provided evidence that GRK2 mediates desensitisation of this receptor in HEK293 cells (Dale et al., 2000). The characteristics of the IP response differ for each of the above mentioned studies. Both the time course of IP production (Hermans and Maloteaux, 1996; Tang et al., 1998) and the magnitude of the IP response depend on the experimental system under study. In fact, the same receptor can have different IP responsiveness in different cell types. This may be due to differing levels of receptor expression, and may also depend upon the size and/or rate of recycling of the PIP<sub>2</sub> pool in different cell types (Forrest-Owen et al., 1999). It is therefore necessary to optimise the IP assay for the investigation of V1b-R desensitisation in the cellular system under study.

This research involved the development of a model system that could be used to assess the involvement of GRK5 in desensitisation of the V1b-R using RNAi. The use of RNAi methodology dictated that a primary culture of pituitary corticotrophs could not be used for this research. Thus, a model system that used V1b-R-transfected HEK293 cells was developed. HEK 293 cells (transiently transfected with the GPCR of interest) have previously been used by the Lefkowitz group to look at the involvement of GRKs in signalling by the angiotensin II receptor (Kim et al., 2005; Wei et al., 2003) and the V2 vasopressin receptor (Ren et al., 2005). An advantage of using HEK 293 cells for this research is that the genetic sequence of human GRKs are known, and siRNAs for these GRKs have been designed and used by Lefkowitz's group to specifically silence GRKs in these cells. In this chapter, the development and optimisation of methods needed to observe desensitisation in V1b-R-transfected HEK293 cells using the inositol phosphate assay is reported. The final protocol for observing desensitisation using this model system, along with a summary of the aspects investigated during the development of the protocol, is given in section 3.5 at the end of this chapter.

## **3.2 STANDARD METHODS AND MATERIALS**

### **3.2.1 Materials**

For the sources of all materials used in this study, refer to Appendix A.

### **3.2.2 Solutions and media**

For the details of all solutions and media used in this study, refer to Appendix B.

### **3.2.3 Steps of the inositol phosphate assay**

The IP assay invariably involves the following major steps; labeling of cells with *myo*-[<sup>3</sup>H]inositol, stimulation of cells with GPCR agonist in the presence of Li<sup>+</sup>, collection of cell lysates, separation of accumulated IPs, and counting of radioactivity. The precise details vary between studies; however the overall concept is the same. The flow diagram below (Figure 3.1) outlines the steps of a typical IP assay for this study. This method was used to measure total IP production in response to stimulation of cells with AVP.

HEK293 or CHO-V1b cells were plated into 24-well plates at a density of  $1.25 \times 10^5$  cells/well or  $7 \times 10^4$  cells/well, respectively, in 0.5mL of appropriate culture medium (without antibiotics). The plates were incubated at 37°C overnight (approximately 22 hours) to allow the cells to adhere and reach a confluence of 70-80% for HEK293 and 80-90% for CHO-V1b. The HEK293 cells were then transfected with the plasmid prV1b-R, or the vector pALTER-MAX (as described in section 2.7). CHO-V1b cells stably express the V1b-R, and so transfection was not required. All cells were

incubated for a further 5-6 hours to allow for transfection of the HEK293 cells prior to removal of the medium for labeling with *myo*-[<sup>3</sup>H]inositol.

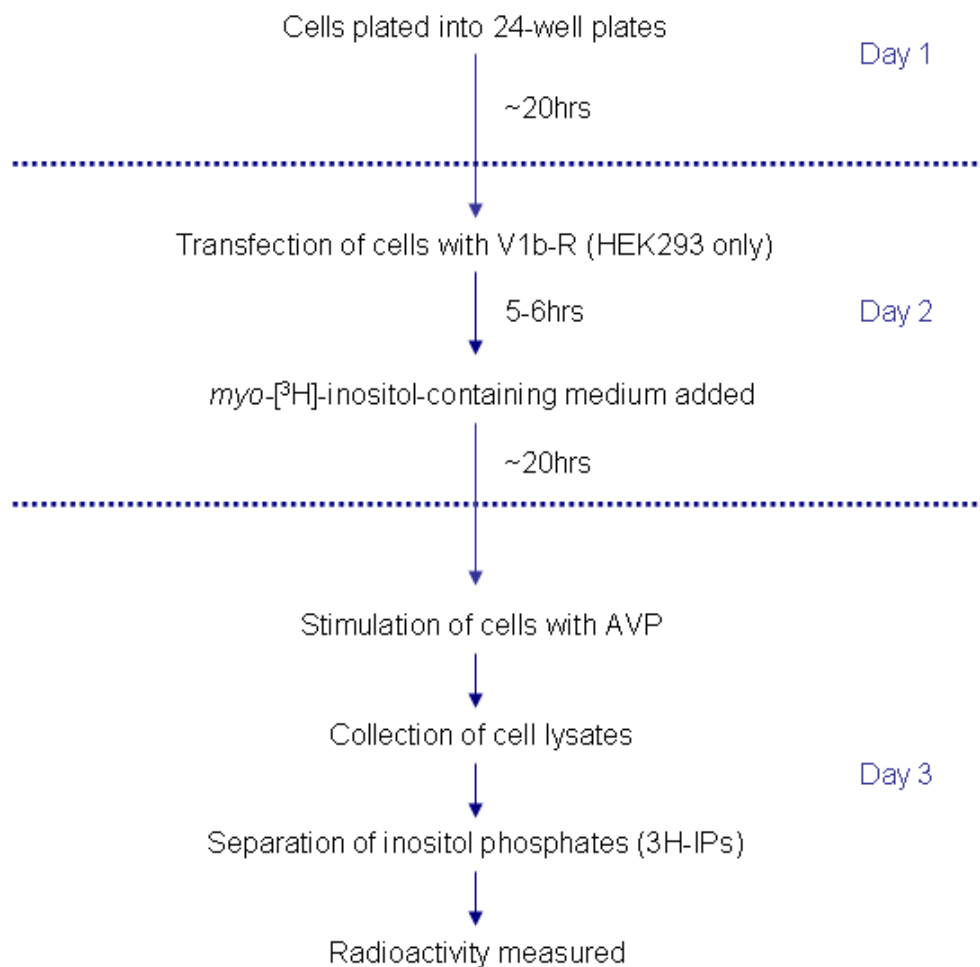


**Figure 3.1. The steps of a typical IP assay.**

### 3.2.4 Cell labeling with *myo*-[<sup>3</sup>H]inositol

For labeling the medium was first aspirated from each well. The cells were then washed once with 0.5mL of pre-warmed phosphate buffered saline (see Appendix B for details) to remove inositol containing medium. 0.5mL of inositol-free culture medium containing 0.32μM *myo*-[<sup>3</sup>H]inositol (see Appendix B for details) was then added to each well.

The cells were then incubated overnight at 37°C in a CO<sub>2</sub> incubator to allow the *myo*-[<sup>3</sup>H]inositol to be incorporated into PIP<sub>2</sub> via the inositol metabolism of the cells. The following incubation times have been reported for labeling of HEK293 cells for IP assays; 18-24hrs (Freedman et al., 1997), 16-24hrs (Oppermann et al., 1996) and 17-22hrs (Iwata et al., 2005). This suggests that the length of the tracer incubation is not particularly critical. The results reported in this study however, indicate that the duration of tracer incubation impacts the magnitude of apparent IP response (see results in section 3.4.1.3). For this reason, both HEK293 and CHO-V1b cells were incubated with *myo*-[<sup>3</sup>H]inositol for as close as possible to 20 hours (unless otherwise indicated).

Following tracer incubation, the *myo*-[<sup>3</sup>H]inositol containing medium was removed from the wells by aspiration. The medium can also be removed by “dumping” the plate if desired as IP assay results were very similar regardless of the method of medium removal (Table 3.1). “Dumping” involved inverting the plate to remove medium from all wells simultaneously.

### 3.2.5 Stimulation of the cells with AVP

Immediately following removal of the tracer-containing medium, each well was washed once with 0.5mL of pre-warmed normal culture medium (MEM for HEK293, or AMEM for CHO-V1b) containing 0.1% BSA (w/v, see Appendix B for details). This wash was to remove the unbound tracer and the serum (HIHS) in the medium. Immediately following the wash, the cells were stimulated with AVP as described for each experiment.

**Table 3.1. Testing the method of removal of *myo*-[<sup>3</sup>H]inositol containing medium.** Following incubation of CHO-V1b cells with *myo*-[<sup>3</sup>H]inositol, the medium was removed by either aspiration or “dumping”. The cells were then treated with either 100nM or 0nM AVP (un-stimulated control) for 15 minutes in the presence of 10mM LiCl. Results represent one experiment, performed in duplicate.

Method of removal of <i>myo</i> -[ <sup>3</sup> H]inositol containing medium	AVP treatment (nM)	IP response (% of control)	SEM (%)
Aspiration	0	100.0	1.8
	100	357.8	10.4
"Dump" of the plate	0	100.0	3.5
	100	345.7	14.0

For a single AVP treatment, the cells were exposed to AVP by the addition of 0.5mL/well of medium + 0.1% BSA + 10mM LiCl ± AVP. For desensitisation experiments the cells were exposed to a “pre-treatment” by the addition of 0.5mL of medium + 0.1% BSA ± AVP (in the absence of LiCl). They were then washed twice using 0.5mL medium + 0.1% BSA + 10mM LiCl per wash, and exposed to a second (“test”) treatment by the addition of 0.5mL of medium + 0.1% BSA + 10mM ± AVP (unless otherwise stated). The plates were placed into a CO<sub>2</sub> incubator at 37°C during exposure to AVP. The AVP treatment concentrations and durations used for each experiment are indicated in the text.

### 3.2.6 Collection of cell lysates

At the end of the AVP treatment period the plate was immediately removed from the incubator and placed onto ice. The reaction was then stopped and the cells lysed by the addition of 0.5mL ice-cold “stop” solution (containing KOH/borate/EDTA (Felder et al., 1989), see Appendix B for details). Once the stop solution was added, the lysate could then be stored for later analysis if required. For example, cells incubated with stop solution for 15 minutes at 37°C produced a very similar IP response to those where the “stop” solution was neutralised immediately following its addition (Table 3.2). In general, the plate was incubated for 1 minute on ice to ensure complete lysis of the cells and the stop solution was then neutralised by the addition of 0.5mL of “neutralisation” solution containing 7.5% HCl.

**Table 3.2. Lack of effect of duration of cells stop solution incubation on IP assay result.** CHO-V1b cells were treated with either 100nM or 0nM AVP (un-stimulated control) for 15 minutes in the presence of 10mM LiCl. The reaction was stopped by the addition of ice-cold “stop” solution, and the cells were incubated with this solution for either <1 minute on ice or 15 minutes at 37°C. Results represent one experiment, performed without replicates.

Duration of incubation with stop solution	AVP treatment (nM)	IP response (% of control)
15 minutes	0	100.0
	100	186.8
<1 minute	0	100.0
	100	234.0

The solution in the wells should be a light pink colour at this stage indicating that the phenol-red containing mixture is neutral. The resin manufacturer (BioRad) states that the pH of the samples must be close to 7 for the anion-exchange resin to function properly. There was some variation in the colour of the samples, some samples were bright pink indicating slightly high pH (alkali) or orange/yellow indicating slightly low pH (acid), however this did not appear to effect the outcome of the IP assay (results not shown).

### 3.2.7 Separation of inositol phosphates

The water soluble cell extracts (collected as described above) were separated by anion-exchange chromatography using AG1-X8 resin (formate form). Each of the IPs can be eluted in a separate fraction by the sequential addition of solutions containing increasing levels of formate (Downes and Michell, 1981). For this study, the total IPs were collected in a single fraction using a shortened version of this method (for an example, see Shacham et al., 2005).

To prepare the columns, 2mL of a 1:1 slurry of AG1-X8 resin:ddH<sub>2</sub>O (ie. 10g/10mL) was added to a Polyprep® chromatography column (BioRad) using a glass pipette. The water was allowed to drip from the columns leaving a final bed volume of approximately 1.6mL. For each well, the lysate was vigorously re-pipetted (5-6 times) and then applied to a column. The samples (and the buffers) were added to the columns slowly and evenly just above the surface of the resin bed with the tip against the side of the column to minimise resin disturbance. The columns were allowed to



drip through after each addition. Free inositol was eluted by washing the column with 10mL of ddH<sub>2</sub>O. Then 8mL of elution buffer II (5mM sodium tetraborate/60mM sodium sodium formate, see Appendix B for details) was used to elute glycerophosphoinositides. Total IPs were then eluted into a fresh tube using 3mL of elution buffer VI (0.1M ammonium formate/0.1M formic acid, see Appendix B for details).

It is also possible to rinse and re-use the packed columns on the same day. Columns were washed first with 10mL of “regeneration” solution (see Appendix B for details) and then washed three times with 10mL of distilled deionised water (ddH<sub>2</sub>O). To test the effects of the column regeneration, CHO-V1b cells were stimulated with 0nM or 100nM AVP for 15 minutes in the presence of LiCl and the IPs were then separated using either freshly poured or regenerated columns. The IP response of the cells stimulated with 100nM AVP was 395.4±62.1% of the control when fresh columns were used, or 380.1% when regenerated columns were used (Table 3.3). Therefore, there appears to be no apparent impact of column regeneration on the IP assay results. Despite this, fresh columns were poured for each separation (unless otherwise stated).

**Table 3.3. Lack of effect of column regeneration on the IP assay results.** Cells were treated with either 100nM or 0nM AVP (un-stimulated control) for 15 minutes in the presence of 10mM LiCl. The IPs were separated using either freshly poured columns, or columns regenerated after previous use on the same day. Results represent one experiment, performed in duplicate for fresh columns or with no replicates for regenerated columns.

Columns	AVP treatment (nM)	IP response (% of control)	SEM (%)
Fresh	0	100.0	23.7
	100	395.4	62.1
Regenerated	0	100.0	-
	100	380.1	-

### 3.2.8 Scintillation counting

To measure the amount of [ $^3\text{H}$ ]-IPs present in eluted fractions the amount of radioactivity in each sample was determined using scintillation counting. The aqueous sample was first combined with NBCS104 scintillation cocktail to obtain a clear homogeneous mixture. Scintillation mixtures containing >7.7% of elution buffer VI (ie. 1mL elution buffer:12mL of scintillant) remained in an emulsion upon mixing. Hence it was not practical to use the entire 3mL eluted fraction. The eluted fraction was mixed, and then 1mL was transferred to a 20mL scintillation vial containing 12mL of NBCS104 scintillation cocktail. The vial was capped firmly, and then shaken vigorously until the mixture cleared.

Samples were counted using the “CPM count” function of a Wallac 1410 scintillation counter. The counts per minute (CPM) function can be used when all samples are expected to have similar counting efficiencies because the CPM is an expression of the relative amount of radioactivity in each sample. The counting efficiency of six representative samples was found to be  $33.9 \pm 0.1\%$  (within the range of 30-45% reported for  $^3\text{H}$ ) hence the efficiency was very similar for the samples tested and counting the CPM was a valid way to compare the samples. The counter determines the CPM by fitting a reference spectrum to the spectrum of the unknown sample. The software then calculates, based on stored information, what CPM value produces that spectrum.

Each sample was counted for 10 minutes using the CPM function. This produced a readout of the following parameters for each sample: CPM (corrected counts per minute), SQPI (spectral quench parameter for  $^3\text{H}$ ) and CPM1 (uncorrected CPM). The SQPI value (which represents the quenching of the sample) was typically 106-110 for all samples. The counter calculated the CPM value of each sample by performing background and chemiluminescence correction of the raw counts (CPM1) for that sample.

### 3.2.9 Data Analysis

For details of the data analysis see section 2.8.1.

### **3.3 HEK293 TRANSFECTION PROTOCOL DEVELOPMENT AND ASSESSMENT USING THE INOSITOL PHOSPHATE ASSAY**

#### **3.3.1 Testing the inositol phosphate assay method using HEK293 cells transfected with the V1b-R**

In an initial experiment the inositol phosphate assay was used to assess the IP response of HEK293 cells transfected with the V1b-R. HEK293 cells were plated (as described in section 2.7) into a standard uncoated plate. They were then transfected with the V1b-R 24-hours later (at a confluence of approximately 70%) using the cationic liposomal transfection reagent Lipofectamine 2000 (LF2000). Based on the manufacturers recommendation 1.6 $\mu$ L of LF2000 and 0.8 $\mu$ g of prV1bR plasmid DNA were used for transfection for this experiment (see section 2.7 for the detailed protocol). Approximately 6 hours after the LF2000/DNA solution was added to each well the cells were washed and then labeled with *myo*-[ $^3$ H]inositol (as described in section 3.2). Following labeling, on the following day, the cells were washed once with 0.5mL of MEM + 0.1%BSA, and then exposed to 100nM AVP for 15 minutes (0.5mL MEM + 0.1%BSA + 10mM LiCl + 100nM AVP added to each well). Released inositol phosphates (IPs) were then collected, separated by anion-exchange chromatography, and counted using a scintillation counter (see section 3.2).

The counts obtained (mean CPM) did not differ significantly between cells stimulated with 100nM AVP and un-stimulated cells (0nM AVP) (Table 3.6) indicating that there was no measurable increase in IP production in response to stimulation with 100nM AVP. There could have been many possible reasons for this:

1. The transfection may have been unsuccessful, resulting in a lack of V1b-R expression. Hence the cells did not respond to stimulation with AVP as would be expected if they were expressing the V1b-R receptor.
2. There may have been too much cell loss from the wells during the medium changes to get a measurable response to AVP.
3. The concentration of AVP and/or exposure time used were ineffective at stimulating an increased IP production.

4. Separation and elution of [3H]IP from the anion exchange columns was not working effectively.

To determine if the procedure used for the IP assay was working, a Chinese Hamster ovary cell line stably transfected with V1b-R (CHO-V1bR) was used. This was because this cell line stably expresses the V1b- R and adheres strongly to culture plates, therefore excluding the first and second possible reasons. An IP assay was carried out as described above for HEK293 cells.

Stimulation of CHO-V1b with 100nM AVP resulted in an IP response that was  $357.8 \pm 1.8\%$  of the un-stimulated control (Table 3.7). This indicates that the protocols used for labeling and stimulating the cells, and separating the IPs are working. Two of the possible reasons given above, remain for why there was no measurable IP increase with AVP stimulation of transfected HEK293 cells:

1. The transfection was not successful.
2. Extensive cell loss precluded measurement of an IP response to AVP.

Therefore, experiments were designed to address these possibilities.

**Table 3.6. Stimulation of V1b-R transfected HEK293 cells with 100nM AVP.** Transfected cells were exposed to 100nM or 0nM AVP (un-stimulated control) for 15 minutes in the presence of 10mM LiCl. The mean CPM was determined and used to calculate the IP response (% of control). Data are the results of one experiment, performed in triplicate.

AVP treatment (nM)	Mean CPM	IP response (% of control)	SEM (%)
0	312.9	100.0	4.9
100	315.6	99.1	1.9

**Table 3.7. Stimulation of CHO-V1b cells with 100nM AVP.** CHO-V1b cells were exposed to 100nM or 0nM AVP (un-stimulated control) for 15 minutes in the presence of 10mM LiCl. The mean CPM was determined and used to calculate the IP response (% of control). Data are the results of one experiment, performed in duplicate.

AVP treatment (nM)	Mean CPM	IP response (% of control)	SEM (%)
0	106.5	100.0	10.4
100	381.1	357.8	1.8

### 3.3.2 Optimisation of transfection

V1b-R transfection of HEK293 cells was assessed by testing whether transfected cells respond to AVP stimulation and produce IP<sub>3</sub>. Firstly, a second plasmid DNA solution was prepared from glycerol stocks of prV1b-R transformed DH5 $\alpha$  cells using the Qiagen plasmid purification method (described in section 2.5.6). This plasmid preparation had a DNA concentration of 333.9 ng/ $\mu$ L, which was approximately 5-fold greater than the DNA used for the previous transfection (66.4 ng/ $\mu$ L). Using the DNA preparation with the higher concentration of DNA, different transfection protocols were tested to determine the amounts of DNA and transfection reagent, Lipofectamine 2000 (LF2000), that would result in successful transfection. These concentrations were varied within the ratios recommended for optimising transfection with LF2000; DNA: LF2000 ratio of 1:1 to 1:3 (see Table 3.8). CHO-V1b cells were used as a positive control in parallel with HEK293 cells for this experiment. The CHO-V1b cells were plated into a standard 24-well plate at a density of  $8 \times 10^4$  cells/well. The HEK293 cells were plated into a poly-D-lysine coated plate (Becton Dickinson Biosciences) at a density of  $1.25 \times 10^5$  cells/well (as described in section 2.7). Both cell types had reached a confluence of 70-80% at the time of HEK293 cell transfection. The poly-D-lysine coated plates used for the HEK293 cells noticeably reduced cell loss during medium changes compared to the standard un-coated plates used previously (discussed in section 2.3).

The transfected HEK293 cells showed an increase in IP production to 134.7-192.5% of the corresponding un-stimulated control. A previous transfection of HEK293 cells with 0.8 $\mu$ g of DNA (from a different preparation) and 1.6 $\mu$ L LF2000 did not result in a measurable increase in IP production (Table 3.6), whereas the same transfection protocol resulted an IP response that was 182.8% of the un-stimulated control for this experiment (Table 3.8). In addition, the CPM values of both the 100nM AVP-treated and un-stimulated control wells were higher than the previous transfection. The increased DNA concentration in the purified plasmid solution may have contributed to this improvement in the results. The manufacturers of the DNA purification kit (Qiagen) state that good quality DNA that is relatively free of impurities is required for plasmid transfection. Of course by increasing the concentration of the DNA, less volume is required for transfection and so impurities would be more diluted. Thus, the plasmid DNA preparation with a

**Table 3.8. Testing of different concentrations of LF2000 and DNA for transfection of HEK293 cells.** HEK293 cells, transfected with the reagents shown in the table below, were exposed to 100nM or 0nM AVP (un-stimulated control) for 15 minutes in the presence of 10mM LiCl. The IP response (% of control) is shown. Data are the results of one experiment, performed without replicates.

Transfection Reagents		Ratio DNA:LF2000	AVP treatment (nM)	CPM	IP response (% of control)
DNA	LF2000				
0.8µg	1.6µL	1:2	0	1417.6	100.0
			100	775.7	182.8
0.8µg	2.4µL	1:3	0	1218.9	100.0
			100	687.6	177.3
1.0µg	1.0µL	1:1	0	858.5	100.0
			100	637.4	134.7
1.0µg	2.0µL	1:2	0	910.5	100.0
			100	473.0	192.5

DNA concentration of 333.9ng/µL was used for all subsequent transfections of HEK293 cells. The improved HEK293 cell adherence may also have contributed to the improvement in the results.

The largest increases in IP production were observed for cells transfected with DNA and LF2000 in a ratio of 1:2; conversely the smallest difference was exhibited by the wells transfected with a DNA to LF2000 ratio of 1:1. The protocol provided with the LF2000 reagent states that a ratio of 1:2 to 1:3 is optimal for most cell types, so it is possible that a low ratio of LF2000 to DNA limits the transfection efficiency. More replicates would be required to confirm this.

The CPM values obtained for those wells transfected with 0.8µg of DNA were typically higher than for those transfected with 1.0µg of DNA. This is interesting as one might expect a larger amount of DNA to result in greater levels of V1b-R expression in the cells, and in turn a larger CPM due to increased IP production. The results indicate that this is not the case. It may be that more efficient transfection is achieved using 0.8µg of DNA, or that high levels of LF2000 and/or DNA are toxic to the cells. 0.8µg of DNA is the amount recommended in the protocols provided with the LF2000 for transfection in a 24-well plate.

The results (Table 3.8) show that transfection has been successful and that the HEK 293 cells are expressing the V1b-R, however further experiments were needed to investigate the optimal amounts of DNA and LF2000 for transfection. This involved carrying out replicates (n=2) of the

same transfection protocol used above to determine whether the differences obtained are reproducible. Two of the four transfection protocols previously tested were used, both with a ratio of DNA to LF2000 of 1:2. For this experiment, HEK 293 cells were plated into poly-D-lysine plates at a density of  $1.25 \times 10^5$  cells/well and transfected at a confluence of approximately 75%.

Transfection with 0.8 $\mu$ g DNA:1.6 $\mu$ L LF2000 and 1.0 $\mu$ g DNA:2.0 $\mu$ L LF2000 resulted in IP responses that were  $209.4 \pm 29.3\%$  and  $209.1 \pm 14.1\%$  of the corresponding un-stimulated controls, respectively (as shown in Figure 3.2). Therefore, the results did not differ between the two transfection protocols tested. For all further experiments 0.8 $\mu$ g of DNA and 1.6 $\mu$ L of LF2000 per well was used (as described in detail in section 2.7), as the results indicate these amounts are appropriate for successful transfection.

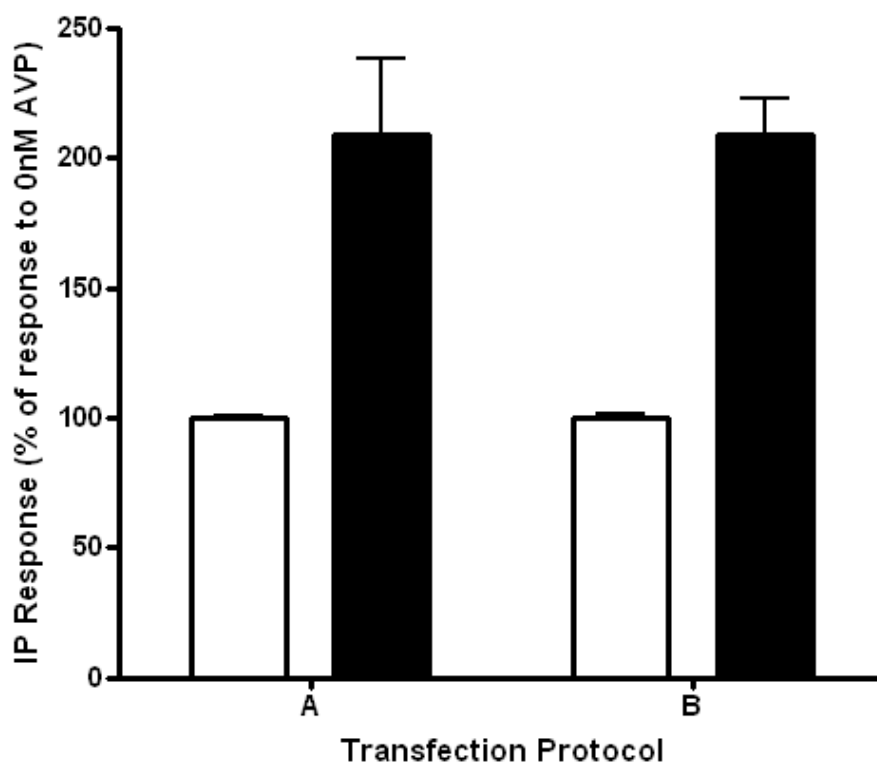


**Figure 3.2. Effect of different concentrations of LF2000 and DNA on transfection of HEK293 cells.** HEK293 cells were transfected with either 0.8 $\mu$ g DNA:1.6 $\mu$ L LF2000 (transfection protocol A) or 1.0 $\mu$ g DNA:2.0 $\mu$ L LF2000 (transfection protocol B) per well. The transfected cells were exposed to 100nM or 0nM AVP (un-stimulated control) for 15 minutes in the presence of 10mM LiCl. The IP response of cells stimulated with 100nM AVP (black bars) is expressed as the mean percentage response compared to the corresponding un-stimulated control (open bars)  $\pm$  SEM. Data represent the results of two experiments, one performed in duplicate, the other without replicates.

### 3.3.3 Optimisation of HEK293 cell adherence using the inositol phosphate assay

Observations of the HEK293 cells at various stages of the IP assay (using an inverted microscope) revealed that a high proportion of cells detach from the plastic surface of standard 24-well plates (Nunc) when the culture medium is changed. During an IP assay, this cell loss appeared to be most pronounced during the wash prior to addition of *myo*-[<sup>3</sup>H]inositol containing medium. This may be because the cell attachment was reduced following transfection. This seems a reasonable assumption, as when transfected and un-transfected cells were compared, there is a higher proportion of unattached cells in the transfected wells immediately prior to a medium change, and after changing the medium the degree of cell loss was greater for transfected cells. This was addressed by testing different plate-coating procedures, and plate types, in order to improve the adhesion of HEK293 cells to the culture plate (discussed in section 2.3.4). The adhesion of HEK293 cells to each of the following 24-well plate types was tested using the IP assay: a plate poly-D-lysine (PDL) coated by the manufacturer (Becton Dickinson Biosciences), and a standard Nunc plate poly-D-lysine coated in our laboratory (prepared as described in section 3.3.4.1) with 5µg or 2.5 µg of PDL per cm<sup>2</sup> of plate area. The HEK293 cells were plated into the various plates at a density of 1.25 x 10<sup>5</sup> cells/well and transfected 24 hours later at a confluence of approximately 80% with 1.6µL of LF2000 and 0.8µg of prV1bR plasmid DNA. The cells were washed, and then exposed to 100nM or 0nM AVP for 15 minutes.

**Table 3.9. Testing the effect of different plate types/poly-D-lysine coating procedures on the IP response of HEK293 cells.** HEK293 cells were plated into the various treated plates, transfected and then exposed to 100nM or 0nM AVP (un-stimulated control) for 15 minutes in the presence of 10mM LiCl. The mean CPM was determined and used to calculate the IP response (% of control). Data are the results of one experiment, performed in duplicate.

Plate type	AVP treatment (nM)	Mean CPM	IP response (% of control)	SEM (%)
Poly-D-lysine coated (Becton Dickinson Biosciences)	0	245.5	100.0	1.8
	100	817.0	332.8	17.5
Poly-D-lysine coated (5µg/cm <sup>2</sup> of plate area)	0	468.9	100.0	7.3
	100	1484.7	316.6	19.7
Poly-D-lysine coated (2.5µg/ cm <sup>2</sup> of plate area)	0	381.9	100.0	5.6
	100	1332.8	349.0	20.8



It seems a reasonable assumption (based on observations of cell loss during the IP assay) that the greater the cell number that remained in the well for the duration of the assay, the greater the absolute IP production (mean CPM). On this basis, the poly-D-lysine plates coated in our laboratory with 5µg and 2.5 µg of PDL per cm<sup>2</sup> of plate area gave the best results with a mean CPM in un-stimulated wells of 468.9 and 381.9 respectively (Table 3.9). The pre-coated plates from Becton Dickinson Biosciences also generated good results with a mean CPM in un-stimulated wells of 245.5. For reasons of convenience, pre-coated plates from Becton Dickinson Biosciences were used for the all further IP assays using HEK293 cells. It should also be noted that the IP response (%) of cells stimulated with 100nM AVP was similar for each of the plate types tested (Table 3.9).

### **3.3.4 The IP response of V1b-R-transfected HEK293 cells to AVP stimulation**

Following optimisation of the HEK293 transfection with the V1b-R, it was necessary to establish that the same transfection protocol resulted in a reproducible IP response to AVP stimulation. HEK293 cells were plated into a poly-D-lysine coated plate (Becton Dickinson Biosciences) at a density of  $1.25 \times 10^5$  cells/well. Approximately 24 hours later, at a confluence of 70-80%, the HEK293 cells were transfected using 0.8µg of DNA and 1.6µL of LF2000 per well. The V1b-R-transfected HEK293 were stimulated with 100nM AVP for 15 minutes, and the IP production was determined and expressed as a percentage of the un-stimulated control (Figure 3.3).

Stimulation of V1b-R-transfected HEK293 cells with 100nM AVP for 15 minutes resulted in a statistically significant increase in the IP response, to  $235.5 \pm 23.4\%$  of the un-stimulated control (Figure 3.3) (*t*-test, \*\*  $P < 0.02$ ). In order to show that this response is mediated by the V1b-R the response of cells transfected with the prV1bR was compared to two controls; pALTER-MAX vector-transfected and un-transfected (mock- transfected using 100µL of normal culture medium) HEK293 cells. The IP response of the cells to stimulation with 100nM VP for 15 minutes (in the presence of 10mM LiCl) was determined and expressed as a percentage of the un-stimulated controls for that transfection protocol (Figure 3.4). The absolute values (CPM) for the mean IP

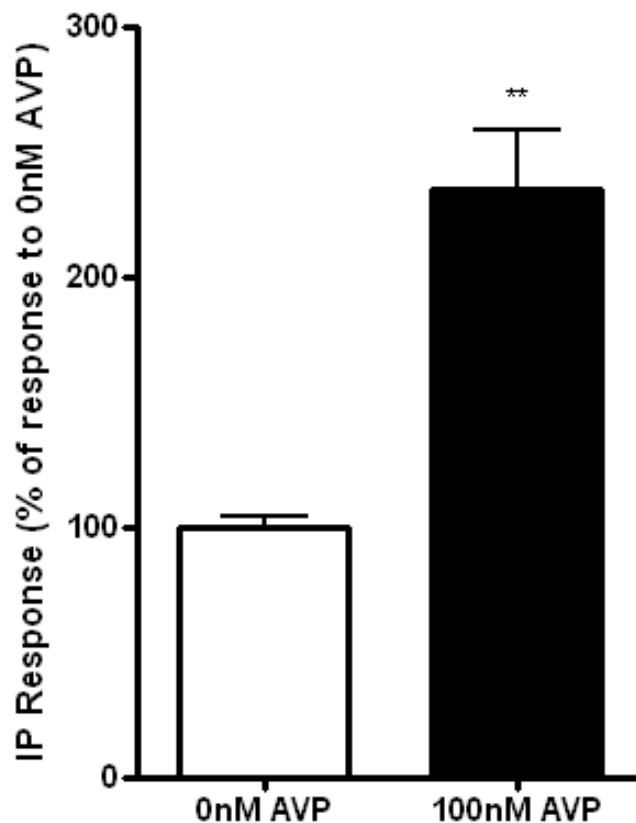


**Figure 3.3. IP response of HEK293 cells transfected with the V1b-R.** HEK293 cells were transfected with the V1b-R using 0.8 $\mu$ g DNA and 1.6 $\mu$ L per well. The transfected cells were exposed to 100nM or 0nM AVP (un-stimulated control) for 15 minutes in the presence of 10mM LiCl. The IP response of cells stimulated with 100nM AVP (black bars) is expressed as the mean percentage response compared to the corresponding un-stimulated control (open bars)  $\pm$  SEM. Data represent the results of three experiments, each performed in duplicate. Asterisks indicate a statistically significant difference between the IP response of cells exposed to 100nM AVP compared to the un-stimulated control (*t*-test, \*\*  $P < 0.02$ ).

responses of un-treated controls were very similar for each transfection; 274.0 for prV1bR-transfected, 229.0 for pAlter-transfected, and 274.9 for un-transfected.

Stimulation of prV1bR-transfected cells with 100nM AVP resulted in an IP response that was  $230.5 \pm 20.3\%$  of the corresponding un-stimulated control. The pALTER-MAX vector serves as a control for the transfection. The pALTER-MAX-transfected cells did not respond to stimulation with AVP, showing that the transfection itself did not cause the IP response seen in prV1bR-transfected cells. Also, un-transfected cells did not respond to stimulation with AVP. Together, these results show that the response of V1b-R-transfected HEK293 cells to AVP is mediated by the V1b-R.

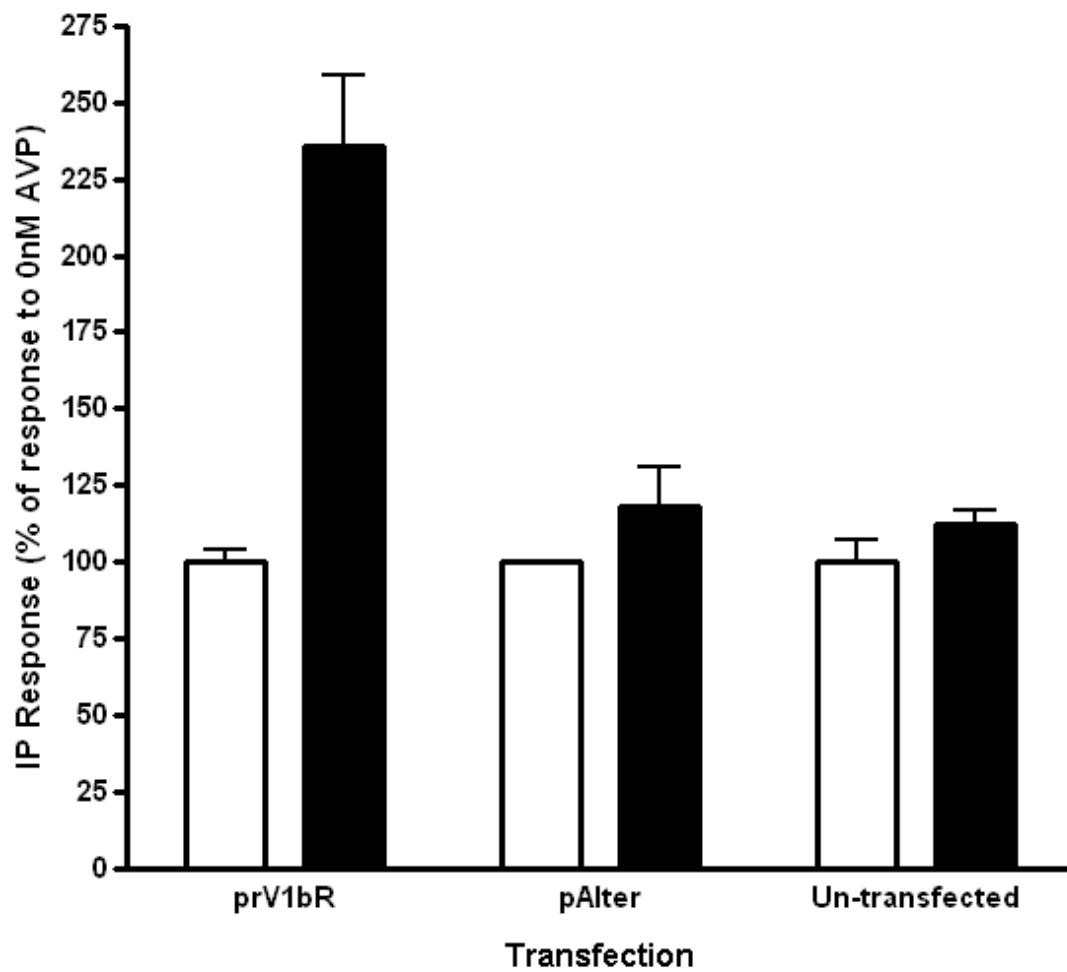


**Figure 3.4. IP response of HEK293 cells transfected with prV1b-R or pALTER-MAX, or un-transfected.** HEK293 cells were transfected with either prV1b-R or pAlter using 0.8 $\mu$ g DNA and 1.6 $\mu$ L per well. For un-transfected cells 100 $\mu$ L of normal culture medium was added to each well at the time of transfection. The transfected cells were exposed to 100nM or 0nM AVP (un-stimulated control) for 15 minutes in the presence of 10mM LiCl. The IP response of cells stimulated with 100nM AVP (black bars) is expressed as the mean percentage response compared to the corresponding un-stimulated control (open bars)  $\pm$  SEM. Data represent the results of one experiment, performed in duplicate.

### **3.4 DEVELOPMENT OF AN ASSAY FOR MEASURING DESENSITISATION OF THE IP RESPONSE TO AVP**

#### **3.4.1 Rationale for using CHO-V1b cells**

A marked response to AVP stimulation can be seen in V1b-R-transfected HEK293 cells, so the next step was to develop a protocol for desensitisation. A protocol was designed for testing desensitisation of the IP response to AVP in V1b-R-transfected HEK 293 cells based on recent research conducted by others in our laboratory. A single pre-treatment with 5nM AVP for 5 minutes was found to be capable of inducing significant desensitisation of the ACTH response to AVP in sheep anterior pituitary cells (Hassan, 2001). Also, the magnitude of this desensitisation increased with increasing pre-treatment concentration and duration (Hassan, 2001). In early experiments however, HEK293 cells did not show desensitisation when exposed to 5nM AVP for 15 minutes, followed by stimulation with 100nM AVP for 15 minutes (results not shown). Chinese hamster ovary (CHO) cells stably expressing the V1bR (CHO-V1b) were therefore used in initial experiments to investigate whether desensitisation of the V1b-mediated response to AVP could be detected using the inositol phosphate assay. Using CHO-V1b cells meant that there was no need for transfection with the V1b-R; making these experiments simpler and less expensive than if transiently transfected HEK293 cells were used. Several parameters influencing the desensitisation response were investigated using CHO-V1b.

#### **3.4.2 The inositol phosphate response of CHO-V1b cells to AVP stimulation**

Initial experiments established that CHO-V1b cells reproducibly respond to stimulation with AVP. CHO-V1b cells (plated and labeled as described in section 3.2) were exposed to 100nM AVP for 15 minutes (in the presence of 10mM LiCl), and the IP production was determined and expressed as a percentage of the un-stimulated control (Figure 3.5). Stimulation of CHO-V1b with 100nM

AVP for 15 minutes resulted in a statistically significant increase in the IP response, to  $456.1 \pm 57.7\%$  of the un-stimulated control (*t*-test,  $P < 0.05$ )

The IP response (% of control) of AVP-stimulated CHO-V1b cells was consistently larger than that observed for V1b-R-transfected HEK293 cells assayed at the same time (as shown in the data presented in Figure 3.5). In addition, the absolute IP production (CPM) was also greater for CHO-V1b cells than for V1b-R-transfected HEK293 cells (results not shown). This suggests that the V1b-R may be expressed at a higher level in the CHO-V1b cells than in transiently transfected HEK293 cells. Hence, the same AVP concentration elicits a larger IP response. There are other possible reasons for a differing IP response from the two cell types. For example, the IP response

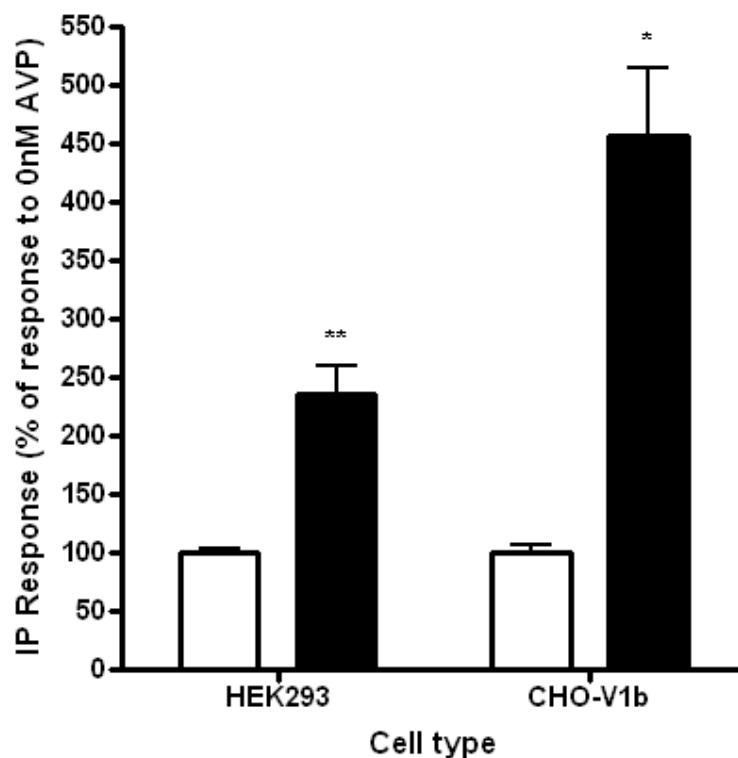


**Figure 3.5. IP response of V1b-R-transfected HEK293 cells and CHO-V1b cells to AVP stimulation.** V1b-R-transfected HEK293 cells or CHO-V1b cells were exposed to 100nM or 0nM AVP (un-stimulated control) for 15 minutes in the presence of 10mM LiCl. The IP response of cells stimulated with 100nM AVP (black bars) is expressed as the mean percentage response compared to the corresponding un-stimulated control (open bars)  $\pm$  SEM. Data represent the results of three experiments, each performed in duplicate. Asterisks indicate a statistically significant difference between the IP response of cells exposed to 100nM AVP compared to the un-stimulated control for the same cell type (*t*-test, \*\*  $P < 0.02$ , \*  $P < 0.05$ ).

may depend upon the size and/or rate of recycling of the PIP<sub>2</sub> pool in different cell types (Forrest-Owen et al., 1999). Therefore, while the CHO-V1b cells serve as a useful tool for optimisation of V1b-R desensitisation, it should be kept in mind that the kinetics and magnitude of the desensitisation may differ somewhat in the HEK293 cells.

#### 3.4.2.1 The effect of AVP treatment concentration

In order to determine what AVP concentrations would be suitable for desensitisation experiments a dose response curve for the V1b-R was generated. CHO-V1b cells were exposed to the following concentrations of AVP for 15 minutes (in the presence of 10mM LiCl): 0, 0.1, 1, 5, 10, 50, 100, 1000 and 10000nM. The concentrations used were selected based on previous studies in our laboratory looking at the ACTH response of ovine anterior pituitary cells to AVP (Hassan, 2001).

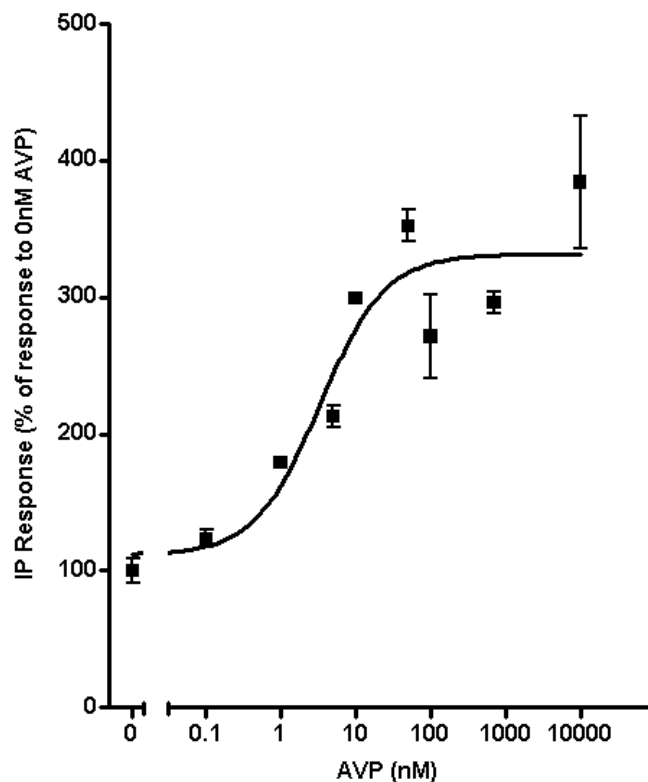


**Figure 3.6. Effect of AVP concentration on IP response.** CHO-V1b cells were exposed to the various concentrations of AVP for 15 minutes (in the presence of 10mM LiCl). The IP responses of cells are expressed as the mean percentage response compared to un-stimulated control (0nM AVP)  $\pm$  SEM. Data represent the results of one experiment, performed in duplicate.

A sigmoidal curve was fitted to the resulting data (Figure 3.6) using Graphpad Prism software. The IP response of the cells appeared to reach a maximum of approximately 320% of the un-stimulated control. An AVP concentration of 100nM AVP was sufficient to elicit the maximum IP response, and was therefore the concentration chosen to use to test the IP response of the cells to AVP. The lowest concentration that resulted in an IP response that was significantly above basal was 1nM AVP. These findings are very similar to those of previous studies of the V1b-R in our laboratory conducted by measuring the ACTH response to AVP in sheep anterior pituitary cells (Johnson, 1992).

#### 3.4.2.2 The effect of AVP treatment duration

The magnitude of the IP response was also found to be dependent on the duration of incubation with AVP. CHO-V1b cells were exposed to 100nM AVP for 5, 10, 15 or 30 minutes and the resulting IP response was determined. All treatment durations resulted in an IP response above basal, and the magnitude of the response increased with increasing duration (Figure 3.7). The absolute IP production (CPM) was approximately 2-fold greater for cells stimulated with AVP for 30 minutes, compared to those stimulated for 15 minutes (results not shown).

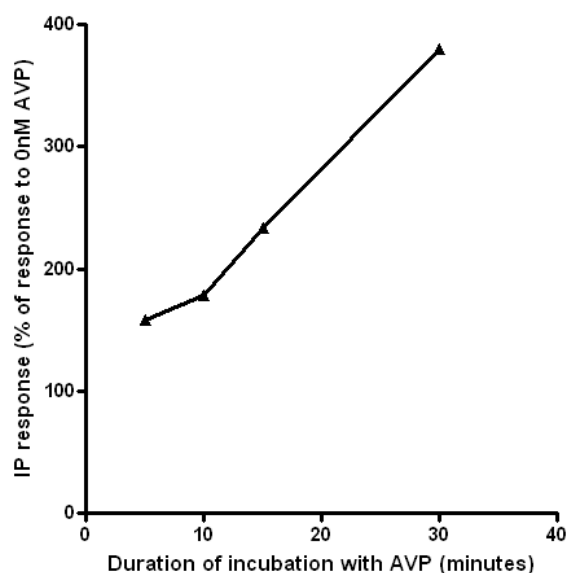


**Figure 3.7. Effects of varying the duration of AVP treatment on the IP response.** CHO-V1b cells were exposed to 100nM or 0nM AVP (un-stimulated control) for 5, 10, 15 or 30 minutes in the presence of 10mM LiCl. The IP response (% of control) is shown. Data are the results of one experiment, performed without replicates.

### **3.4.3 Desensitisation of the inositol phosphate response of CHO-V1b cells to AVP stimulation**

Chinese hamster ovary cells stably transfected with the V1b-R (CHO-V1b) were used to investigate whether desensitisation of the V1b-R-mediated response to AVP could be detected. To induce desensitisation cells were exposed to a pre-treatment with a relatively low AVP, and the IP response to a subsequent treatment (“test” treatment) with a high AVP concentration was determined. Ideally the AVP concentrations and durations used for desensitisation experiments should reflect endogenous AVP stimulation but also give an optimal readout for reproducible quantitation. An AVP concentration of 5nM was selected as a pre-treatment for desensitisation experiments because it lies within the steepest part of the dose response curve for the V1b-R (ie. elicits an IP response above basal) (Figure 3.6). In addition, 5nM AVP has been used by others in our lab to induce desensitisation of the V1b-R-mediated ACTH response of anterior pituitary cells and is within the range of AVP concentrations measured endogenously (Hassan, 2001; Mason et al., 2002). As mentioned above, an AVP concentration of 100nM AVP was sufficient to elicit the maximum IP response (Figure 3.6), and was therefore the concentration chosen for the test treatment with AVP.

For desensitisation experiments CHO-V1b cells were plated and labeled with *myo*-[<sup>3</sup>H]inositol as described earlier (section 3.2). Following labeling, the next day, the cells were washed once with 0.5mL/well AMEM + BSA, and then exposed to an AVP pre-treatment by the addition of 0.5mL/well AMEM + BSA + AVP. Immediately following the pre-treatment, the cells were washed twice with 0.5mL/well AMEM + BSA + 10mM LiCl (unless otherwise stated). For the test treatment the cells were exposed to 100nM AVP by the addition of 0.5mL/well AMEM + BSA + 10mM LiCl + 100nM AVP. The IP response of the cells to the test treatment was determined and expressed as a percentage IP response of cells exposed to medium without AVP during the 15 minute pre-treatment incubation (ie. non-pretreated controls).

In the first experiment desensitisation the pre-treatment regime used was 5nM AVP for 15 minutes (in the absence of LiCl). The cells were then exposed to 100nM AVP for 15 minutes (in the presence of 10mM LiCl) for the test treatment. See Figure 3.8 for a diagrammatical representation



of the AVP protocol used for this experiment. Appropriate un-stimulated controls were included as shown in Table 3.8 and Figure 3.8.

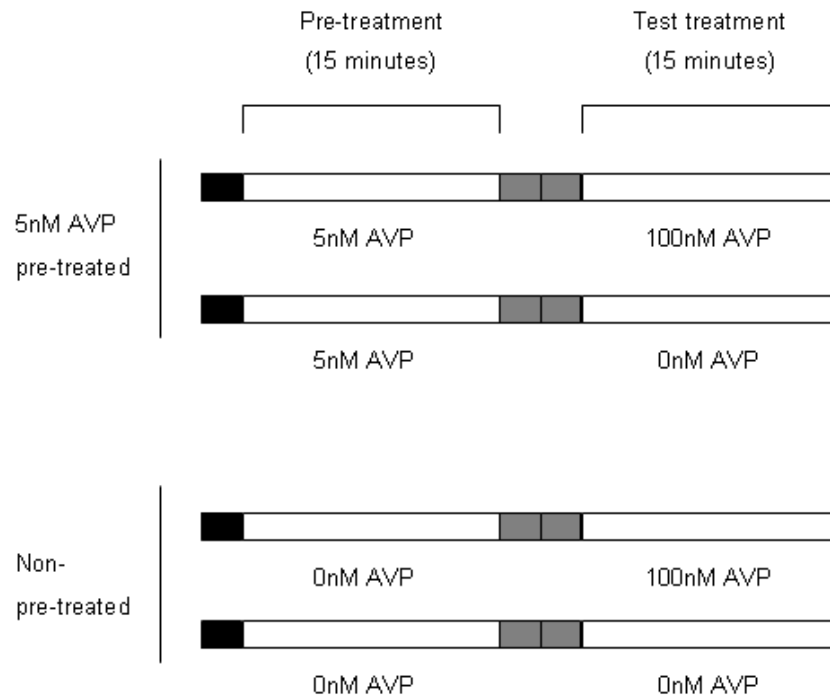


**Figure 3.8. Diagrammatic representation of the AVP treatment protocol used to measure desensitisation in CHO-V1b.** Each line represents a different well. Cells were first washed once with AMEM + BSA (black bars), then pre-treated with either 5nM AVP (5nM AVP pre-treated) or 0nM AVP (non-pre-treated control) for 15 minutes. Following pre-treatment the cells were immediately washed twice with MEM + BSA + 10mM LiCl (grey bars) then exposed to either 100nM AVP or 0nM AVP (unstimulated control) for 15 minutes. The IP response of the cells to the test treatment was determined and expressed as a percentage IP response of cells exposed to medium without AVP during the 15 minute pre-treatment incubation (ie. non-pretreated controls) (Table 3.8).

**Table 3.8. Testing the desensitisation protocol using CHO-V1b cells.** For pre-treatment CHO-V1b cells were exposed to either 5nM (pre-treated) or 0nM AVP (control) for 15 minutes (in the absence of LiCl). The cells were immediately washed twice with medium containing 10mM LiCl and then exposed to either 100nM or 0nM AVP. The mean counts per minute (CPM) were determined, and used to calculate the IP response (expressed as the percentage of the non-pre-treated control  $\pm$  SEM). Data are the results of one experiment, performed in duplicate.

Protocol	AVP <sub>pre-treatment</sub> (nM)	AVP <sub>test</sub> (nM)	Mean CPM	IP response (% of control)	SEM (%)
Control	0	0	132.2	100	10.6
	0	100	765.6		
Pre-treated	5	0	366.9	82.8	5.6
	5	100	891.4		

The IP response of the pre-treated CHO-V1b cells was reduced to  $82.8 \pm 5.6\%$  of the non-pre-treated control (Table 3.8). This indicates that desensitisation had occurred. However, it was smaller in magnitude than that previously reported for AVP-desensitisation of the ACTH response in ovine anterior pituitary cells ( $66.3 \pm 3.7\%$ ;  $n=10$  with 5nM AVP pre-treatment for 15 minutes) (Hassan, 2001; Mason et al., 2002). One might expect the mean CPM to be lower for desensitised cells (5nM AVP pre-treatment + 100nM AVP test treatment) compared to the non-pre-treated control (0nM AVP pre-treatment + 100nM AVP test treatment), however this was not the case for this experiment. Cells that were exposed to a 5nM AVP pre-treatment + 0nM AVP test treatment had a mean CPM of 366.9 which was much greater than the mean CPM for cells exposed to 0nM AVP pre-treatment/0nM AVP test treatment (132.2). Presumably, the 5nM AVP pre-treatment resulted in the production of IPs which were not broken down before the test treatment. IPs appeared to be carried over from the pre-treatment (or were continuing to accumulate), and this may explain why the magnitude of desensitisation was smaller than expected.

#### 3.4.3.1 The effect of lithium chloride

Lithium blocks an enzyme involved in the breakdown of IPs (as discussed earlier), and hence causes the IPs to accumulate as they are produced. Therefore, for the desensitisation protocol tested above the cells were pre-treated with AVP in the absence of LiCl, washed with 10mM LiCl containing medium and then exposed to the test AVP treatment in the presence of 10mM LiCl (Figure 3.8). The LiCl is included in the test treatment so that the IPs produced can be measured, in contrast LiCl was not included in the pre-treatment to allow breakdown of the IPs produced at this stage. However, as shown (Table 3.8) IPs are carried over from the pre-treatment to the test treatment. In order to minimise this IP “carry over”, and hence maximise the measureable desensitisation, the effect of LiCl on accumulation of IPs was investigated. In order to investigate the effect of LiCl on the accumulation of IPs during AVP stimulation, CHO-V1b cells were stimulated with 100nM AVP (or 0nM AVP for controls) for 15 minutes in the presence (+ LiCl) or absence (- LiCl) of 10mM LiCl.

The IP response of cells stimulated with 100nM AVP in the presence of 10mM LiCl (100nM + LiCl) was  $348.8 \pm 9.9\%$  of the unstimulated control (exposed to 0nM AVP) (Figure 3.9). As

expected, this was the largest IP response measured as the cells were exposed to LiCl for the longest period of time. Cells stimulated with 100nM AVP without any exposure to LiCl (100nM – LiCl) generated an IP response of  $200.4 \pm 15.4\%$  of the control. This shows that the absolute [ $^3\text{H}$ ]IP levels in the cell were elevated by continuous stimulation with 100nM AVP.

To investigate the rate of IP breakdown upon removal of AVP-containing medium, following exposure of the cells to 100nM (in the absence of LiCl) the cells were immediately washed to remove AVP. Cells were washed twice with 0.5mL/well of either LiCl containing medium (wash + LiCl) or medium without LiCl (wash – LiCl) (Figure 3.9). The cells washed after AVP treatment produced an IP response slightly less than that of unwashed cells (compared to unstimulated control) indicating that IP breakdown occurred following removal of the AVP. Cells washed with LiCl after incubation (wash + LiCl) produced an IP response slightly greater than those washed without LiCl (wash - LiCl) compared to the control. This suggests that the relatively short (approximately 2 minute) exposure of the cells to LiCl during the washes may be sufficient to block IP breakdown.

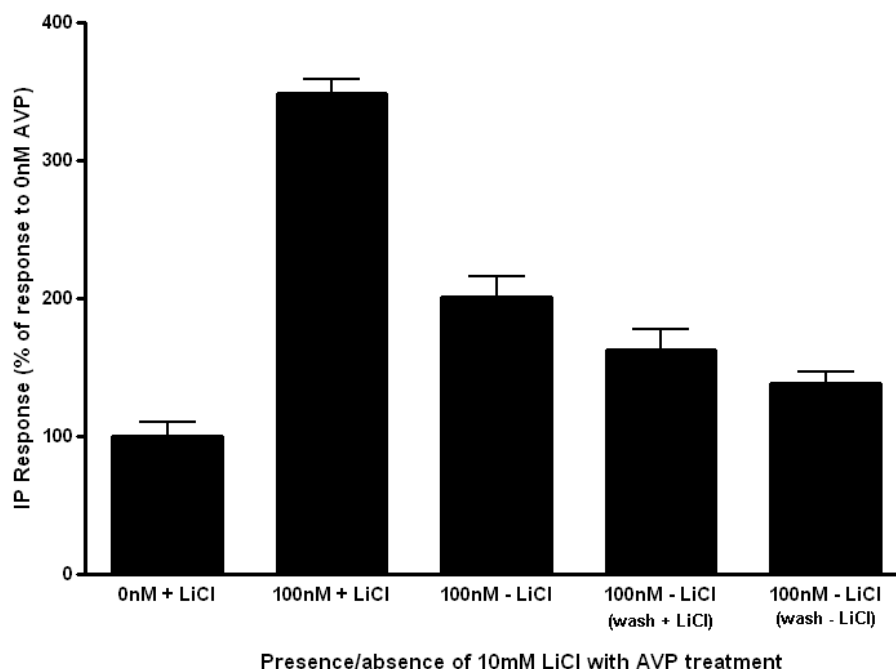


**Figure 3.9. Effects of LiCl on the IP response of CHO-V1b cells to 100nM AVP.** CHO-V1b cells were exposed to 100nM (or 0nM AVP for control) for 15 minutes in the presence (+) or absence (-) of 10mM LiCl. Following the AVP treatment the cells were washed with medium either with (+) or without (-) 10mM LiCl where indicated. The IP response (% of control) is shown. Data are the results of one experiment, performed in duplicate.

The results suggest that it may be possible to reduce IP “carry over” from the pre-treatment to the test treatment by altering the timing of LiCl exposure. To test the effect of removing LiCl from the wash medium on measurable desensitisation, cells were rapidly washed twice with 0.5mL/well of either AMEM + BSA + 10mM LiCl (+ LiCl) or with AMEM + BSA (-LiCl) between the pre-and test treatments (Figure 3.10 (A)).

The IP response was reduced to 81.2% for pre-treated cells washed with LiCl, and 78.6% for pre-treated cells washed without LiCl (Figure 3.11 (A)). Therefore, it appears removal of LiCl from the wash medium did not lead to an increase in the magnitude of the desensitisation. Also, the CPM values were much lower for cells washed without LiCl (results not shown). This indicated that pre-exposure of the cells to LiCl prior to the test treatment is needed in order to maximise the CPM measured and hence improve the accuracy of the results.

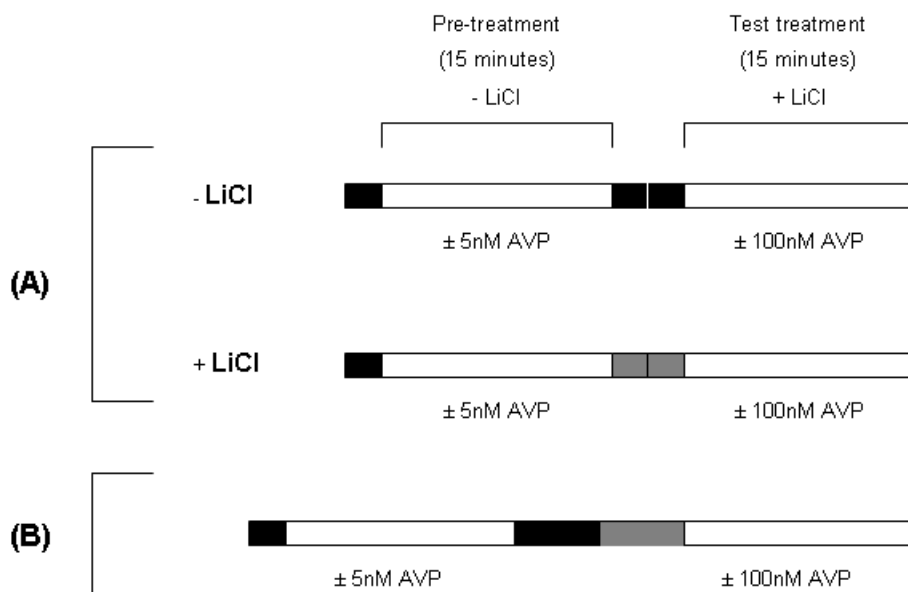


**Figure 3.10. Diagrammatic representation of the AVP treatment protocol used to test the effects of LiCl on measurable desensitisation in CHO-V1b.** All wells were first washed once with AMEM + BSA (black bars), then pre-treated with either 5nM AVP (5nM AVP pre-treated) or 0nM AVP (non-pre-treated control) for 15 minutes in the absence of LiCl. For wash protocol (A) the cells were then washed twice rapidly with MEM + BSA (black bars, - LiCl) or with MEM + BSA + 10mM LiCl (grey bars, + LiCl). For wash protocol (B) the cells were washed first with MEM + BSA (black bars) then with MEM + BSA + 10mM LiCl (grey bars). All cells were then exposed to either 100nM AVP or 0nM AVP (unstimulated control) for 15 minutes in the presence of LiCl. The IP response of the cells to the test treatment was determined and expressed as a percentage IP response of cells exposed to medium without AVP during the 15 minute pre-treatment incubation (ie. non-pretreated controls) (Figure 3.11).

In an attempt to minimise the IP “carry over” the effect of increasing the duration of the washes was tested. Each of the two washes was increased to 5 minutes to allow sufficient time for IP breakdown (Figure 3.10 (B)). Also the first of the two washes was performed with medium without LiCl, and the second with medium with LiCl. This wash regime did not result in a measurable reduction in IP production during the test incubation (Figure 3.11 (B)). This was possibly because the time between pre- and test AVP treatments allowed the cells to at least partially recover from the pre-treatment.

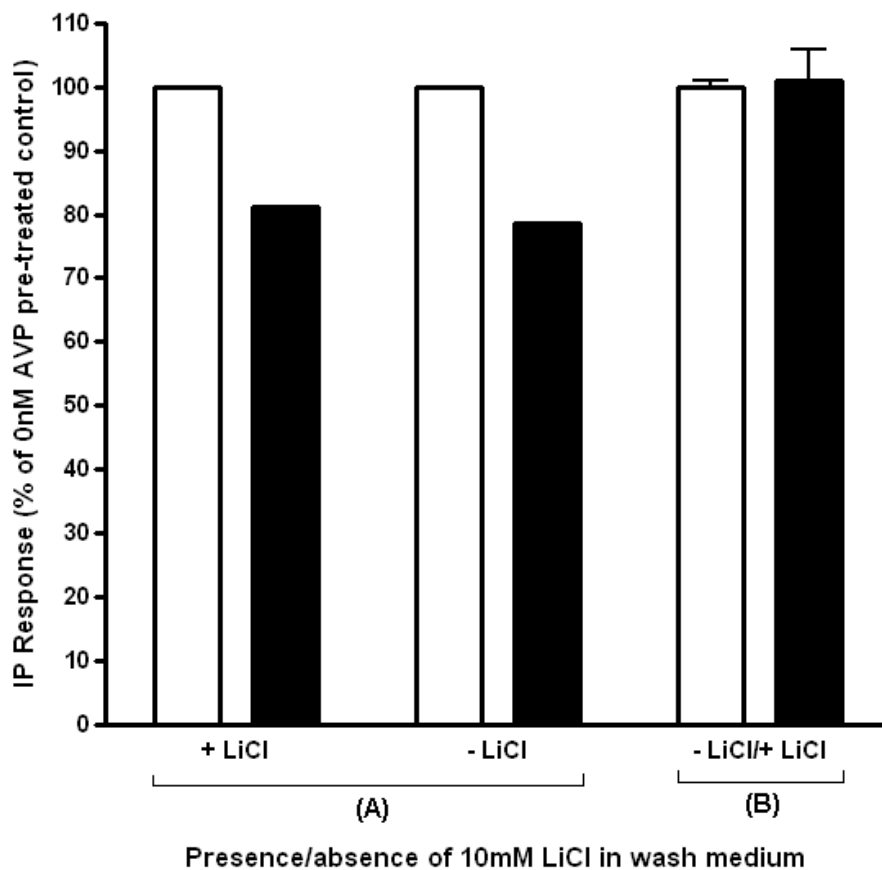


**Figure 3.11. Effects of LiCl in the wash medium on the measured desensitisation of CHO-V1b.** CHO-V1b cells were exposed to either 0nM (control, open bars) or 5nM AVP (pre-treated, black bars) for 15 minutes in the absence of LiCl for the pre-treatment. The cells were then either: (A) washed twice rapidly with medium with (+ LiCl) or without (- LiCl) 10mM LiCl, or (B) subjected to two 5 minute washes; first with medium without LiCl, then with LiCl containing medium (- LiCl/+ LiCl). The IP response to a subsequent treatment with 100nM AVP for 15 minutes is shown (expressed as the % of the appropriate 0nM AVP pre-treated control). Data are the results of one experiment, performed in duplicate for protocol (B) or without replicates for protocol (A).

### 3.4.3.2 The effect of AVP pre-treatment duration

From the results shown above it appeared that manipulation of LiCl exposure was unlikely to minimise the “carry over” of IPs from the pre- to the test AVP treatments. It was believed that the IP “carry over” could be minimised by reducing the IPs produced in response to the pre-treatment and this could be achieved by reducing the duration of the pre-treatment. Desensitisation of the IP response of PLC-coupled GPCRs has been shown to occur with a single pre-treatment with a duration as low as 3 minutes (Freedman et al., 1997; Oppermann et al., 1996). In addition, a significant reduction (to ~80% of control) of the ACTH response to V1b-R stimulation occurred within 5 minutes in ovine anterior pituitary cells (Hassan et al., 2003). Therefore, the effect of decreasing the AVP pre-treatment duration to 5 minutes was investigated.

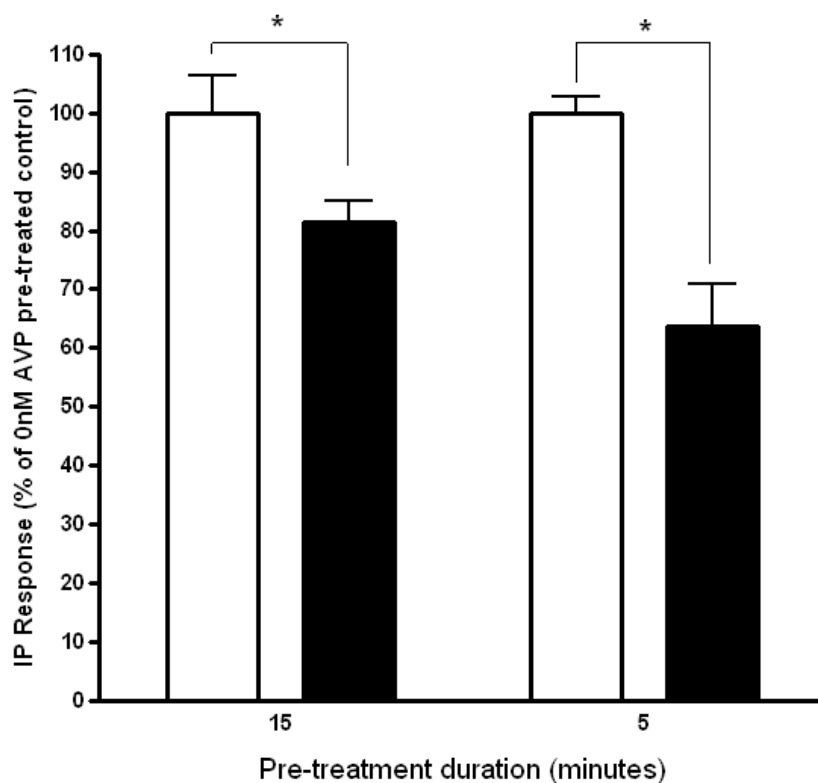


**Figure 3.12. Effects on measurable desensitisation of reducing the duration of the pre-treatment to 5 minutes.** CHO-V1b cells were exposed to either 0nM (control, open bars) or 5nM AVP (pre-treated, black bars) for 5 or 15 minutes in the absence of LiCl for the pre-treatment. The cells were then washed twice rapidly with medium with LiCl. The IP response to a subsequent treatment with 100nM AVP for 15 minutes is shown (expressed as the % of the appropriate 0nM AVP pre-treated control). Data are the results of two experiments, each performed in duplicate.

CHO-V1b cells were exposed to 5nM AVP for 5 or 15 minutes, washed rapidly twice with LiCl containing medium, and then stimulated for 15 minutes with 100nM AVP. The IP response was reduced to  $81.5 \pm 3.6\%$  of the non-pre-treated control for cells pre-treated for 15 minutes, or to  $63.6 \pm 7.4\%$  for cells pre-treated for 5 minutes (Figure 3.12). Both pre-treatment durations resulted in a significant reduction in the IP response to the test treatment (*t*-test, \*  $P < 0.05$ ), however greater desensitisation was seen with a 5 minute pre-treatment. Stimulation for 5 minutes with 5nM is sufficient to initiate the process of desensitisation, while the short exposure time minimised the IPs produced during pre-treatment.

### 3.4.3.3 The effect of AVP pre-treatment concentration

To determine the effect on the magnitude of desensitisation of increasing the AVP concentration of the pre-treatment CHO-V1b cells were exposed to a 5 minute pre-treatment with 0, 5, 20 or 100nM AVP. The IP response to a subsequent stimulation with 100nM AVP for 15 minutes was measured.

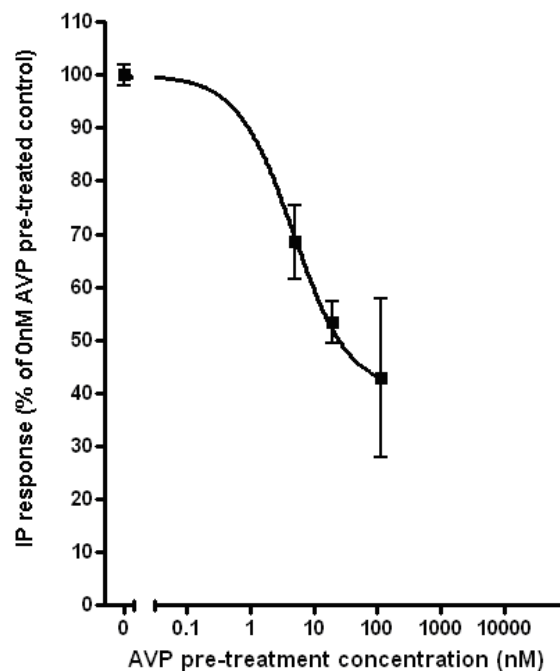


**Figure 3.13. Effect of AVP concentration used in pre-treatment on magnitude of desensitisation.** CHO-V1b cells were exposed to 0, 5, 20 or 100nM AVP for 5 minutes in the absence of LiCl for the pre-treatment. The cells were then washed twice rapidly with medium containing LiCl. The IP response to a subsequent treatment with 100nM AVP for 15 minutes is shown (expressed as the % of the 0nM AVP pre-treated control). Data are the results of one experiment, performed in duplicate.

Desensitisation exhibited dose-dependence: with an increase in the AVP concentration of the pre-treatment the magnitude of desensitisation increased (Figure 3.13). For example, pre-treatment with 20nM AVP reduced the IP response to  $53.3 \pm 4.8\%$  of the non-pre-treated control, compared to  $68.5 \pm 7.9\%$  for pre-treatment with 5nM AVP (Figure 3.13). Although increasing the AVP concentration of the pre-treatment appeared to increase the magnitude of the desensitisation, it is desirable to measure desensitisation with a concentration of AVP that is within the range measured endogenously. The peak AVP concentration measured in the pituitary portal circulation of the rat is  $<2\text{nM}$  (Plotsky et al., 1985), therefore an AVP concentration of 5nM is closer to physiological. Desensitisation can be measured in CHO-V1b cells with a 5 minute 5nM AVP pre-treatment which is within the physiological range for rat and sheep (Mason et al., 2002).

### **3.5 DESENSITISATION OF THE INOSITOL PHOSPHATE RESPONSE TO AVP USING V1b-R-TRANSFECTED HEK293 CELLS**

For practical reasons, mentioned above, CHO-V1b cells were used to optimise the IP assay protocol for the desensitisation of the V1b-R. However, the V1b-R may have different IP responsiveness in different cell types (as discussed above). Therefore it was necessary to confirm that the protocol used to induce desensitisation in CHO-V1b cells was also appropriate for investigating V1b-R desensitisation in HEK293 cells.

#### **3.5.1 Desensitisation of the inositol phosphate response to AVP using V1b-R-transfected HEK293 cells**

Since pre-treatment with 5nM AVP for 5 minutes caused significant, reproducible desensitisation to a subsequent AVP stimulation in CHO-V1b cells, this concentration and duration of AVP treatment was tested in HEK293 cells transfected with the V1b-R. For desensitisation experiments HEK293 cells were transfected with the V1b-R, then labeled with *myo*[ $^3\text{H}$ ]-inositol (as described



above). Following transfection and labeling, the cells were pre-treated with 5nM AVP for 5 minutes, rapidly washed twice with LiCl containing medium and then stimulated with 100nM AVP for 15 minutes. The IPs produced were then collected and measured (as described above).

Following pre-treatment, the IP response to AVP stimulation was reduced to  $62.8 \pm 9.1\%$  of that seen in control cells that were not pre-treated (Figure 3.14) (*t*-test, \*\*  $P < 0.02$ ). Therefore, desensitisation can be induced in V1bR-transfected HEK293 cells by a brief pre-treatment with a physiologically relevant concentration of AVP.

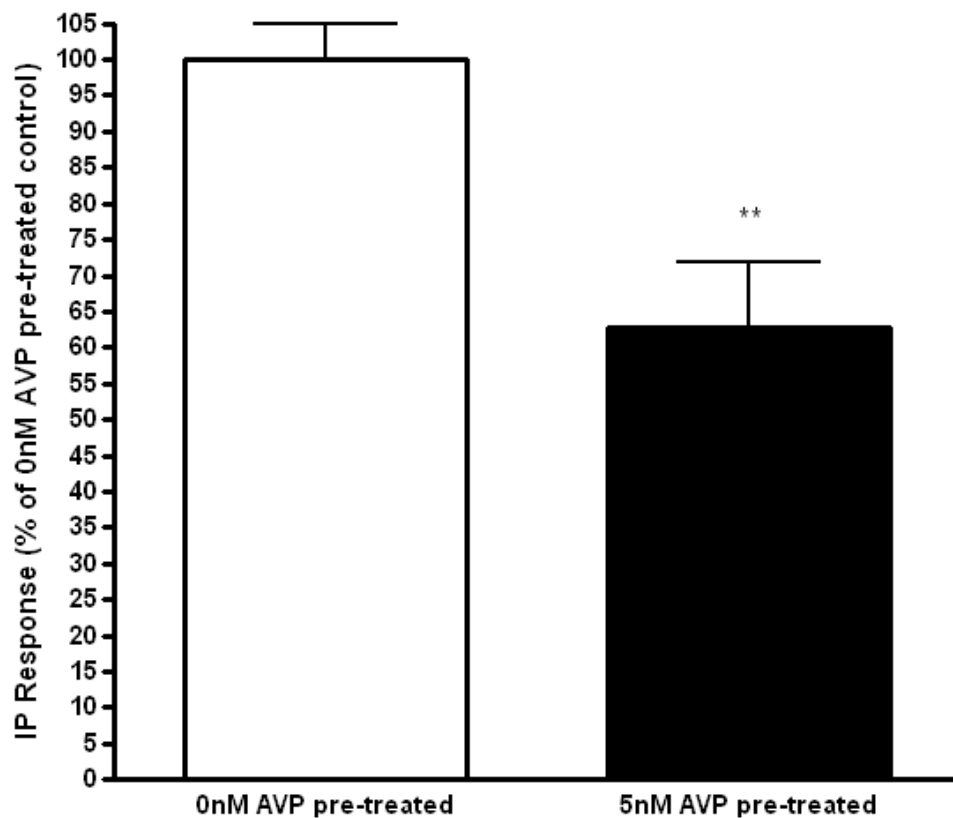


**Figure 3.14. Desensitisation of the IP response to AVP in V1b-R-transfected HEK293 cells.** V1b-R-transfected HEK293 cells were exposed to either 0nM (open bar) or 5nM AVP (black bar) for 5 minutes in the absence of LiCl for the pre-treatment. The cells were then washed twice rapidly with medium containing LiCl. The IP response to a subsequent treatment with 100nM AVP for 15 minutes is shown (expressed as the % of the 0nM AVP pre-treated control). Data are the results of four experiments, each performed in duplicate. (*t*-test, \*\*  $P < 0.02$ ).

### 3.5.1.1 The effect of AVP pre-treatment concentration

The effect of increasing the AVP concentration of the pre-treatment on desensitisation of the IP response in HEK293 cells was investigated. V1b-R-transfected HEK293 cells were exposed to a 5 minute pre-treatment with 0, 5 or 50nM AVP, and the IP response to a subsequent stimulation with 100nM AVP for 15minutes was determined. Pre-treatment with 50nM AVP reduced the IP response to  $64.3 \pm 16.3\%$  of the non-pre-treated control, compared to  $63.2 \pm 28.3\%$  for pre-treatment with 5nM AVP (Figure 3.15).

Therefore, increasing the concentration of the pre-treatment did not appear increase the magnitude of desensitisation (Figure 3.15) in contrast to CHO-V1b cells (see Figure 3.13). These results were inconclusive however, as the SEM values were large.

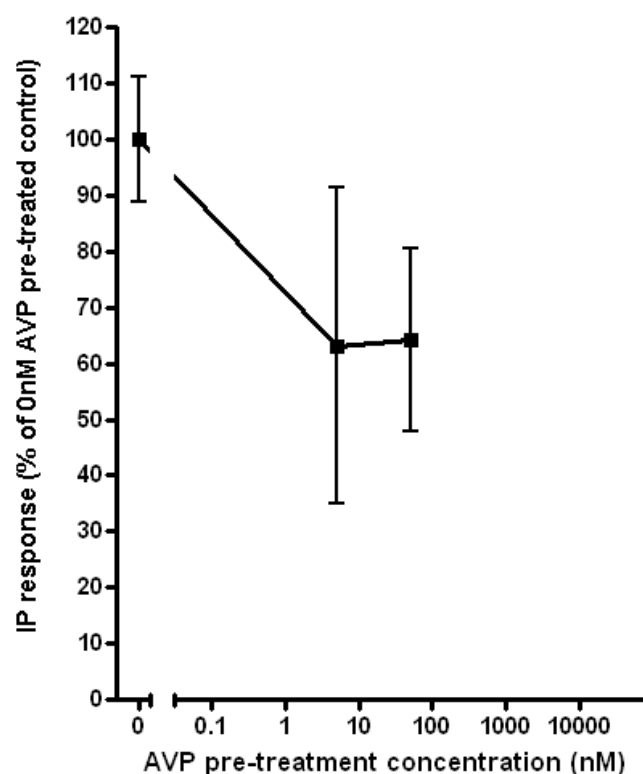


**Figure 3.15. Effects of increasing pre-treatment AVP concentration on magnitude of desensitisation in HEK293 cells.** V1b-R-transfected HEK293 cells were exposed to either 0nM (control, open bars), 5 or 50nM AVP (pre-treated, black bars) for 5 minutes. The IP response to a subsequent treatment with 100nM AVP for 15 minutes is shown (expressed as the % of the appropriate 0nM AVP pre-treated control). Data are the results of one experiment, performed in duplicate.

### 3.5.1.2 The effect of AVP pre-treatment duration

V1b-R-transfected HEK293 cells were pre-treated with 5nM AVP for 5 or 15 minutes to induce desensitisation (as described previously for CHO-V1b). The IP response to a subsequent treatment with 100nM AVP for 15 minutes was then measured.

The IP response was reduced to  $64.7 \pm 8.2\%$  of the non-pre-treated control for cells pre-treated for 15 minutes, or  $41.9 \pm 5.6\%$  for cells pre-treated for 5 minutes (Figure 3.16). Both pre-treatment durations resulted in a significant reduction in the IP response to the test treatment (*t*-test, \*  $P < 0.05$ ). However, greater desensitisation was seen with 5 minute pre-treatment, consistent with the results obtained for CHO-V1b cells. Therefore, stimulation for 5 minutes with 5nM AVP is sufficient to initiate the process of desensitisation of the V1b-R in HEK293 cells.

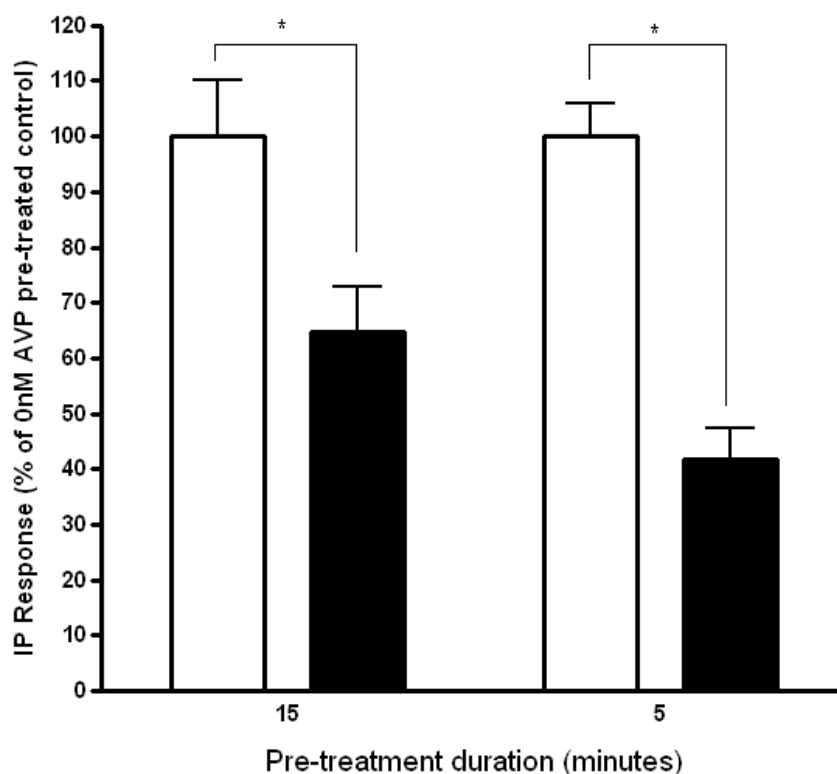


**Figure 3.16. Effect of pre-treatment duration on the magnitude of desensitisation in HEK293 cells.** V1b-R-transfected HEK293 cells were exposed to either 0nM (control, open bars) or 5nM AVP (pre-treated, black bars) for 5 or 15 minutes. The IP response to a subsequent treatment with 100nM AVP for 15 minutes is shown (expressed as the % of the appropriate 0nM AVP pre-treated control). Data are the results of two experiments, each performed in duplicate. (*t*-test, \*  $P < 0.05$ ).

### 3.5.1.3 The effect of the duration of incubation with *myo*[<sup>3</sup>H]-inositol

There was considerable variability in the absolute IP production (CPM) for inositol phosphate assays (IP assays) performed at different times (results not shown). This appeared to have little or no effect on the final results as the IP response was always expressed as a percentage relative to an appropriate control. However examination of the raw data (CPM) of several experiments revealed that there was an increase in CPM with increasing incubation duration of incubation with *myo*[<sup>3</sup>H]-inositol. An experiment was carried out to investigate whether the duration of incubation with *myo*[<sup>3</sup>H]-inositol effects the desensitisation. Other researchers report incubating cells with *myo*[<sup>3</sup>H]-inositol for 18-24 hours (Freedman et al., 1997), 16-24 hours (Oppermann et al., 1996) and 17-22 hours (Iwata et al., 2005) for the inositol phosphate assay. For this experiment, V1b-R-transfected HEK293 cells were incubated with *myo*[<sup>3</sup>H]-inositol for 16, 20 or 24 hours prior to AVP stimulation. The cells were pre-treated for 5 minutes with 5nM AVP, and the IP response to a subsequent stimulation with 100nM AVP was determined (as described previously).

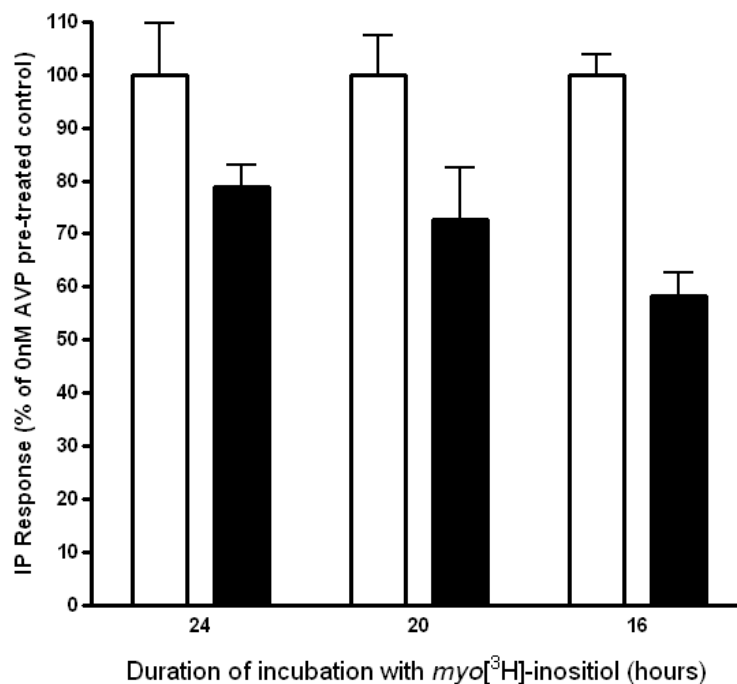


**Figure 3.17. Testing the effect the duration of incubation with *myo*[<sup>3</sup>H]-inositol.** V1b-R-transfected HEK293 cells were labeled with *myo*[<sup>3</sup>H]-inositol for 16, 20 or 24 hours prior to stimulation with AVP. Following labeling the cells were exposed to either 0nM (control, open bars) or 5nM AVP (pre-treated, black bars) for 5 minutes. The IP response to a subsequent treatment with 100nM AVP for 15 minutes is shown (expressed as the % of the appropriate 0nM AVP pre-treated control). Data are the results of one experiment, performed in duplicate.

Interestingly, decreasing the duration of incubation with the tracer to 16 hours was associated with an increase in the magnitude of desensitisation. The IP response of AVP (5nM) pre-treated cells labeled with *myo*[<sup>3</sup>H]-inositol for 16 hours was  $58.2 \pm 4.5\%$  of the non-pre-treated control, compared to  $78.9 \pm 4.1\%$  or  $72.6 \pm 9.7\%$  for cells labeled for 24 or 20 hours respectively (Figure 3.17). However, cells labeled for 16 hours generated very low CPM values. At low CPM values (<150 counts per minute) the accuracy of counting is poor and may compromise the experiment. The low CPM values were probably caused by low uptake and metabolic incorporation of the *myo*[<sup>3</sup>H]-inositol. An incubation time of 20 hours is sufficient to generate measurable CPM values and reproducible IP responses. Therefore, cells were labeled for as close as possible to 20 hours (no less than 18 hours) for each IP assay.

### 3.6 THE FINAL PROTOCOL FOR OBSERVATION OF DESENSITISATION OF THE V1b-R MEDIATED IP RESPONSE IN HEK293 CELLS

The flow diagram below outlines the final protocol developed for the observation of desensitisation of the V1b-R in HEK293 cells using the IP assay (Figure 3.18). These methods can be used to investigate the involvement of GRK5 in this desensitisation using RNAi.

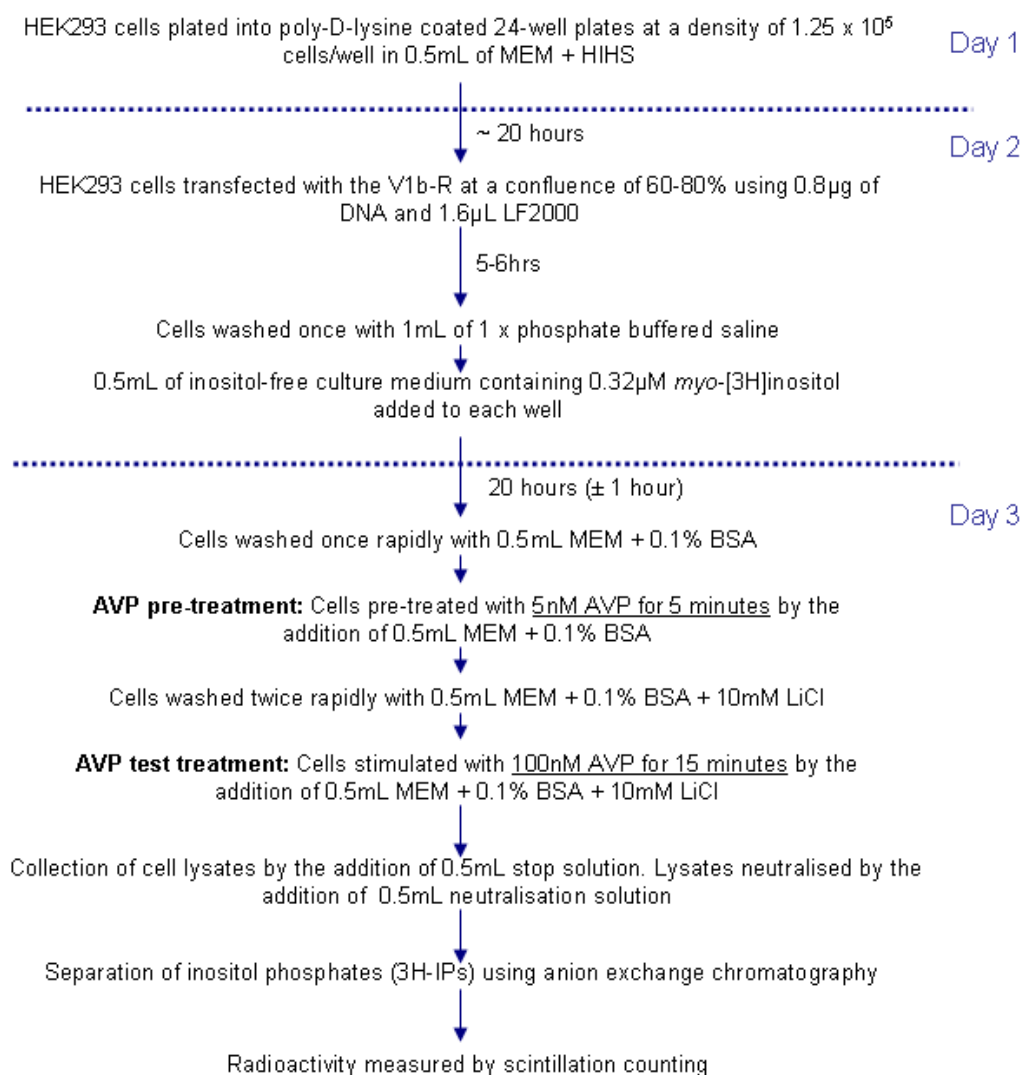


**Figure 3.18. Outline of the final protocol developed for observing desensitisation of the V1b-R mediated IP response to AVP in HEK293 cells.**

## 4

# **ASSESSMENT OF HUMAN G PROTEIN-COUPLED RECEPTOR KINASE 5 EXPRESSION IN HEK293 CELLS USING QUANTITATIVE RT-PCR**

### **4.1 INTRODUCTION**

In order to interpret the results of an RNAi experiment correctly it is important to show that the effects observed are the result of siRNA-specific degradation of the target mRNA. Knockdown of the target should be demonstrated at both the protein and mRNA levels using quantitative techniques to allow for an accurate estimate of the level of reduction. Western blots have been used to quantitatively determine knockdown of GRK proteins following transfection of HEK293 cells with siRNAs (Kim et al., 2005; Ren et al., 2005; Violin et al., 2006). While qRT-PCR has been the method used to demonstrate mRNA knockdown (Cortez et al., 2007; Miao et al., 2007).

Real-time polymerase chain reaction (PCR) can be used to quantify starting amounts of nucleic acid template by analysing the amount of DNA produced during each cycle of PCR (Avison, 2007). It is a form of quantitative PCR (qPCR). Real-time PCR is often preceded by reverse transcription to detect ribonucleic acids (RNA) via their complementary DNA (cDNA). In fact, messenger RNA (mRNA) quantification is one of the most frequent uses of real-time PCR. This method is referred to as quantitative reverse transcription PCR (qRT-PCR). qRT-PCR is the most common method for comparing mRNA levels in different sample populations (Wong and Medrano, 2005) and is often used to assess mRNA levels following knockdown by siRNA (Cortez et al., 2007; Miao et al., 2007). The research presented in this chapter was focused on development

and validation of qRT-PCR methods to assess human G protein-coupled receptor kinase 5 (GRK5) mRNA expression in HEK293 cells.

## **4.2 STANDARD METHODS AND MATERIALS**

### **4.2.1 Materials**

For the sources of all materials used in this study, refer to Appendix A.

### **4.2.2 Solutions and media**

For the details of all solutions and media used in this study, refer to Appendix B.

### **4.2.3 Avoiding RNase contamination**

Ribonuclease enzymes (RNases) degrade RNA and so it essential to eliminate RNase contamination while working with RNA (Avison, 2007). Therefore, some basic precautions were taken to avoid RNase contamination during RNA extraction and reverse transcription. These included: wearing gloves, having dedicated equipment (eg. pipettors), using plasticware (eg. tips and tubes) that is guaranteed RNase-free, and using RNase free reagents and solutions. For plasticware that was recycled (such as the lids of Schott bottles) the plastic was soaked in 0.1% diethylpyrocarbonate (DEPC) made up in ddH<sub>2</sub>O with gentle mixing overnight. The plastic was then wrapped in foil and autoclaved for 15 minutes at 15lb/sq in to eliminate residual DEPC. RNase-free solutions were prepared either by the addition of 0.1% DEPC followed by autoclaving



as before, or by preparing the solutions using RNase-free ddH<sub>2</sub>O (see Appendix B for details for each solution). Glassware and foil was baked at  $\geq 180^{\circ}\text{C}$  for 8 hours to eliminate RNase. In addition, just prior to working with RNA the area of bench to be used was swabbed with either RNasezap (Ambion) or RNase-away (Invitrogen) where possible and RNase-free foil was placed on the bench to provide an RNase-free work surface.

#### **4.2.4 RNA extraction**

##### **4.2.4.1 Preparation of HEK293 cells for RNA extraction**

HEK293 cells were plated into individual poly-D-lysine coated 10cm<sup>2</sup> culture plates at a density of  $8.75 \times 10^5$  cells/plate (unless otherwise indicated) in 2.5mL of normal tissue culture medium (MEM + HIHS). The cells were cultured for approximately 24 hours so that a confluence of 80-90% was reached. The medium was aspirated from each well and the cells were then either used immediately for RNA extraction, or frozen rapidly, by placing the plate onto dry ice, and stored at  $-80^{\circ}\text{C}$  for later RNA extraction (Avison, 2007).

##### **4.2.4.2 RNA extraction**

Total RNA was extracted from HEK293 cells using one of the three methods described below. For each method, the RNA was resuspended in 45 $\mu\text{L}$  of RNase-free ddH<sub>2</sub>O with 1 x RNasesecure (Ambion). The RNA solution was heated to  $65^{\circ}\text{C}$  for 10 minutes (using a Labnet Accublock digital dry bath) to activate the RNasesecure, aliquoted into several tubes and stored at  $-20^{\circ}\text{C}$  for up to two weeks (or stored at  $-80^{\circ}\text{C}$  for longer durations).

For the first method, referred to as the TRIreagent-based method, TRIreagent (Molecular Research Centre, Inc) was used following the manufacturer's instructions. The cells in the plate were lysed by the addition of 1mL of TRIreagent. The lysate was homogenised by repipetting (using a 1mL

Gilson pipette) over the surface of the plate, transferred to a 1.5mL tube and then incubated at room temperature for 5 minutes to allow complete dissociation of nucleoprotein complexes. 1-bromo-3-chloropropane (BCP) (0.1mL) was then added, mixed vigorously by shaking for 15 seconds and incubated at room temperature for 10 minutes. The mixture was then centrifuged at 4°C, 10700rpm for 10 minutes (Eppendorf centrifuge 5417) to separate the phases. The RNA-containing aqueous phase (~500µL) was carefully transferred to a new tube, and the RNA was precipitated by addition of an equal volume of isopropanol. The RNA was pelleted by centrifugation at 4°C, 10700rpm for 10 minutes. The pelleted RNA was washed with 1mL of 75% (v/v) ethanol, air dried for 10 minutes and resuspended in 45µL of RNase-free ddH<sub>2</sub>O with 1 x RNasesecure.

The second method, referred to as the column-based method, used the BP-10 Spin Column Total RNA Minipreps Super Kit (Biopioneer Inc.) following the manufacturer's instructions. The cells were disrupted by the addition of 350µL RLT solution, and homogenised by passing the lysate through a 20-G needle ~20X. An equal volume (350µL) of 70% ethanol was added to the lysate, mixed by repipetting and then transferred to a BP-10 spin column in a 2mL collection tube. The column and collection tube was centrifuged at 8000rpm for 1 minute (Eppendorf centrifuge 5417) at room temperature. The RNA was washed by adding 500µL of RW solution to the column, and then centrifuged as before. This was followed by an additional wash with 500µL RPE solution. The column with bound RNA was then transferred to an RNase-free 1.5mL tube. The RNA was eluted from the column by adding 45µL of RNase-free ddH<sub>2</sub>O containing 1 x RNasesecure, heating the column to 50°C for 2 minutes (using a Labnet Accublock digital dry bath) and then centrifuging at 10000rpm for 1 minute at room temperature.

The third method was essentially a combination of the first two methods; TRIreagent was used to generate an aqueous homogenate containing RNA which was then purified using the column-based method (Dr Aaron Jeffs, University of Otago, *Pers Comm.*). The first part of the method was equivalent to the first steps of the TRIreagent-based method described above. HEK293 cells were lysed by the addition of 1mL of TRIreagent, homogenised by repipetting and the lysate was transferred to a 1.5mL tube. The mixture was incubated at room temperature for 5 minutes. BCP (0.1mL) was then added and mixed vigorously. The mixture was incubated at room temperature

for 10 minutes and then centrifuged at 10700rpm for 10 minutes at 4°C. 400µL of the RNA-containing aqueous phase was carefully transferred to a new tube. The RNA was then purified from the aqueous phase using the column-based method described above. An equal volume (400µL) of 70% ethanol was added to the aqueous phase, mixed by repipetting and then 700µL was transferred to a BP-10 spin column in a 2mL collection tube. The RNA was then washed, and finally eluted from the column as described above for the column-based method.

#### 4.2.4.3 Analysis of RNA

The RNA quality was analysed by native DNA gel electrophoresis. RNA samples were separated by electrophoresis through a 1% agarose/1 x TAE gel (see Appendix B for details) using a Hoeffer HE33 MINNIE Submarine electrophoresis tank and a Power Pac 300 power supply (BIORAD). 5µL of the RNA sample combined with 1µL of gel loading dye (see Appendix B for details) was loaded per well. Precautions were taken to avoid RNase contamination, for example the gel was prepared RNase-free and the electrophoresis tank was wiped with RNasezap or RNase-away prior to loading each gel. Electrophoresis was performed at 100 V for 60 minutes. The DNA was visualised by UV transillumination using the Chemi Genius<sup>2</sup> Bio Imaging System and photographed (GeneSnap from Syngene).

Total RNA was quantified using an ND1000 NanoDrop spectrophotometer. ddH<sub>2</sub>O with 1 x RNase-free was used to zero the spectrophotometer prior to reading each sample. 1µL of the RNA sample was then used to read the RNA concentration (ng/µL) based on the absorbance of the sample at 260nm. The absorbance ratios 260/280 and 260/230 were also recorded for each RNA sample as these values indicate the purity of the RNA.

#### 4.2.5 Reverse transcription

The cDNA was synthesised from total RNA using reverse transcription. This procedure was performed as recommended by the supplier of the Expand Reverse Transcriptase enzyme (Roche).

Reverse transcription was performed using RNase-free solutions and plastic ware, and appropriate precautions were taken to avoid RNase contamination (as described in section 4.2.3 above). The reaction was performed in 0.5mL tubes and heated using a PTC-200 Petlier Thermal Cycler (MJ Research) with a heated lid to avoid evaporation.

To prepare the RNA 0.5-2µg of RNA was combined with 0.25µg of oligo (dT)<sub>12-18</sub> primer and 1 x RNAsure, then made up to 10µL with ddH<sub>2</sub>O. The RNA mixture was denatured at 65°C for 10 minutes, then immediately chilled on ice. 10µL of a reverse transcription mixture (see Appendix B for full details) containing 1 x first-strand reverse transcriptase buffer (250mM Tris-HCl, 200mM KCl, 25mM MgCl<sub>2</sub>, pH 8.3; provided by Roche), 1 x RNAsure, 1 x dithiothreitol (DTT) (an RNA protector), 2mM deoxynucleotides (dNTPs) and 50U of Expand Reverse Transcriptase enzyme was then added to the RNA mixture. The reaction mixture was incubated at room temperature for 10 minutes then heated to 42°C. Reverse transcription was allowed to proceed at 42°C for 4-10 hours. The reaction was inactivated by heating to 70°C for 15 minutes. The cDNA was diluted 5-fold by the addition of 80µL of ddH<sub>2</sub>O and stored at -20°C.

#### **4.2.6 Polymerase chain reaction (PCR)**

##### **4.2.6.1 PCR reactions**

PCR was carried out using either a PTC-200 (MJ Research) or a DNA Engine® (BIORAD) Peltier Thermal Cycler with a heated lid. The standard 20µL PCR reaction contained the following reagents: 2µL 10x Taq polymerase buffer (contains 100mM Tris-HCl, 15mM MgCl<sub>2</sub>, 500mM KCl, pH 8.3; Roche), 2.5µL dNTPs (2mM), 1µL of each primer (forward and reverse) (10pmol/µL), 1µL of MgCl<sub>2</sub> (25mM), 2µL of template DNA, 10.3µL ddH<sub>2</sub>O and 0.2µL Taq polymerase (5U/µL; Roche). The thermal cycling conditions comprised a denaturation step at 94°C for 5 minutes, 35 cycles of 3-step PCR including denaturation for 45 seconds at 94°C, annealing for 45 seconds at 50°C (unless otherwise indicated) and extension for 1 minute at 72°C, and a final extension at 72°C for 5 minutes. Where necessary PCRs were optimised by carrying out annealing temperature

gradients. PCR products were kept at 4°C until used for analysis (on the same day). The sequences of all primers used for PCR are provided in Table 4.1.

#### 4.2.6.2 Agarose gel electrophoresis of PCR products

PCR products were separated by electrophoresis through a 1% agarose/1 x TAE gel (see Appendix B for details) using a Hoeffer HE33 MINNIE Submarine electrophoresis tank and a Power Pac 300 power supply (BIORAD). 5µL of PCR product combined with 1µL of gel loading dye (see Appendix B for details) was loaded per well. Electrophoresis was performed at 85V for 90 minutes. The DNA was visualised by UV transillumination using the Chemi Genius<sup>2</sup> Bio Imaging System and photographed (GeneSnap from Syngene).

### 4.2.7 DNA sequencing

#### 4.2.7.1 DNA preparation

For sequencing reactions the PCR products to be sequenced were purified using the UltraClean<sup>TM</sup>15 DNA purification kit (MO BIO Laboratories, Inc) using the manufacturer's instructions. This purification procedure removes unwanted chemical contaminants from the DNA solution so that they do not interfere with the sequencing reaction. 30µL of PCR product (15µL from each of two different PCR runs) was used for DNA purification. The DNA was combined with 90µL ULTRA SALT by inverting the tube. 6µL of ULTRA BIND (a 50:50 mix of pure silica with buffer) was added to the mixture, combined by shaking the tube and then incubated at room temperature for 5 minutes. During this step, the DNA binds to the silica in the presence of salt. The mixture was centrifuged for 5 seconds to pellet the silica, and the supernatant was then removed. The pellet was resuspended in 1mL of ULTRA WASH (buffered ethanol solution), then centrifuged as before and the supernatant was discarded. The centrifugation step was repeated and all traces of supernatant were removed by aspirating. The pellet was then resuspended in 12µL of

TE8 buffer (see Appendix B for details) by pipetting until a uniform suspension was achieved. The suspension was incubated at room temperature for 5 minutes to allow the DNA to dissociate from the silica. The silica was then pelleted by centrifugation for 1 minute, and the DNA-containing supernatant was immediately transferred to a new tube.

The DNA concentration was estimated by agarose gel electrophoresis of 5 $\mu$ L of sample. Hyperladder I (Bioline), a DNA molecular weight marker with bands of known DNA concentration, was used as a reference.

#### 4.2.7.2 DNA sequencing reactions

PCR products were sequenced by primer sequencing. This was performed by Canterbury Sequencing using the BigDye Terminator v3.1 Cycle Sequencing Kit (Applied Biosystems). 3.3pmol of each primer and 12ng of DNA template (PCR product) were used for each sequencing reaction. The DNA to be sequenced was denatured and the single stranded molecules labeled with fluorescent dideoxynucleotides using the kit reagents. The labeled DNA fragments were analysed automatically in an ABI Prism® 3100 Genetic Analyser (Applied Biosystems). Samples underwent electrophoresis in the system's vertical gel, followed by laser detection and computer analysis. The final data was provided as electronic ABI trace files.

#### **4.2.8 Quantitative reverse transcription polymerase chain reaction (qRT-PCR)**

Two-step quantitative reverse transcription polymerase chain reaction (qRT-PCR) was used to detect expression of GRK5 mRNA. For two step qRT-PCR, the reverse transcription of RNA into cDNA was separated from other reaction steps and performed outside the PCR instrument (as described in section 4.2.5). The subsequent amplification and monitoring was performed according to standard real time PCR procedure with the Stratagene Mx3005P<sup>TM</sup> real time PCR system using the cDNA as a template. Generation of product during qRT-PCR was detected by monitoring the

formation of double-stranded DNA (dsDNA) using SYBR green. This fluorescent dye intercalates dsDNA. Therefore the intensity of fluorescence is proportional to the quantity of DNA present (Avison, 2007).

The qRT-PCR reaction was carried out using a pre-prepared SYBR green qPCR mix that contained all the reagents (except primers and template) required for running qPCR. For this study either SYBR Green supermix (BioRad), FastStart SYBR Green Master (Roche) or a mixture prepared in our laboratory (Dr Jason Song, *Pers Comm.*) was used. The PCR reaction mixture was prepared based on the recommendations of the manufacturer of the FastStart SYBR Green Master (Roche). A standard 20 $\mu$ L qPCR reaction contained the following reagents: 10 $\mu$ L SYBR green qPCR mix (final concentration of 1x), 1 $\mu$ L of each primer (forward and reverse) (10pmol/ $\mu$ L), 1 $\mu$ L of template DNA (cDNA) and 7 $\mu$ L ddH<sub>2</sub>O. The thermal cycling conditions comprised a denaturation step at 95°C for 10 minutes, then 40 cycles of 3-step PCR including denaturation for 30 seconds at 95°C, annealing for 45 seconds at 50-52°C and extension for 45 seconds at 72°C. Unless otherwise stated the fluorescence was measured during the extension phase of the PCR cycle. This was followed by a single cycle including 1 minute at 95°C, 30 seconds at 55°C and finally 30 seconds at 95°C. PCR products were kept at 4°C if required for later analysis.

To normalise for differences in the amount and quality of total cDNA added to the reaction, amplification of  $\beta$ -actin and 18S ribosomal RNA (rRNA) was performed as an endogenous control. The sequences of all primers used for qRT-PCR are provided in Table 4.1.

#### 4.2.8.1 Reference genes

Traditionally, genes thought to have stable expression (“housekeeping genes”) have been employed as controls for gene expression assays. Due to the increased sensitivity of real-time PCR over traditional quantitation techniques, many of the well known “housekeeping genes”, such as glyceraldehydes-3-phosphate dehydrogenase (GAPDH), have in fact been shown to be affected by various treatments, biological processes, and cell types (von Ahsen et al., 1999). Therefore normalisation of qRT-PCR results with a single reference gene can falsely bias results (Wong and

Medrano, 2005). Normalisation of samples against a panel of 2-3 reference genes is recommended (Bustin, 2002).

Two reference genes were used to normalise the GRK5 expression data in this study. These genes also served as a positive control for the reaction. 18S rRNA was used both as a positive control for standard PCR reactions, and as a reference gene for qRT-PCR. 18S rRNA appears to be a good candidate for use as a reference gene for qRT-PCR in HEK293 as a recent study showed that 18S rRNA has constant levels of expression across different human cells lines and following different treatments (Bandaa et al., 2008). The 18S rRNA primers used in this study were designed by Dr Jason Song of the University of Canterbury.

$\beta$ -actin mRNA was used as a second reference gene.  $\beta$ -actin is a widely used reference gene. The primer sequences used for this study were reported by Metaye and colleagues and have previously been used for normalisation of GRK5 mRNA expression in human thyroid tissue using qRT-PCR (Metaye et al., 2002).

#### 4.2.8.2 Analysis of qRT-PCR results

For details of the data analysis see section 2.8.2.

### 4.3 OPTIMISATION OF RNA EXTRACTION FROM HEK293 CELLS

For PCR it is essential to start with RNA that is of acceptable quality for downstream reactions. This was particularly important for sensitive applications such as qRT-PCR as most guidelines for this method insist that successful qRT-PCR is highly dependent on the quality of the RNA (Bustin, 2002). The RNA must meet certain criteria to be considered acceptable (Bustin and Nolan, 2004);



it needs to be relatively free of inhibitors of downstream reactions, minimally degraded, free of DNA contamination and free of nucleases (such as RNase) for storage. It is worth noting that qRT-PCR can be used to amplify DNA fragments as small as 60bp, therefore this technique is suitable for quantitating mRNA levels in samples containing partially degraded RNA (Bustin, 2002). The RNA samples must be free of DNA as any significant DNA contamination will result in inaccurate RNA quantification. In order to establish an appropriate method for total RNA extraction from HEK293 cells, three different methods were tested.

#### **4.3.1 Comparison of TRIreagent and column based methods of RNA extraction**

For testing RNA extraction methods HEK293 cells from the same culture were plated into several plates and then frozen as described in section 4.2.4.1. RNA was extracted from the HEK293 cells using either the TRIreagent or the column-based method (described in detail in section 4.2.4.2). The quality and quantity of the resulting RNA was analysed by gel electrophoresis and spectrophometric analysis using the NanoDrop spectrophotometer.

Gel electrophoresis of the RNA samples on a native DNA gel gave several distinct bands (Figure 4.1). The DNA molecular weight marker (mw) cannot provide a real size comparison, and was only used to assist with the identification of the bands based on their position relative to the marker. The bands corresponded to 28S and 18S ribosomal RNA, and degraded RNA (Figure 4.1). Where DNA contamination occurred this appeared as an additional band close to the origin (as seen in lane 1 above). The level of RNA degradation was estimated from the gel. If the 18S and 28S bands appear as a smear, this indicates that the RNA is highly degraded. Samples containing a large amount of degraded RNA were not used for further reactions. Some degraded RNA also appeared as a distinct band on the gel. For the RNA extracted using the TRIreagent method (lane 2 above) the intensity of the degraded RNA band is approximately equal to the total RNA of the other two bands, so for this sample it was assumed that approximately  $\frac{1}{2}$  of the RNA was degraded. Typically the RNA was more degraded in samples extracted using the TRIreagent-based

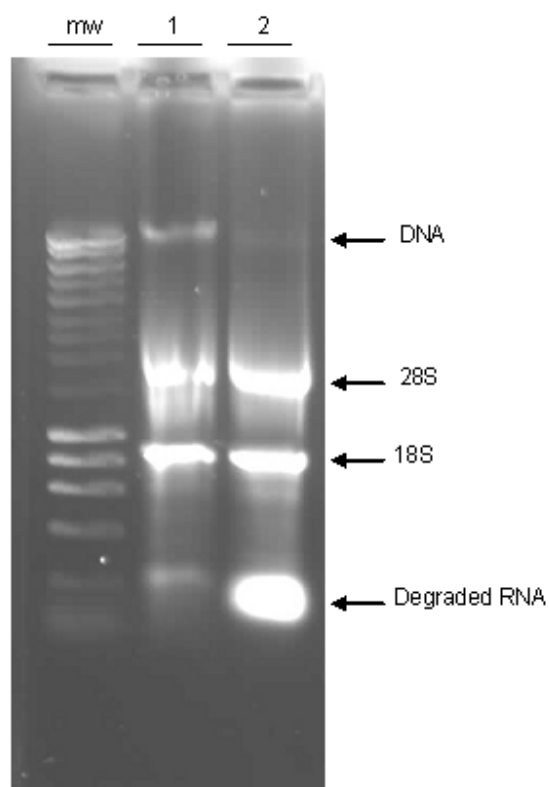


**Figure 4.1. Gel electrophoresis of RNA extracted using either the column (1) or TRIreagent (2) based method.** RNA was extracted from HEK293 cells plated at  $8.75 \times 10^5$  cells/plate and then frozen 24 hours after plating. The DNA molecular weight marker (mw) was Hyperladder I (Bioline).

method (Figure 4.1). RNA extracted using the column-based method was minimally degraded, however DNA contamination was present. The TRIreagent based protocol tended to provide a better yield than the column-based method. RNA yields from equivalent plates of HEK293 cells ranged from 758.1-1236.3ng/ $\mu$ L for the TRIreagent based method, or 727.0-849.1ng/ $\mu$ L for the column-based method. The RNA purity was assessed by spectrophometric analysis using the NanoDrop spectrophotometer. Ideally the absorbance ratios 260/280 and 260/230 should be greater than 1.8 indicating that the RNA was free of protein and carbohydrate contamination, respectively. RNA extracted using the column-based method gave 260/230 ratios of 1.21-1.35 indicating that there may be some carbohydrate contamination in the samples.

In summary, the TRIreagent based protocol provided a slightly better yield than the column-based method however the RNA was typically more degraded. The level of RNA degradation seen in Figure 4.1 was not considered a significant problem for non-quantitative PCR. Therefore, RNA extracted using the TRIreagent method was reverse transcribed and used for non-quantitative PCR. The column based method yielded RNA that was minimally degraded, but contaminated with DNA and carbohydrate which could cause significant problems in further reactions. This RNA was not used for reverse transcription or PCR.

#### **4.3.2 The combined method of RNA extraction**

For the TRIreagent method there is a potential for co-purifying phenolic compounds that can inhibit downstream reactions (Nolan et al., 2006) Therefore, RNA extracted with this method was not used for quantitative PCR in this study. Nolan and colleagues report that their most consistent qRT-PCR results were obtained using column-based protocols for RNA extraction (Nolan et al., 2006). For this research however, this method yielded RNA that was not suitable for further reactions. DNase treatment could be used to remove the DNA contamination. It was preferable however, to use an RNA extraction method that allowed the isolation of virtually DNA-free RNA as DNase can hinder further reactions and its removal can be time consuming and costly (Bustin, 2002). In fact, some researchers only DNase-treat the sample to be amplified when forced to use PCR primers that are not intron spanning (Li et al., 2000).

The combination of RNA extraction from TRIreagent homogenates with a column-based purification step (the combined method) has been shown to give consistently good quality RNA that is relatively free of inhibitors (Dr Aaron Jeffs, University of Otago, *Pers Comm.*). In addition, RNA extracted using the combined method has been shown to perform more reliably in downstream applications such as qRT-PCR than RNA extracted using either the TRIreagent or the column based method alone (Dr Aaron Jeffs, University of Otago, *Pers Comm.*).

The combined method was first tested by extracting RNA from a single plate of HEK293 cells (plated at the same time as the plates used for testing TRIreagent and column based methods) (see lane 1 in Figure 4.2 below). Analysis of the sample by gel electrophoresis gave two distinct bright bands for 18S and 28S RNA, and a very faint band for degraded RNA indicating that RNA degradation was minimal. There was no visible DNA band indicating that there was little or no DNA contamination. The RNA concentration of this sample was 542ng/ $\mu$ L, and the RNA was relatively free of protein (260/280 ratio = 2.01) and carbohydrate contamination (260/230 = 1.79).

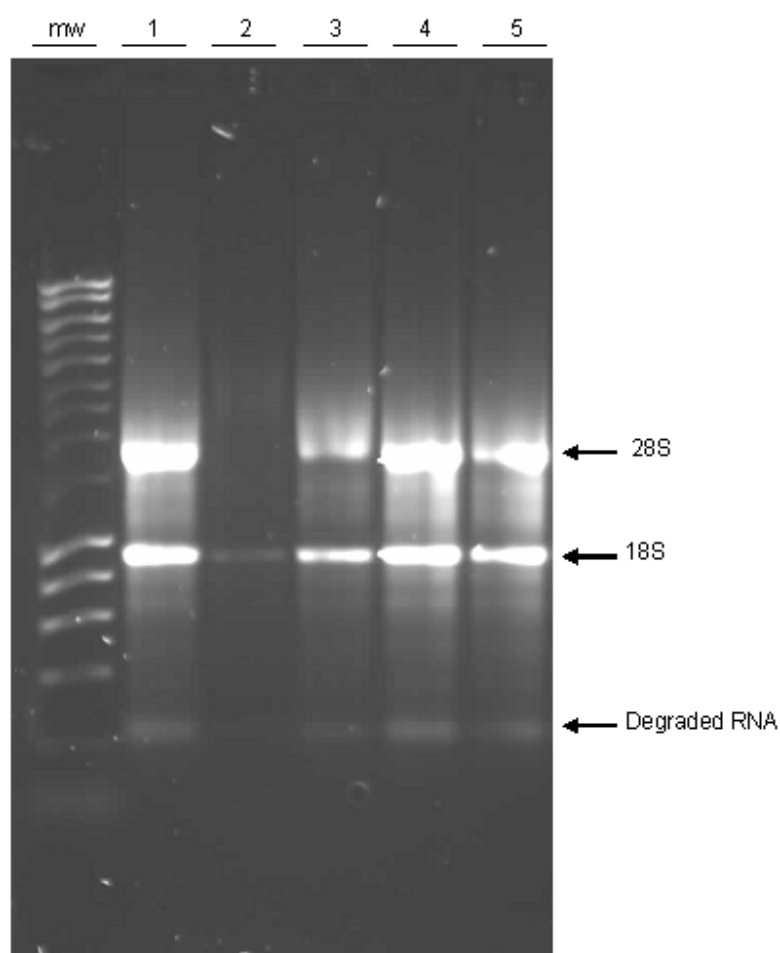


**Figure 4.2. Gel electrophoresis of RNA extracted using the combined method.** RNA was extracted from HEK293 cells plated at  $8.75 \times 10^5$  cells/plate and then frozen 1 day after plating (lane 1), or from cells plated at  $1.25 \times 10^5$  cells/plate and frozen 1 (lane 2), 3 (lane 3), 5 (lane 4) or 7 (lane 5) days after plating. The DNA molecular weight marker (mw) was Hyperladder I (Bioline).

The combined method was then used to extract RNA from HEK293 cells plated at a different cell density to ensure that the methods would enable RNA extraction from samples with varying amounts of starting material (ie. Cells) (Figure 4.2). HEK293 cells were plated at a density of  $1.25 \times 10^5$  cells/plate. The cells were then frozen 1 (lane 2), 3 (lane 3), 5 (lane 4) or 7 (lane 5) days after plating at a confluence of approximately 20, 65, 100 or >100% respectively. RNA of acceptable quality and quantity was extracted from all samples (Figure 4.2). RNA extracted from cells frozen at a confluence of 20% had a very low concentration (101.2ng/ $\mu$ L for the extraction shown here) and hence was not clearly visible on the gel. However, further analysis of this sample with the NanoDrop spectrophotometer and additional gels indicated that the RNA quality was acceptable.

All RNA used for qRT-PCR was extracted using the combined method. The quality and quantity of RNA in each sample was verified by gel electrophoresis and spectrophotometric analysis.

## **4.4 PRIMER DESIGN AND TESTING**

### **4.4.1 Design of primers for PCR amplification of GRK5**

One of two methods was used to design specific primers for the amplification of GRK5. Both methods involved the design of specific primers for PCR and qPCR using the human GRK5 mRNA sequence (NCBI accession number NM 005308) as a template. For all primers a search of the human genome was carried out using the Basic Local Alignment Search Tool (BLAST) to check for matching of each forward (F) and reverse (R) primer to human nucleotide sequences other than GRK5. Primers with a high degree of complementarity (an “expect value” <1 from BLAST) with non-target mRNA sequences, particularly at the 3' end of the primer, were excluded.

In addition, all primers selected were intron-spanning as this would allow the identification of DNA contamination following amplification using PCR (Bustin, 2002).

#### 4.4.1.1 Primer design using Primer3 software

In the first instance, Primer3 primer design software v.0.4.0 (Rozen and Skaletsky, 2000) was used to design primers for amplification of GRK5. The entire human GRK5 mRNA sequence was used as a template, and the product size range was set to 150-250 nucleotides (nt). Primer3 generated a ranked list of 5 primer pairs. Based on the results of the BLAST search a single pair of primers was selected. These primers, which will be referred to as GRK5F and GRK5R, were located at nt 902-921 and 1103-1121 of the human GRK5 mRNA sequence (Figure 4.3), amplifying a predicted 221 nt product. The melting temperature ( $T_m$ ) of GRK5F and GRK5R were 60.1 and 59.9°C respectively (Table 4.1).

#### 4.4.1.2 Multiple alignment of GRK protein sequences and primer design

As discussed earlier (see section 1.3.3), GRK5 is classified as a member of the GRK4 subfamily comprising GRK4, GRK5 and GRK6 (Ferguson, 2001; Yang and Xia, 2006). There is considerable sequence homology between these different GRKs, especially in the N-terminal 185-amino acid region. It was therefore necessary to design specific primers for GRK5 that would not amplify GRK4 or 6. The human mRNA sequences for GRK4 (NCBI accession number NM 182982) and GRK6 (NCBI accession number NM 001004106) were retrieved from the Genbank database ([www.ncbi.nlm.nih.gov](http://www.ncbi.nlm.nih.gov)). To identify regions of GRK5 that were highly conserved across mammalian species, GRK5 mRNA sequences from mouse (*Mus musculus*, NCBI accession number NM 0188869) and rat (*Rattus norvegicus*, NCBI accession number NM 030829) were also retrieved.

The amino acid sequences of the human GRK4 and GRK6, and rat and mouse GRK5 were aligned with the human GRK5 mRNA sequence (NCBI accession number NM 005308) using the multiple

alignment function of ClustalX 1.83 (<http://www-igbmc.u-strasbg.fr/Bioinfo/ClustalX/>) (Thompson et al., 1997) (Figure 4.4).

To avoid co-amplification of the other GRK genes with the target GRK5, the multiple alignment analysis data were used to select areas of the GRK5 mRNA sequence that are different from the other members of the GRK4 subfamily for GRK5 specific PCR primer design. PCR primers that bound within regions of GRK5 that were highly conserved between the different species and divergent from human GRK4 and 6 were designed using Primer Premier (Abd-Elsalam, 2003). GRK5F1 and GRK5R1 were located at nt 1500-1519 and 1843-1862 (Figure 4.3), amplifying a predicted 360 nt product. GRK5F2 and GRK5R2 were located at nt 1953-1975 and 2221-2243 (Figure 4.3), amplifying a predicted 290 nt product. The T<sub>m</sub> of the primers is indicated in Table 4.1.

**Table 4.1. Primers used for PCR and qPCR.** The sequence and melting temperature (T<sub>m</sub>) of each primer is indicated, as well as the size of the expected product for each primer pair.

Primer name	Sequence	T <sub>m</sub> (°C)	Product size (nt)
GRK5 F	5'- AAA GAG GAA AGG GGA GTC CA -3'	60.1	221
GRK5 R	5'- AGA GGA TCT CTG CCG CAT AA -3'	59.9	
GRK5 F1	5'- CTG CTC ACG AAA GAT GCG AA -3'	60.0	360
GRK5 R1	5'- CGG AGG GTG GTT TCT GTT CA -3'	60.5	
GRK5 F2	5'- AAC CAC CAC ATA AAC TCA AAC CA -3'	58.9	290
GRK5 R2	5'- AAT GTT CAC CAA AGA CAA ATC CA -3'	58.9	
18S F <sup>a</sup>	5' - TACCGTCCTAGTCTCAACCATAA – 3'	53.0	319
18S R <sup>a</sup>	5' - CAGACAAATCGCTCCACCAA -3'	52.0	
β-actin F <sup>b</sup>	5'- TCC CTG GAG AAG AGC TAC G -3'	53.0	131
β-actin R <sup>b</sup>	5'- GTA GTT TCG TGG ATG CCA CA -3'	52.0	

<sup>a</sup> Primers were designed by Dr J. Song of the University of Canterbury

<sup>b</sup> Primers were designed by Metaye and colleagues (Metaye et al, 2002)

```

841 gccaggttcg ggccacgggt aaaatgtatg cctgcaagcg cttggagaag aagaggatca
901 aaaagaggaa aggggagtcc atggccctca atgagaagca gatcctcgag aaggtcaaca
      → F
961 gtcagtttgt ggtcaacctg gcctatgcct acgagaccaa ggatgcaactg tgcttggtcc
1021 tgaccatcat gaatgggggt gacctgaagt tccacatcta caacatgggc aacctgggt
1081 tcgaggagga gcgggccttg ttttatgagg cagagatcct ctcgggctta gaagacctcc
      ← R
1141 accgtgagaa caccgtctac cgagatctga aacctgaaaa catcctgtta gatgattatg
1201 gccacattag gatctcagac ctgggcttgg ctgtgaagat ccccgaggga gacctgatcc
1261 gcggccgggt gggcactgtt ggctacatgg ctccagaggt cctgaacaac cagaggtacg
1321 gcctgagccc cgactactgg ggccttggct gcctcatcta tgagatgac gagggccagt
1381 cgccgttccg cggccgcaag gagaagtgga agcgggagga ggtggaccgc cgggtcctgg
1441 agacggagga ggtgtactcc cacaagttct ccgaggaggc caagtccatc tgcaagatgc
1501 tgctcacgaa agatgcgaag cagaggctgg gctgccagga ggagggggct gcagaggtea
      → F1
1561 agagacaccc cttcttcagg aacatgaact tcaagcgctt agaagccggg atgttgacc
1621 ctcccttcgt tccagacccc cgcgctgtgt actgtaagga cgtgctggac atcgagcagt
1681 tctccactgt gaagggcgtc aatctggacc acacagacga cgacttctac tccaagttct
1741 ccacgggctc tgtgtccatc ccatggcaaa acgagatgat agaaacagaa tgctttaagg
1801 agctgaacgt gtttggacct aatggtaccc tcccgccaga tctgaacaga aaccacctc
      ← R1
1861 cggaaccgcc caagaaaggg ctgctccaga gactcttcaa gcggcagcat cagaacaatt
1921 ccaagagttc gcccagctcc aagaccagtt ttaaccacca cataaactca aaccatgta
      → F2
1981 gctcgaaact caccggaagc agctagtctt ggctctggcc tccaagtcca cagtggaacc
2041 agcccagacc cttctcctta gaagtggaa tagtgaggcc cctgctctgg tggggctgcc
2101 aggggagacc ccgggagccg gggaaggagg ccgtccatcc cgtcgacgta gaacctcgag
2161 gtttctcaaa gaaatttcca ctcaagctctg ttttccgagg cggccccggc cggggtggat
2221 tggtattgtc ttgtgtgaac attgcaatag aaatccaatt ggatacgaca acttgacgt
      ← R2

```

**Figure 4.3. Human GRK5 mRNA sequence showing primer sites.** Primer binding sites are indicated as follows: GRK5 F/R (yellow), GRK5 F1/R1 (green), GRK5 F2/R2 (blue).



		1	60
HumGRK4	(1)	MELENIVANSLLKARQGGYGKKSGRSKKQKEILFLPPVSSQSELKHSIEKOYSSLCQKQ	
HumGRK6	(1)	MELENIVAMVLLKAREGGGGRKKGSKKKRQMQQFPHISQCEELRLSLERDYHSLCERQ	
HumGRK5	(1)	MELENIVAMVLLKAREGGGGRKKGSKKKQKEILKFPFHSQCEDLRRTIDRDYSLCQKQ	
MusGRK5	(1)	MELENIVAMVLLKAREGGGGRKKGSKKKQKEILKFPFHSQCEDLRRTIDRDYSLCQKQ	
RatGRK5	(1)	MELENIVAMVLLKAREGGGGRKKGSKKKQKEILKFPFHINQCEDLRRTIDRDYSLCQKQ	
		61	120
HumGRK4	(61)	PIGRLLFRQFCETRPGLKRIEFLDAVAEYEVADDEDSDCLSLIDRFFNDKLAAPLPE	
HumGRK6	(61)	PIGRLLFRQFCATRPGLSRCAFLDGAEEYVTPDDKRRACRQLTQNFSLHTGPDLLPE	
HumGRK5	(61)	PIGRLLFRQFCETRPGLKRIEFLDAVAEYEVTPDEKLGKKEIMTKYLTPKSPVFIAQ	
MusGRK5	(61)	PIGRLLFRQFCETRPGLKRIEFLDAVAEYEVTPDENLGAKKEIMTKYLTPKSPVFIAQ	
RatGRK5	(61)	PIGRLLFRQFCETRPGLKRIEFLDAVAEYEVTPDENLGAKKEIMTKYLTPKSPVFIAQ	
		121	180
HumGRK4	(121)	IPPDVYTECRGLKEENSSKKAEECTRVANVYLRGEPFEEVQESSVFSQFLQWKQLERQ	
HumGRK6	(121)	VPRQLVINCTQRLAQ-GPCKDLQELTRLTHEVLSVAPFADYLDSEYFNRLQWKQLERQ	
HumGRK5	(121)	VGQDLVSQTEKKLLQ-KPCKELSSACAQSVHEVLRGEPFHEVLDSEYFNRLQWKQLERQ	
MusGRK5	(121)	VGQDLVSQTEKKLLQ-SPKCKELSSACAQSVHEVLRGEPFHEVLDSEYFNRLQWKQLERQ	
RatGRK5	(121)	VGQDLVSQTEKKLLQ-SPKCKELSSACAQSVHEVLRGEPFHEVLDSEYFNRLQWKQLERQ	
		181	240
HumGRK4	(181)	PVTKNTFRHYRVLGKGGFGEVCACQVRATGKMYACKRLKKRIKKRKGESMALNEKQILE	
HumGRK6	(180)	PVTKNTFRQYRVLGKGGFGEVCACQVRATGKMYACKRLKKRIKKRKGESMALNEKQILE	
HumGRK5	(180)	PVTKNTFRQYRVLGKGGFGEVCACQVRATGKMYACKRLKKRIKKRKGESMALNEKQILE	
MusGRK5	(180)	PVTKNTFRQYRVLGKGGFGEVCACQVRATGKMYACKRLKKRIKKRKGESMALNEKQILE	
RatGRK5	(180)	PVTKNTFRQYRVLGKGGFGEVCACQVRATGKMYACKRLKKRIKKRKGESMALNEKQILE	
		241	300
HumGRK4	(241)	KVQSRFVVSLAYAYETKDALCLVLTLMNGGDLKPHIYNLGNPGFDEQRAVFYAAELCCGL	
HumGRK6	(240)	KVMSRFVVSLAYAYETKDALCLVLTLMNGGDLKPHIYHMCQACFPEARAVFYAAELCCGL	
HumGRK5	(240)	KVMSQFVVMLAYAYETKDALCLVLTLMNGGDLKPHIYNMGNPGFDEARAVFYAAELCCGL	
MusGRK5	(240)	KVMSQFVVMLAYAYETKDALCLVLTLMNGGDLKPHIYNMGNPGFDEARAVFYAAELCCGL	
RatGRK5	(240)	KVMSQFVVMLAYAYETKDALCLVLTLMNGGDLKPHIYNMGNPGFDEARAVFYAAELCCGL	
		301	360
HumGRK4	(301)	EDLHREIRIVYRDLKPENILLDDHGHIRISDLGLATEIPEGQVRVGRVGTGVYMAPEVVMN	
HumGRK6	(300)	EDLHREIRIVYRDLKPENILLDDHGHIRISDLGLAVHVPEGQTIKGRVGTGVYMAPEVVMN	
HumGRK5	(300)	EDLHRENTVYRDLKPENILLDDHGHIRISDLGLAWKIPEGDLIRGRVGTGVYMAPEVLMN	
MusGRK5	(300)	EDLHRENTVYRDLKPENILLDDHGHIRISDLGLAWKIPEGDLIRGRVGTGVYMAPEVLMN	
RatGRK5	(300)	EDLHRENTVYRDLKPENILLDDHGHIRISDLGLAWKIPEGDLIRGRVGTGVYMAPEVLMN	
		361	420
HumGRK4	(361)	EKYTFSPDMMGLGCLLYEMTIQCHSPKPKYKPKWKKEEVDQRIKNDTEYSEKFSQDAKSI	
HumGRK6	(360)	ERYTFSPDMMGLGCLLYEMTIQCHSPKPKYKPKWKKEEVDRLVKEVPPEYSEKFSQARSL	
HumGRK5	(360)	QRYGLSPDYMLGLGCLLYEMTIQCHSPKPKYKPKWKKEEVDRRVLETEEVYSHKFSQAKSI	
MusGRK5	(360)	QRYGLSPDYMLGLGCLLYEMTIQCHSPKPKYKPKWKKEEVDRRVLETEEVYSHKFSQAKSI	
RatGRK5	(360)	QRYGLSPDYMLGLGCLLYEMTIQCHSPKPKYKPKWKKEEVDRRVLETEEVYSHKFSQAKSI	
		421	480
HumGRK4	(421)	CKMLLTQKPSKRLGCRGEGAGVKKHVEPKDINFRLDAMMLEPPFCEDPRAVYCKDVLD	
HumGRK6	(420)	CSQLLCKDPAERLGCRRGGSAREVKEHLLPKKLNFRLDAGMLEPPFKPDPAVYCKDVLD	
HumGRK5	(420)	CKMLLTQKPSKRLGCRGEGAGVKKHVEPKDINFRLDAGMLEPPFVDPRAVYCKDVLD	
MusGRK5	(420)	CKMLLTQKPSKRLGCRGEGAGVKKHVEPKDINFRLDAGMLEPPFVDPRAVYCKDVLD	
RatGRK5	(420)	CKMLLTQKPSKRLGCRGEGAGVKKHVEPKDINFRLDAGMLEPPFVDPRAVYCKDVLD	
		481	540
HumGRK4	(481)	IEQFSVWKGIVLDTADEDFYARFATGCVSLPWQNMETESGCEKDIKSESEELPLDLDK	
HumGRK6	(480)	IEQFSVWKGIVLEPTDQDFYQKATGCVSLPWQNMETETECQELNWFGLDGSVPDLDW	
HumGRK5	(480)	IEQFSVWKGIVLDHTDDDFYSKFTGCVSLPWQNMETETECQELNWFPGNGTLPPDLNR	
MusGRK5	(480)	IEQFSVWKGIVLDHTDDDFYSKFTGCVSLPWQNMETETECQELNWFPGNGTLSPDLNR	
RatGRK5	(480)	IEQFSVWKGIVLDHTDDDFYSKFTGCVSLPWQNMETETECQELNWFPGNGTLSPDLNR	
		541	593
HumGRK4	(541)	NIHTVYSRPNRGFFYRLRRGGCLTMVPSKEKEVEPKQC-----	
HumGRK6	(540)	KGQPPAP-PKKGLLQRLSRQDCCGNCSDSEELPTRL-----	
HumGRK5	(540)	N-HPPEP-PKKGLLQRLRRQHQNSKSSPSSKTSFNHHINSNHVSSNSTGSS	
MusGRK5	(540)	S-QPPEP-PKKGLLQRLRRQHQNSKSSPPTKTSNHRINSNHINSNSTGSS	
RatGRK5	(540)	S-QPPEP-PKKGLLQRLRRQHQNSKSSPPTKTSNHRINSNHINSNSTGSS	

**Figure 4.4. Multiple alignment of the amino acid sequences of human (Hum), rat and mouse (Mus) GRK5, and human GRK4 and GRK6.** Alignment performed using ClustalX 1.83. Amino acids conserved across all sequences (black) and those conserved across >3 of the sequences (grey) are indicated.

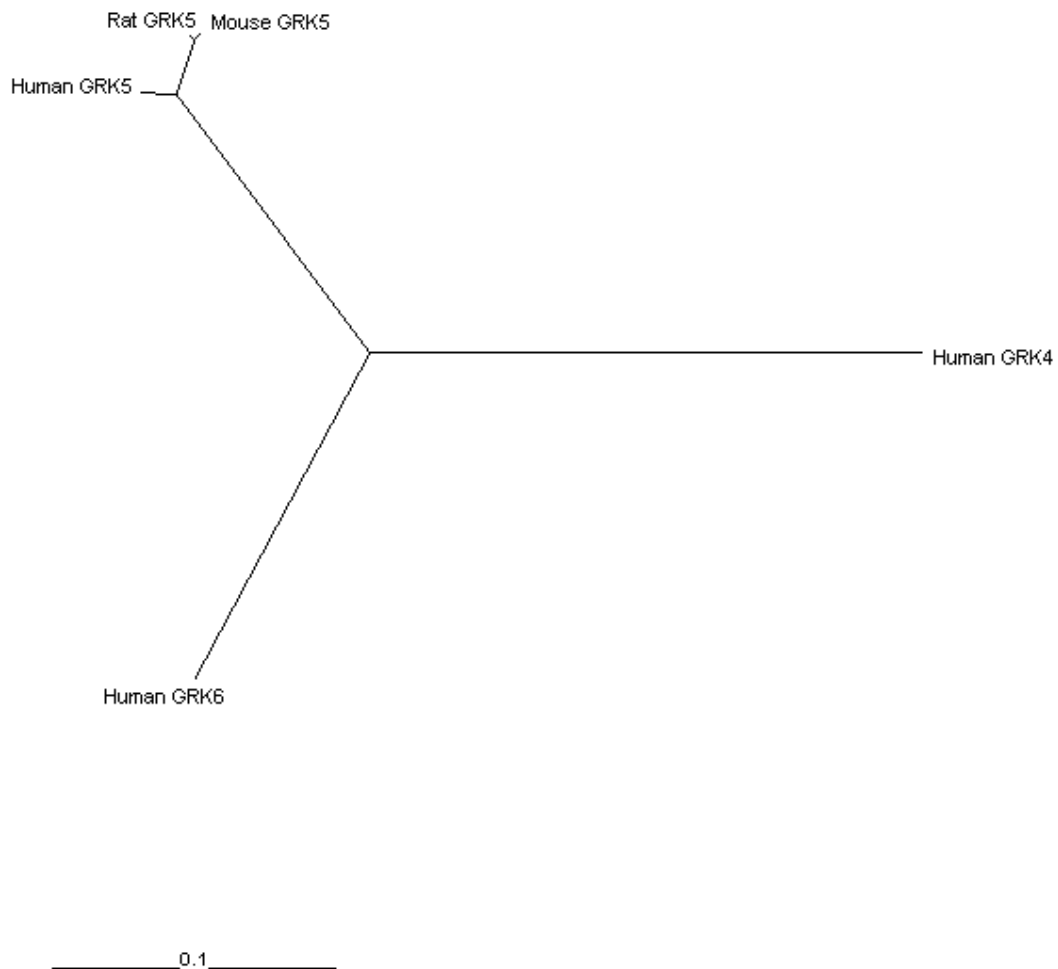


**Figure 4.5. Phylogenetic tree showing relationships between human, rat and mouse GRK5, and human GRK4 and 6.** Genetic distances were calculated from multiple alignment data of the GRK protein sequences using ClustalX 1.83 which employs the neighbour-joining method (Saitou and Nei, 1987).

The multiple alignment data was also used to generate a phylogenetic tree using ClustalX 1.83 which employs the neighbour-joining method (Saitou and Nei, 1987) (Figure 4.5). The tree shows that human GRK5 has a greater sequence similarity with GRK5 from rat and mouse than with other members of the GRK4 subfamily (GRK4 and GRK6) in humans.

#### 4.4.2 Primer testing using PCR

##### 4.4.2.1 The positive control: 18S ribosomal RNA

18S rRNA was used as a positive control for all PCR work. Primers were located at nt 1046-1073 and nt 1348-1365 of the human 18S sequence (NCBI accession number NR 003286), amplifying a predicted 319 nt product (Table 4.1). The  $T_m$  of 18S F and 18S R were 53°C and 52°C respectively. A single product of the expected size was amplified when PCR was performed with an annealing temperature of 50°C (Figure 4.6).

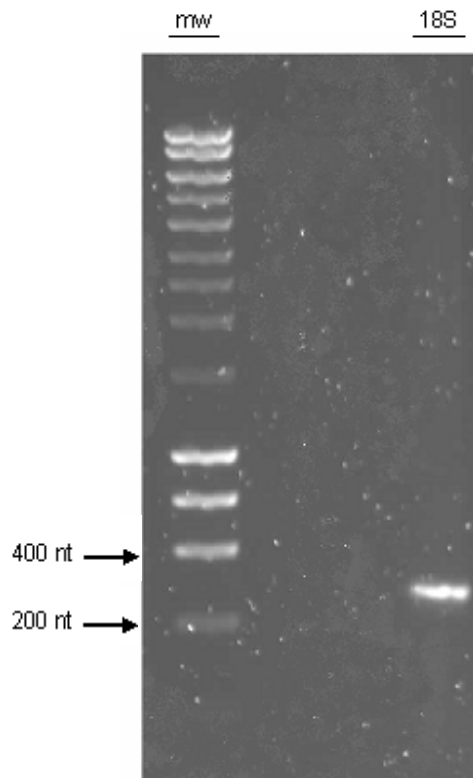


**Figure 4.6. PCR amplification of 18S ribosomal RNA.** PCR products were analysed on a 1% agarose/1 x TAE gel. The expected PCR product for 18S rRNA was 319 nt.

#### 4.4.2.2 GRK5 specific primers: GRK5F/R

PCR was performed using the primer pair GRK5F/R (designed using Primer3 software) and an annealing temperature of 50°C. Analysis of the PCR products on a gel revealed two bands, a reasonably bright band (1 in Figure 4.7) and a very faint band (2 in Figure 4.7). The faint band was thought to be the desired product, as this band was closest to the expected size (221 nt) based on comparison with the molecular weight marker (mw). There are a number of possible reasons for the second band, including co-amplification of a non-target sequence or primer-dimer.

In an attempt to eliminate the formation of any non-specific product, annealing temperature gradients were carried out. PCR was performed using 5 different annealing temperatures ranging from 50-60°C (Figure 4.8). Although it appeared that the intensity of the band for the desired product (2 in Figure 4.8) increased with increasing annealing temperature the non-target product (1 in Figure 4.8) also remained. In fact the two bands appeared to be of equal intensity at 60°C. An additional annealing temperature gradient was carried out using temperatures ranging from 60-70°C, however the amount of product was very low (results not shown). Increasing the magnesium concentration in the PCR reaction mixture also failed to eliminate the non-specific product (results not shown). Subsequent sequencing of the PCR products pointed to the presence of a second non-target product. Therefore, these primers were not suitable for PCR amplification of GRK5. Based on these results, the method of primer design was reviewed and two new primers pairs were selected (as described above in section 4.4.1.2).

#### 4.4.2.3 GRK5 specific primers: GRK5F1/R1 and GRK5F2/R2

PCR was performed using the primer pairs GRK5F1/R1 and GRK5F2/R2 (designed using multiple alignment analysis) and an annealing temperature of 50°C. Both primer pairs amplified single products of the expected size (360 nt for GRK5F1/R1 and 290 nt for GRK5F2/R2) (Figure 4.9). The primer pair GRK5F/R was also included, and, as seen previously PCR, produced two products.

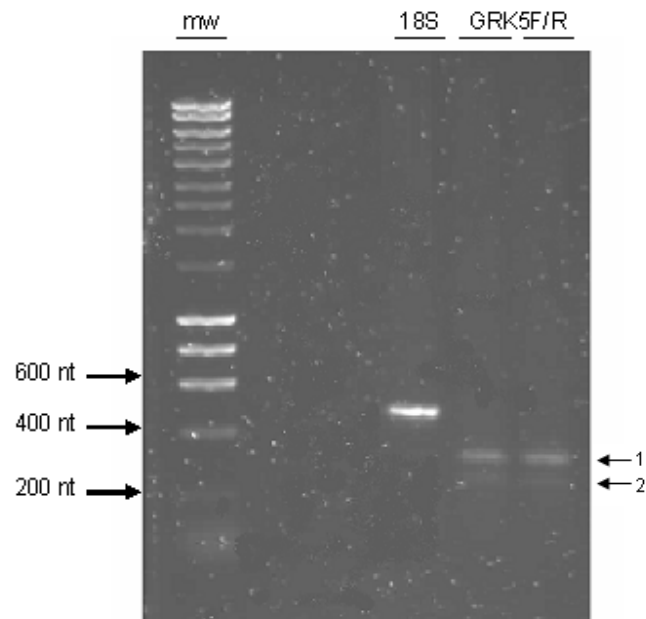


**Figure 4.7. PCR amplification of GRK5 with GRK5F/R primers.** PCR products were analysed on a 1% agarose/1 x TAE gel. The expected PCR product for GRK5F/R was 221 nt. Amplification of 18S rRNA was included as a positive control. The DNA molecular weight marker (mw) was Hyperladder I (Bioline).

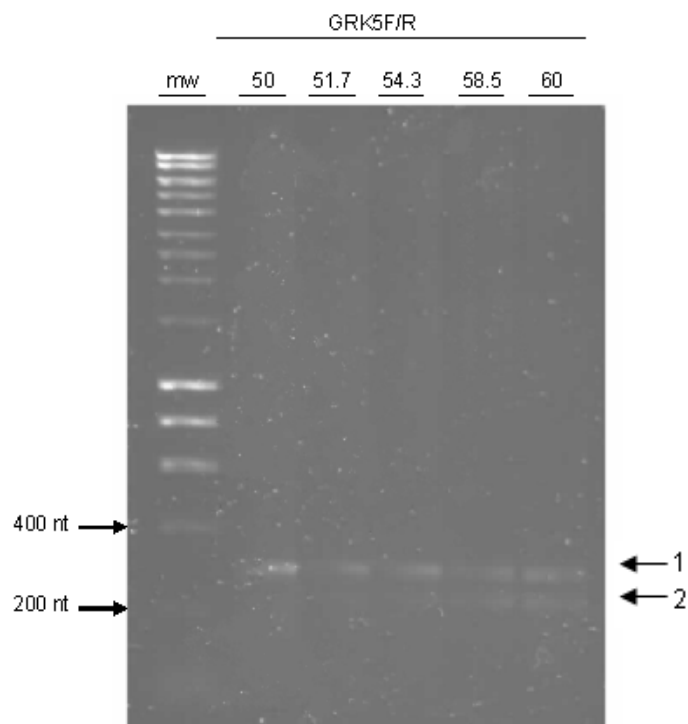


**Figure 4.8. Annealing temperature gradient PCR of GRK5 with GRK5F/R primers.** PCR was carried out using annealing temperatures of 50-60°C. PCR products were analysed on a 1% agarose/1 x TAE gel. The expected PCR product for GRK5F/R was 221 nt. The DNA molecular weight marker (mw) was Hyperladder I (Bioline).

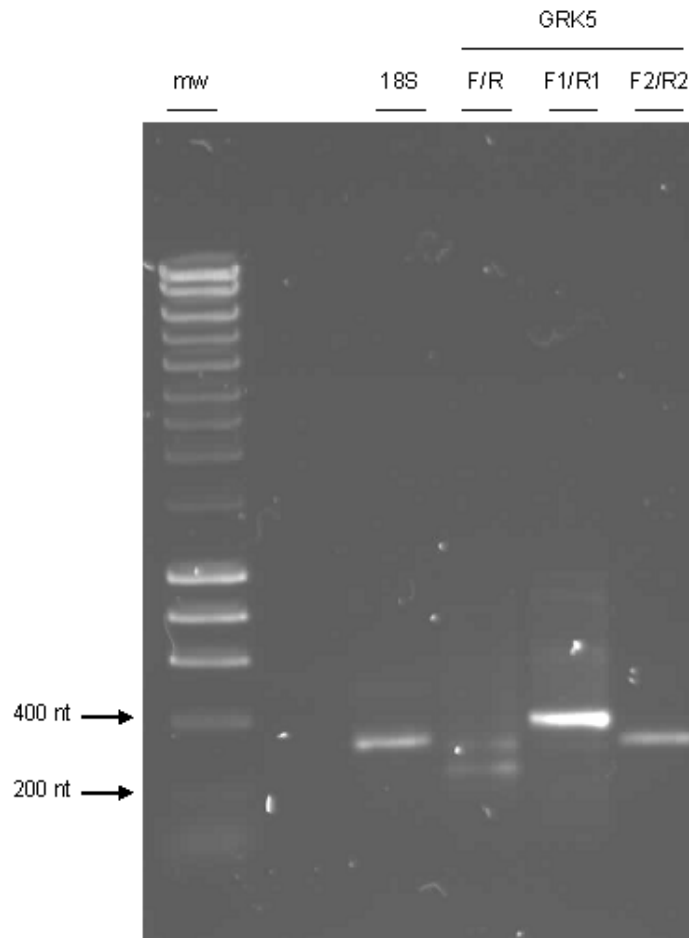


**Figure 4.9. PCR amplification of GRK5 with GRK5F/R, GRK5F1/R1 and GRK5F2/R2 primers.** PCR products were analysed on a 1% agarose/1 x TAE gel. The expected PCR product sizes were 360 nt for GRK5F1/R1 and 290 nt for GRK5F2/R2. Amplification of 18S rRNA was included as a positive control. The DNA molecular weight marker (mw) was Hyperladder I (Bioline).

#### 4.4.3 Primer testing using quantitative PCR

Quantitative PCR (qPCR) was used to confirm the presence of a single product for amplification of GRK5. qPCR was performed as described in section 4.2.8 using all three primer pairs for GRK5 (GRK5F/R, GRK5F1/R1 and GRK5F2/R2). Amplification of 18S rRNA was included as a positive control. All reactions were performed using the SYBR Green supermix (BioRad), and at an annealing temperature of 50°C.

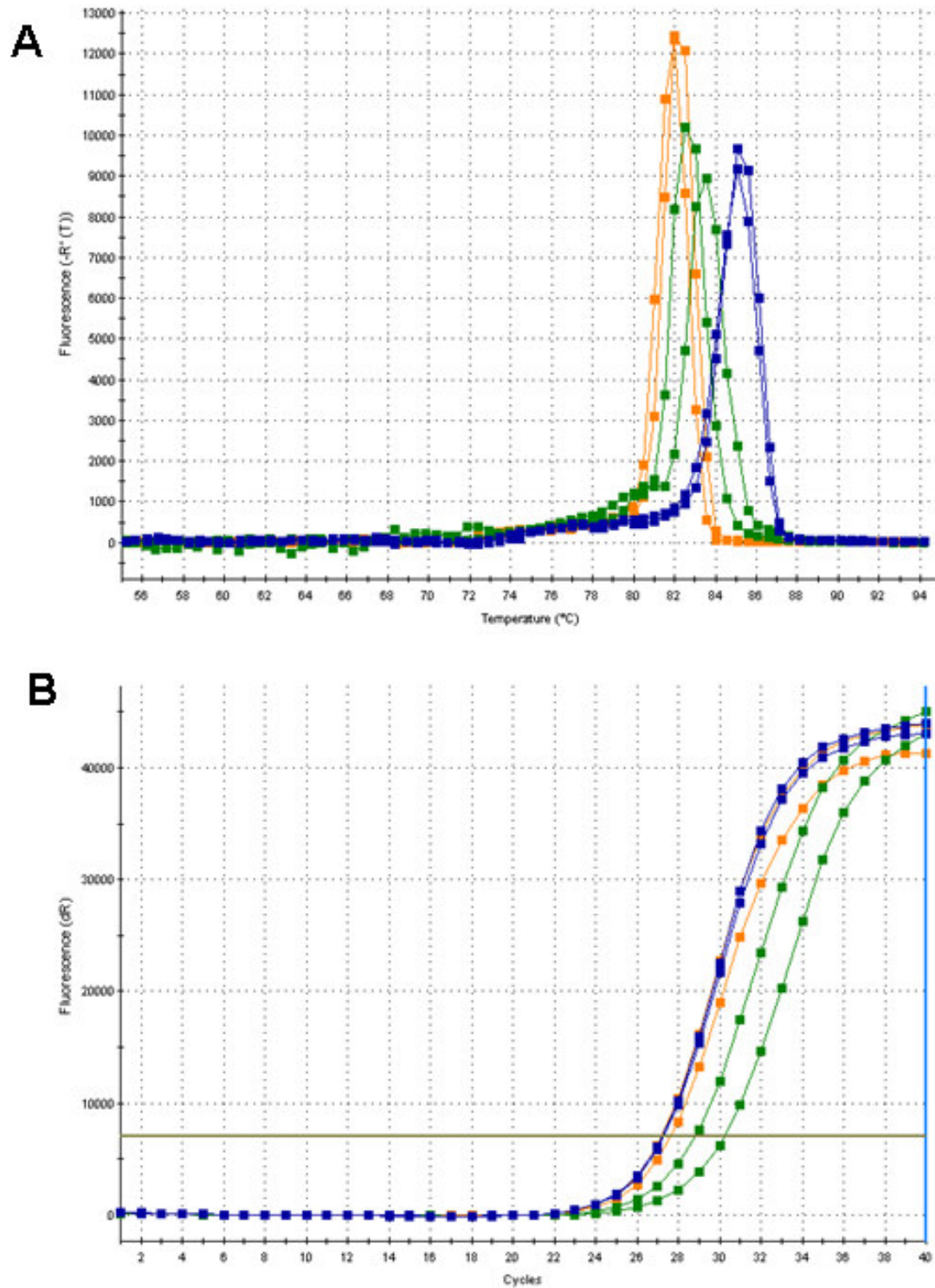


**Figure 4.10.** Dissociation curves (A) and amplification plots (B) for qPCR performed using GRK5F/R (orange), GRK5F1/R1 (green) and GRK5F2/R2 (blue) primers. Each reaction was performed in duplicate.

Dissociation curve analysis (automatically performed by the Mx3005P<sup>TM</sup> software) showed a single product specific melting temperature for each primer pair as follows: at approximately 82°C for GRK5F/R, 83°C for GRK5F1/R1, and 85°C for GRK5F2/R2 (Figure 4.10). Also the positive control, 18S rRNA, generated a single product specific melting temperature of approximately 84°C (not shown). The amplification plot showed that the GRK5F2/R2 primer pair amplified GRK5 with the highest efficiency (ie. it had the lowest Ct value, 27.3). In addition, this primer pair generated the most reproducible results as the replicates were very close.

Specificity of the PCR products was checked with gel electrophoresis (Figure 4.11). This resulted in a single product of the expected size as follows: (GRK5F/R 221 nt, GRK5F1/R1 360 nt, GRK5 F2/R2 290 nt, and 319 nt for 18S. This result for GRK5F/R was somewhat surprising as the attempts to optimise non-quantitative PCR to generate a single product for this primer pair had been unsuccessful. It seems most likely that the increased sensitivity of qPCR compared to non-quantitative PCR is the reason for this difference.

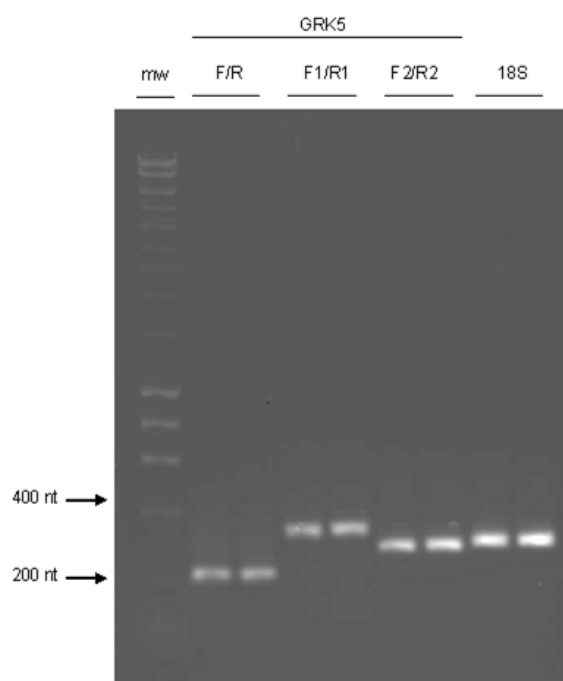


**Figure 4.11. qPCR amplification of GRK5 with GRK5F/R, GRK5F1/R1 and GRK5F2/R2 primers.** 18S was included as a positive control. qPCR products were analysed on a 1% agarose/1 x TAE gel. The expected PCR product sizes were 221 nt for GRK5F/R, 360 nt for GRK5F1/R1, 290 nt for GRK5F2/R2 and 319 nt for 18S rRNA. The DNA molecular weight marker (mw) was Hyperladder I (Bioline).



#### **4.4.4 Sequencing of the human GRK5 PCR product**

The qPCR products for GRK5F/R, GRK5F1/R1 and GRK5F2/R2 were sequenced using methods described in section 4.2.7. Primer sequencing was performed in both forward and reverse directions, and where necessary were reverse complemented using Primer Premier (Abd-El salam, 2003). The identities of the sequences were investigated by carrying out a nucleotide BLAST search of the human genome. For each sequence the only mRNA match was the target, human GRK5 mRNA (NCBI accession number NM 005308).

All three primer pairs tested specifically amplified GRK5 and gave single product for qPCR. Therefore, any of these primer pairs appeared to be suitable for GRK5 expression studies. Only one primer pair for GRK5 was required, however. Based on the qPCR efficiency and primer specificity, the primer pair GRK5F2/R2 was selected for further studies.

Additional qPCR reactions were performed to confirm that the results for GRK5F2/R2 were reproducible, and the products were used to carry out additional sequencing reactions to confirm the sequence. The sequences of the GRK5F2/R2 products were aligned with the corresponding partial human GRK5 mRNA sequence using ClustalX 1.83 (Figure 4.12). This provided confirmation that qPCR using HEK293 cDNA with GRK5F2/R2 primers invariably resulted in the amplification of human GRK5 mRNA giving a product of the expected size (290 nt) and sequence.

			1951	2000			
GRK5F2	(1)		-----ATGT	CAGCTCGA-CTC-MCCGGA-GC			
GRK5F2	(1)		-----ATGT	M-GCTCGA-CTC-MCCGGA-GC			
GRK5F2	(1)		-----ATGT	MAGCTCGAACTC-MCCGGA-GC			
GRK5R2 rc	(1)		-AACCA	CCACATTAA-CTCAAACCATGT	CAGCTCGAACTC	CA	CCGGAAGC
GRK5R2 rc	(1)		-AACCA	CCACATTAAACTCAAACCATGT	CAGCTCGAACTC	CA	CCGGAAGC
GRK5R2 rc	(1)		TAACCA	CCACATTAAACTCAAACCATGT	CAGCTCGAACTC	CA	CCGGAAGC
GRK5mRNA	(1951)		TAACCA	CCACATAAA-CTCAAACCATGT	CAGCTCGAACTC	CA	CCGGAAGC
Consensus	(1951)		AACCA	CCACAT AA CTCAAACCATGT	CAGCTCGAACTC	CA	CCGGAAGC
			2001	2050			
GRK5F2	(24)		AGCTAGTTTCGGCTCTGGCCTCCAAGTCCACAGTGAAC	CAGCCAGACC			
GRK5F2	(23)		AGCTAGTTTCGGCTCTGGCCTCCAAGTCCACAGTGAAC	CAGCCAGACC			
GRK5F2	(25)		AGCTAGTTTCGGCTCTGGCCTCCAAGTCCACAGTGAAC	CAGCCAGACC			
GRK5R2 rc	(49)		AGCTAGTTTCGGCTCTGGCCTCCAAGTCCACAGTGAAC	CAGCCAGACC			
GRK5R2 rc	(50)		AGCTAGTTTCGGCTCTGGCCTCCAAGTCCACAGTGAAC	CAGCCAGACC			
GRK5R2 rc	(51)		AGCTAGTTTCGGCTCTGGCCTCCAAGTCCACAGTGAAC	CAGCCAGACC			
GRK5mRNA	(2000)		AGCTAGTTTCGGCTCTGGCCTCCAAGTCCACAGTGAAC	CAGCCAGACC			
Consensus	(2001)		AGCTAGTTTCGGCTCTGGCCTCCAAGTCCACAGTGAAC	CAGCCAGACC			
			2051	2100			
GRK5F2	(74)		CTTCTCCTTAGAAGTGGAAGTAGTGGAGCCCC	CTGCTGGTGGGGCTGCC			
GRK5F2	(73)		CTTCTCCTTAGAAGTGGAAGTAGTGGAGCCCC	CTGCTGGTGGGGCTGCC			
GRK5F2	(75)		CTTCTCCTTAGAAGTGGAAGTAGTGGAGCCCC	CTGCTGGTGGGGCTGCC			
GRK5R2 rc	(99)		CTTCTCCTTAGAAGTGGAAGTAGTGGAGCCCC	CTGCTGGTGGGGCTGCC			
GRK5R2 rc	(100)		CTTCTCCTTAGAAGTGGAAGTAGTGGAGCCCC	CTGCTGGTGGGGCTGCC			
GRK5R2 rc	(101)		CTTCTCCTTAGAAGTGGAAGTAGTGGAGCCCC	CTGCTGGTGGGGCTGCC			
GRK5mRNA	(2050)		CTTCTCCTTAGAAGTGGAAGTAGTGGAGCCCC	CTGCTGGTGGGGCTGCC			
Consensus	(2051)		CTTCTCCTTAGAAGTGGAAGTAGTGGAGCCCC	CTGCTGGTGGGGCTGCC			
			2101	2150			
GRK5F2	(124)		AGGGGAGACCCCGGAGCCGGGGAAGGAGGCCGTC	CATCCGTCGACGTA			
GRK5F2	(123)		AGGGGAGACCCCGGAGCCGGGGAAGGAGGCCGTC	CATCCGTCGACGTA			
GRK5F2	(125)		AGGGGAGACCCCGGAGCCGGGGAAGGAGGCCGTC	CATCCGTCGACGTA			
GRK5R2 rc	(149)		AGGGGAGACCCCGGAGCCGGGGAAGGAGGCCGTC	CATCCGTCGACGTA			
GRK5R2 rc	(150)		AGGGGAGACCCCGGAGCCGGGGAAGGAGGCCGTC	CATCCGTCGACGTA			
GRK5R2 rc	(151)		AGGGGAGACCCCGGAGCCGGGGAAGGAGGCCGTC	CATCCGTCGACGTA			
GRK5mRNA	(2100)		AGGGGAGACCCCGGAGCCGGGGAAGGAGGCCGTC	CATCCGTCGACGTA			
Consensus	(2101)		AGGGGAGACCCCGGAGCCGGGGAAGGAGGCCGTC	CATCCGTCGACGTA			
			2151	2200			
GRK5F2	(174)		GAACCTC	GAGGTTTCTCAAAGAAATTTCCACTCAGGTCTGTTT	CCGAGG		
GRK5F2	(173)		GAACCTC	GAGGTTTCTCAAAGAAATTTCCACTCAGGTCTGTTT	CCGAGG		
GRK5F2	(175)		GAACCTC	GAGGTTTCTCAAAGAAATTTCCACTCAGGTCTGTTT	CCGAGG		
GRK5R2 rc	(199)		GAACCTC	GAGGTTTCTCAAAGAAATTTCCACTCAGGTCTGTTT	CCGAGG		
GRK5R2 rc	(200)		GAACCTC	GAGGTTTCTCAAAGAAATTTCCACTCAGGTCTGTTT	CCGAGG		
GRK5R2 rc	(201)		GAACCTC	GAGGTTTCTCAAAGAAATTTCCACTCAGGTCTGTTT	CCGAGG		
GRK5mRNA	(2150)		GAACCTC	GAGGTTTCTCAAAGAAATTTCCACTCAGGTCTGTTT	CCGAGG		
Consensus	(2151)		GAACCTC	GAGGTTTCTCAAAGAAATTTCCACTCAGGTCTGTTT	CCGAGG		
			2201	2250			
GRK5F2	(224)		CGGCCCGGCCGGGGTGGATTGGATTGTGTTTCCGGTGAACATW	-----			
GRK5F2	(223)		CGGCCCGGCCGGGGTGGATTGGATTGTCTTTGGGTGAACATW	AAG---			
GRK5F2	(225)		CGGCCCGGCCGGGGTGGATTGGATTGTCTTTGGGTGAACATTA	-----			
GRK5R2 rc	(248)		CGGCCCGGCCGGGGTGGATT	-----			
GRK5R2 rc	(249)		CGGCCCGGCCGGGGTGGATT	-----			
GRK5R2 rc	(250)		CGGCCCGGCCGGGGTGGATT	-----			
GRK5mRNA	(2200)		CGGCCCGGCCGGGGTGGATTGGATTGTCTTTGGTGAACATTGCAATAG				
Consensus	(2201)		CGGCCCGGCCGGGGTGGATTGGATTGT	TT G GA T			

**Figure 4.12. Multiple alignment of the nucleotide sequences of the products amplified using GRK5F2/R2 with the partial GRK5 mRNA sequence.** The results of three forward (GRK5F2) and three reverse (GRK5R2) sequencing reactions are shown. Reverse sequences were reverse complemented (rc) using Primer Premier, and the alignment was performed using ClustalX 1.83. Amino acids conserved across all sequences (black) and those conserved across >3 of the sequences (grey) are indicated.

#### 4.4.5 Determination of the amplification efficiency of the primer pairs used for GRK5 expression studies

The amplification efficiencies of the primers to be used for GRK5 expression studies were determined by carrying out qPCR with serial dilutions of GRK5 cDNA. HEK293 cDNA was serially diluted 5-fold to give the following dilutions: undiluted, 1/5, 1/25, 1/125, 1/625. qPCR was then performed using the primer pairs GRK5F2/R2, 18SF/R and  $\beta$ -actinF/R. All reactions were performed using the SYBR Green supermix (BioRad), and at an annealing temperature of 50°C. Dissociation curves showed a single product specific melting temperature for each primer pair as follows: at 86.3°C for GRK5F2/R2, 84.9°C for  $\beta$ -actin and 84.4°C for 18S (data for undiluted cDNA shown in Figure 4.13). Specificity of the PCR products was assessed with gel electrophoresis (Figure 4.14). This resulted in a single product of the expected size for each primer pair as follows: GRK5F2/R2 290 nt, 18SF/R 319 nt and  $\beta$ -actinF/R 131 nt.

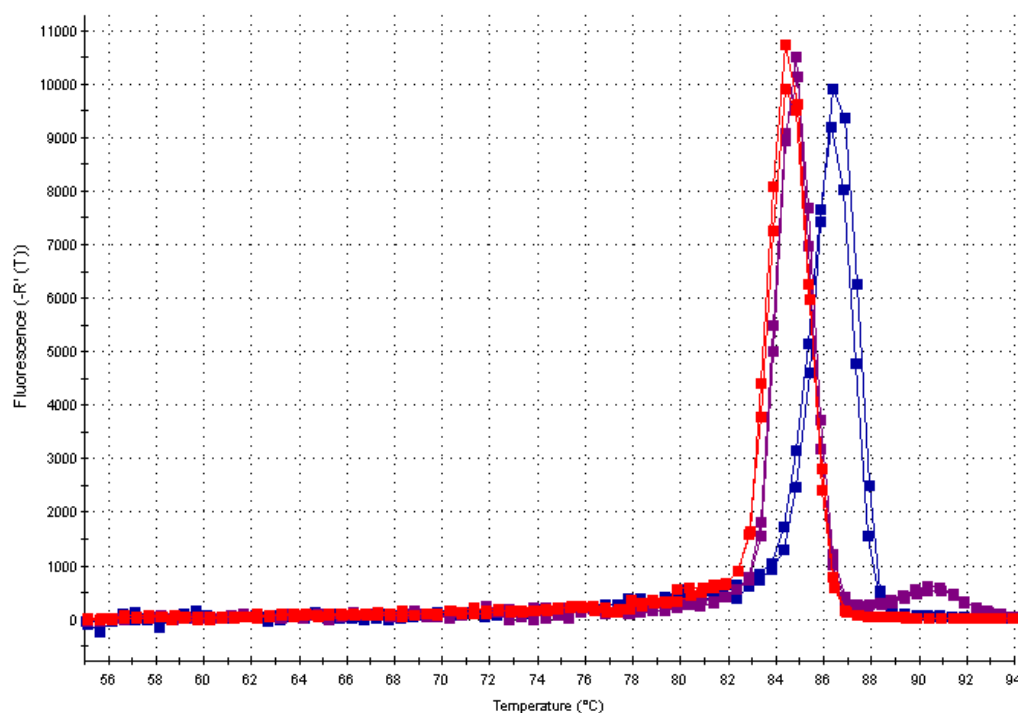


**Figure 4.13.** Dissociation curves for qPCR performed using GRK5F2/R2 (blue), 18SF/R (purple) and  $\beta$ -actinF/R (red) primers. Each reaction was carried out using undiluted cDNA and performed in duplicate.

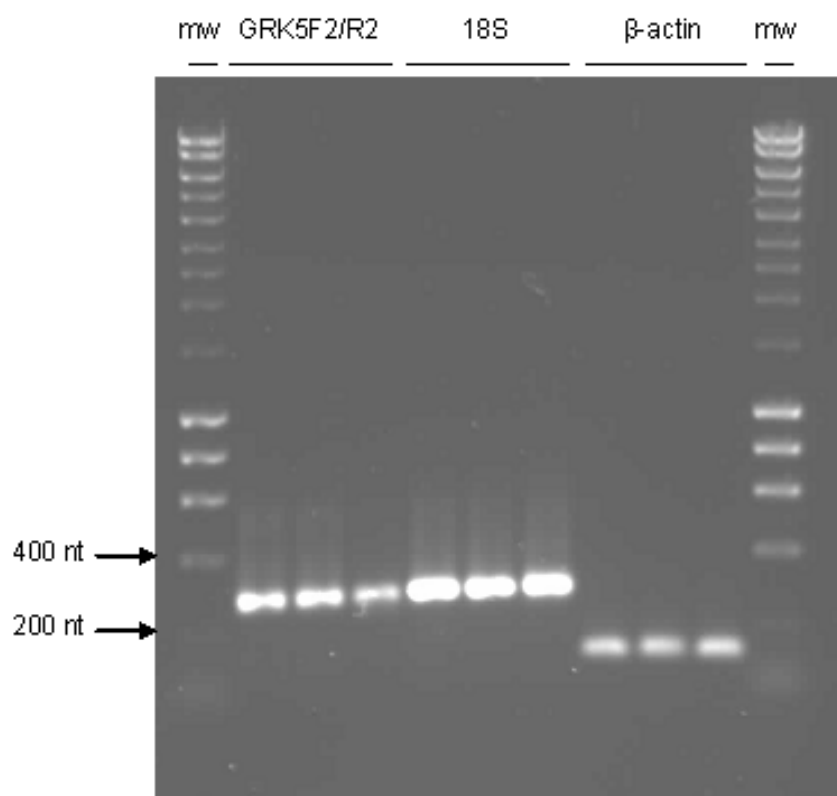


**Figure 4.14. qPCR amplification of GRK5 with GRK5F2/R2, 18S and  $\beta$ -actin using undiluted (1), 1/5 or 1/25 diluted cDNA.** qPCR products were analysed on a 1% agarose/1 x TAE gel. The expected PCR product sizes were as follows: GRK5 290 nt, 18S rRNA 319 nt and  $\beta$ -actin 131 nt. The DNA molecular weight marker (mw) was Hyperladder I (Bioline).

The Mx3005P<sup>TM</sup> software was used to generate standard curves for each primer pair using pre-entered information regarding the cDNA dilution (expressed as an initial quantity relative to the undiluted cDNA) and the Ct value for each sample (Figure 4.15). The amplification efficiency for each primer pair was calculated from the appropriate standard curve (as described in section 2.8.2). Amplification efficiencies were 89.6%, 90.1% and 78.2% for GRK5F2/R2, 18S rRNA and  $\beta$ -actin respectively. These efficiencies were considered acceptable for qPCR. These values were then used to perform data analysis for GRK5 expression studies (as described in section 2.8.2).

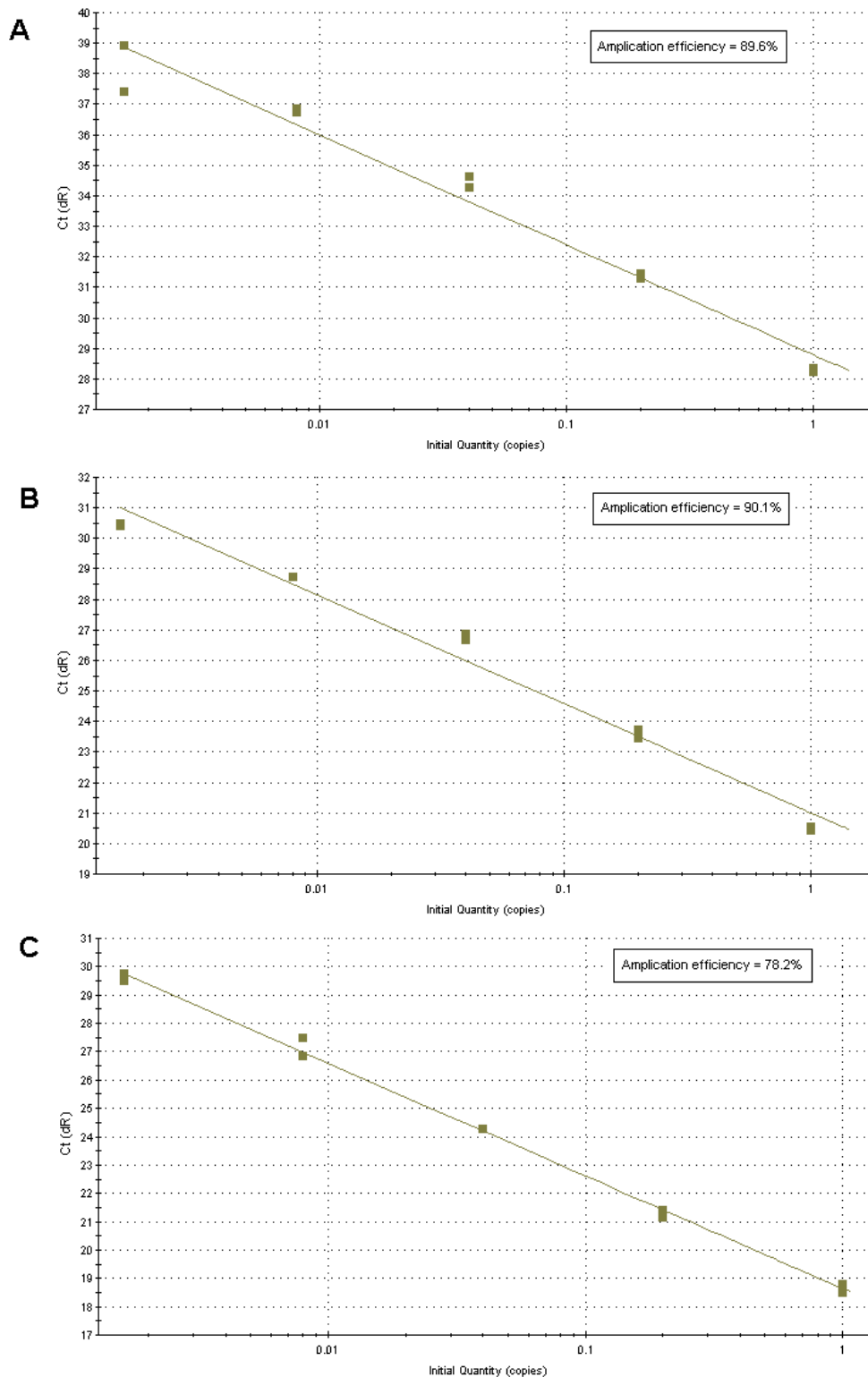


**Figure 4.15. Standard curves for the calculation of amplification efficiencies for GRK5F2/R2 (A), 18SF/R (B) and  $\beta$ -actinF/R (C) primers. Each reaction was performed in duplicate.**

## **4.5 ASSESSMENT OF HUMAN GRK5 EXPRESSION IN HEK293 CELLS USING QUANTITATIVE PCR**

GRK5 expression studies were performed to investigate whether the methods developed in this study would allow siRNA-mediated knockdown of GRK5 mRNA to be measured. Previous studies have shown that following siRNA transfection, qRT-PCR can be used to measure a reduction in mRNA expression as small as 40-45% (Miao et al., 2007). Therefore, it was necessary to determine whether a change in GRK5 expression of this magnitude could be accurately measured using the methods described in this study.

Experiments were designed to test the effects HEK293 cell culture age (passage number) and culture conditions on GRK5 expression. This served two purposes:

1. The expression data would allow the assessment of the impact of cell culture methods on GRK5 expression.
2. If small changes in GRK5 expression were accurately measured this would validate the methods used.

In addition, the GRK5 expression in three different human cancer cell lines was measured for comparison with the expression in HEK293 cells. It was hypothesised that the GRK5 expression in the different cell lines would vary considerably. If differences in GRK5 expression could be accurately measured, this would assist in the validation of the qRT-PCR methods described in this study.

### **4.5.1 Reference RNA: A positive control for GRK5 expression studies**

It has been shown using Northern blot analysis that GRK5 mRNA is expressed in a variety of human tissues, with the highest levels in heart, placenta and lung > skeletal muscle > brain, liver, pancreas > kidney (Kunapuli and Benovic, 1993). These findings are consistent with bovine data (Premont et al., 1994). It therefore seems reasonable that the GRK5 expression in HEK293 cells (a kidney-derived cell line) may be lower than its expression in human cells originating from other tissues. It must be noted however, that the HEK293 cells are far from typical kidney cells and in

fact show unexpected similarities to neuronal cells (Shaw et al., 2002). A pooled RNA sample was provided as a kind gift from Dr Anna Pilbrow, Cardioendocrine Research Group, Christchurch School of Medicine and Health Sciences. Total RNA was extracted from normal human tissue (21% kidney, 64% bowel, 10% ovary) obtained from the Christchurch tissue bank. The RNA samples were then pooled with 5% commercial human heart RNA (Stratagene). It was hypothesised that this “reference RNA” sample would have higher GRK5 expression than HEK293 cells, and so may be useful as a positive control for qRT-PCR reactions. This RNA was reverse transcribed as described in section 4.2.5, and the resulting cDNA will be referred to below as “reference cDNA”.

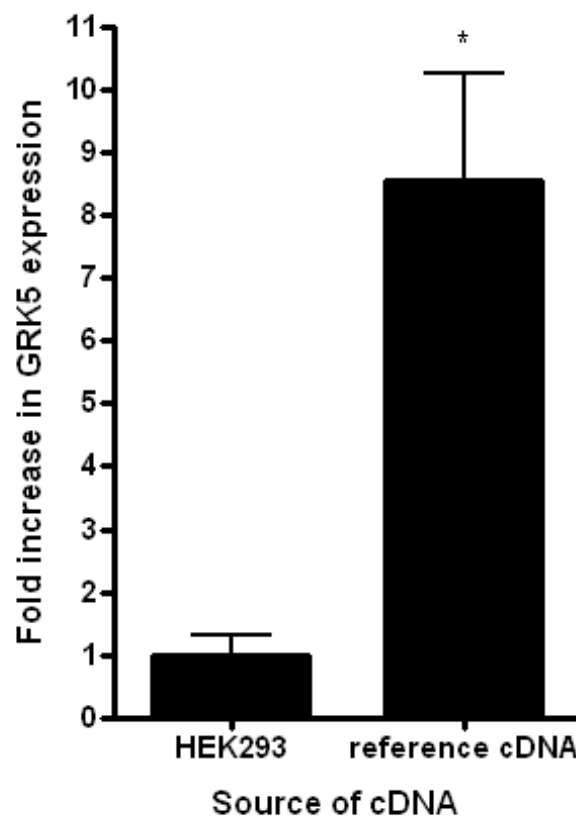


**Figure 4.16. GRK5 expression in HEK293 cells compared to the reference cDNA.** GRK5 expression in HEK293 cells and the reference cDNA was investigated using qRT-PCR. Data were normalised using 18S rRNA and  $\beta$ -actin expression, and expressed as a fold increase relative to the HEK293 cells. Data are the results of two qPCR runs, each performed in duplicate. (*t*-test, \*  $P < 0.05$ ).

#### 4.5.1.1 GRK5 expression in the reference cDNA

GRK5 expression in the reference cDNA and HEK293 cells was determined using qRT-PCR. The qPCR was performed as described in section 4.2.8 using either SYBR Green supermix (BioRad) or FastStart SYBR Green Master (Roche). The data for GRK5 was normalised to expression of 18S rRNA and  $\beta$ -actin, and expressed as a fold increase relative to results for HEK293 cells (set as 1). The results represent the data from two qPCR runs with each reaction performed in duplicate (Figure 4.16). The two qPCR runs were performed using different cDNA preparations generated from the same RNA sample.

The GRK5 expression was significantly greater ( $8.6 \pm 1.7$  fold) in the reference cDNA relative to HEK293 (*t*-test,  $P < 0.05$ ). Therefore, the reference cDNA sample was often included as a positive control for the amplification of GRK5 using qRT-PCR, particularly during optimisation of the qPCR reaction.

#### 4.5.2 Optimisation of the SYBR green reaction mix for amplification of GRK5 using qPCR

In initial experiments, qPCR using HEK293 cDNA, GRK5F2/R2 primers and commercial SYBR green mixes such as FastStart SYBR Green Master (Roche) sometimes resulted in poor amplification of GRK5. For some qPCR runs the amplification curve was poorly defined or the Ct value was particularly high (ie.  $>35$ ), and in either case the results were discarded. In order to reduce the variability between qPCR runs the SYBR green reaction mix was optimised for the amplification of GRK5. Three SYBR green mixes (which will be referred to below as SYBR A, SYBR B1 and SYBR B2) were prepared by Dr Jason Song (School of Biological Sciences, University of Canterbury, *Pers Comm.*). SYBR A and B differed in their contents, whereas SYBR B1 and SYBR B2 were prepared identically. These mixes were tested alongside the Roche SYBR mix. qPCR was performed as described in section 4.2.8 using GRK5F2/R2 and the reference gene  $\beta$ -actin was included as a positive control.



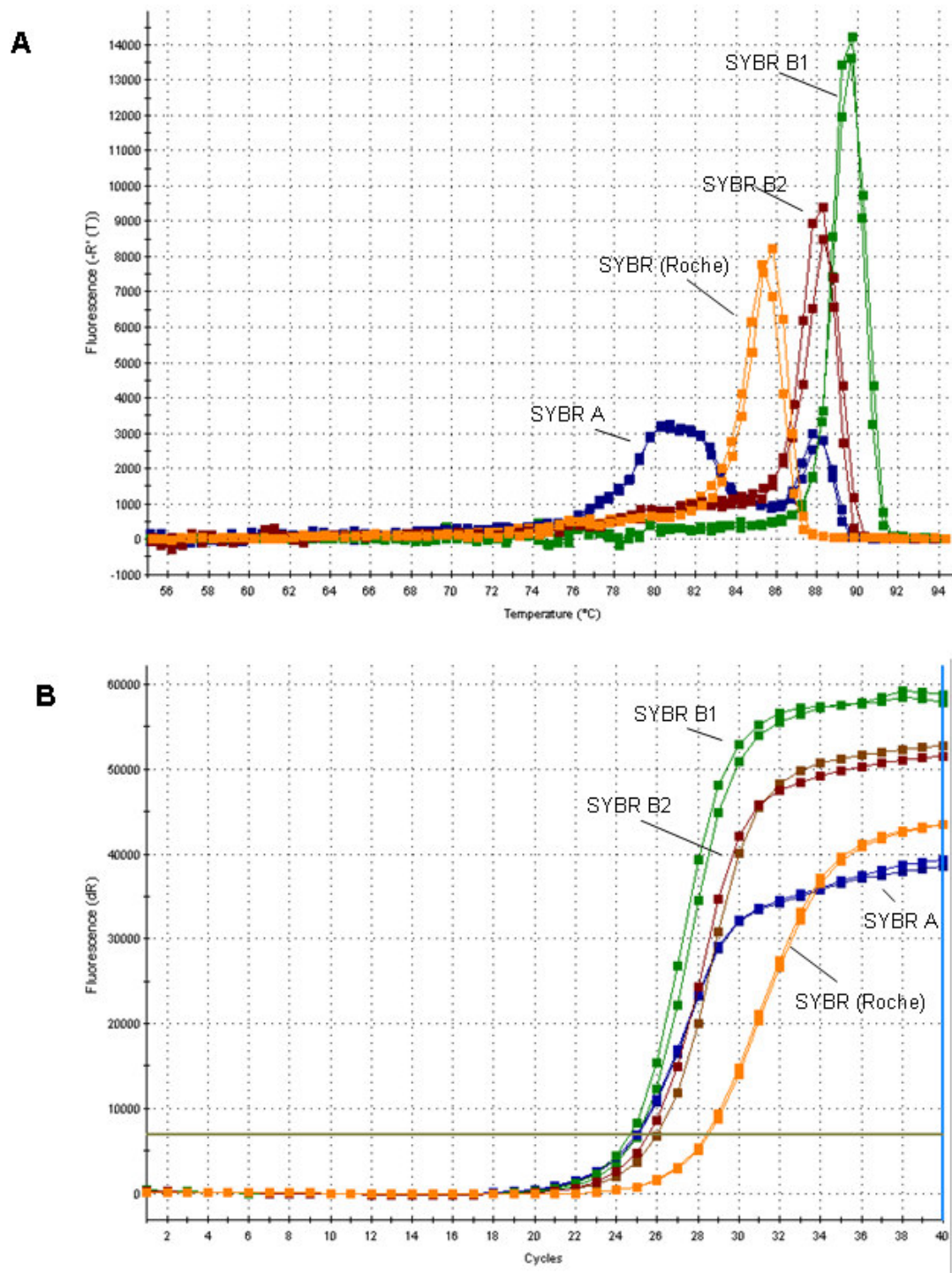


**Figure 4.17.** Dissociation curves (A) and amplification plots (B) for qPCR amplification of GRK5 using one of four different SYBR green qRT-PCR mixes. Results for amplification of GRK5 using SYBR A, B1 and B2 (made in our laboratory, Dr Jason Song, *Pers Comm.*), and FastStart SYBR Green Master (Roche) is shown. Each reaction was performed in duplicate.

All mixes produced good results for the amplification of  $\beta$ -actin (results not shown). However, the results were variable for the amplification of GRK5 (Figure 4.17). The SYBR A mix performed poorly in this experiment; resulting in the formation of a non-specific product (early peak in Figure 4.17, A) and produced a poorly-shaped amplification curve (Figure 4.17, B). Although the commercial mix (Roche) produced acceptable results, the Ct value for the Roche mix (Ct = 28.5) was much higher than that for other SYBR mixes (24.7-26.0). Thus results generated using the Roche mix were more likely to fall outside of the range that could be accurately measured (Ct <35) if the GRK5 expression was very low. The SYBR B mixes, SYBR B1 and SYBR B2, performed the best for amplification of GRK5 (Figure 17). SYBR B1 and SYBR B2 were equivalent mixtures prepared at different times and yet produced slightly different results for the Ct and melting temperature. This highlighted the importance of using SYBR mix from a single master mix for all qPCR reactions in a single run.

For all further qPCR runs one of the following SYBR mixes was used: SYBR Green supermix (BioRad), FastStart SYBR Green Master (Roche) or the “SYBR B” (SYBR B1 or SYBR B2) mixture prepared in our laboratory (Dr Jason Song, *Pers Comm.*). For experiments where very low GRK5 expression was observed (for example see section 4.5.4), only the BioRad or the “SYBR B” mix was used because these allowed the most accurate detection of GRK5 at low expression levels.

### **4.5.3 EXPERIMENT 1: Assessment of the effects of HEK293 culture age on GRK5 expression**

There is considerable evidence that the number of passages that a mammalian cell culture has undergone influences the characteristics of the cells (Freshney, 1987). For example, freshly thawed NIH3T3 cells were more efficiently transfected than cells that had undergone 8 passages (Hawley-Nelson and Shih, 1995). In addition, the growth rate of HEK293 cells increased rapidly between the 12th and 34th passage since thaw (Park et al., 2004). The effect of HEK293 culture age (passage number) on the expression of GRK5 was investigated.

#### 4.5.3.1 Preparation of cDNA from HEK293 cells of different culture age

A single tube of HEK293 cells was thawed and passaged over an approximately 3 month period. The cells were plated for RNA extraction and analysis at the 2<sup>nd</sup>, 10<sup>th</sup>, 18<sup>th</sup> and 26<sup>th</sup> passages. At the time of subculture, HEK293 cells were plated into individual 10cm<sup>2</sup> plates at a density of  $8.75 \times 10^5$  cells/plate. The cells were cultured for approximately 24 hours so that a confluence of 80-90% was reached and the cells were then frozen for later RNA extraction. RNA extraction and then reverse transcription were performed at the same time for all samples to be analysed together.

#### 4.5.3.2 GRK5 expression in HEK293 cells of different culture age

The GRK5 expression in HEK293 cells at the 2<sup>nd</sup>, 10<sup>th</sup>, 18<sup>th</sup> and 26<sup>th</sup> passages was determined using qRT-PCR. The qPCR was performed as described in section 4.2.8 using either SYBR Green supermix (BioRad), FastStart SYBR Green Master (Roche) or the “SYBR B” (B1 or B2) mixture. The data for GRK5 was normalised to expression of 18S rRNA and  $\beta$ -actin, and expressed as fold differences relative to results for the 2<sup>nd</sup> passage (set as 1). The results represent the data from four qPCR runs with each reaction performed in duplicate (Figure 4.18). Three qPCR runs were performed using identical cDNA, and a fourth using new cDNA generated from the same RNA as a technical replicate. Biological replicates were not carried out due to the time and resources required to passage HEK293 cells over a 3 month period.

There was no significant difference between the GRK5 expression in HEK293 cells of different passages (Figure 4.18). The standard errors were relatively large however. Replicates within a run were very close, and the large standard errors reflect the variation that occurred between different qPCR runs.

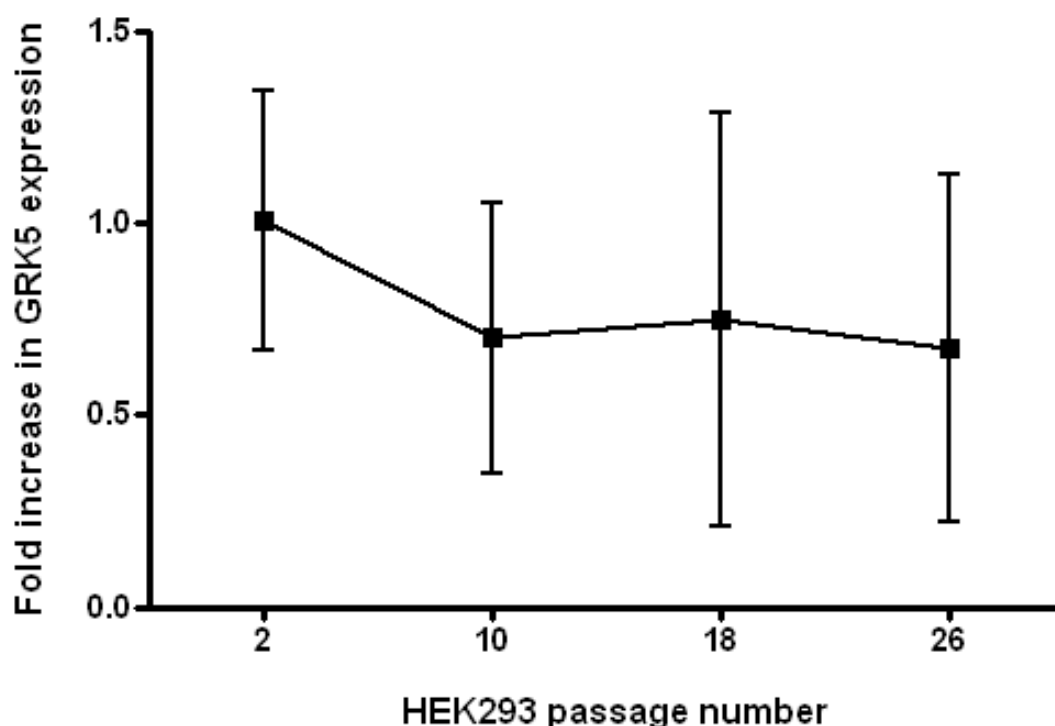


**Figure 4.18. GRK5 expression in HEK293 cells of different culture age (passage number).** The GRK5 expression in HEK293 cells at the 2<sup>nd</sup>, 10<sup>th</sup>, 18<sup>th</sup> and 26<sup>th</sup> passage was investigated using qRT-PCR. Data were normalised using 18S rRNA and  $\beta$ -actin expression, and expressed as fold increases relative to the 2<sup>nd</sup> passage. Data represent the mean  $\pm$  SEM and are the results of four qPCR runs (n=4), each performed in duplicate.

#### **4.5.4 EXPERIMENT 2: Assessment of the effects of HEK293 cell culture conditions on GRK5 expression**

It is well known that mammalian cells at different phases of the growth cycle behave differently with respect to proliferation, enzyme activity and synthesis of specific products (Freshney, 1987). For routine maintenance of the HEK293 cells, the cells were subcultured as recommended by the supplier of the cells (ATCC). HEK293 cells were subcultured when they reached a confluence of approximately 80% and plated so that they reached a confluence of no less than 30% the following day. This regime was designed to maintain the cells in the exponential growth phase. If the cells were plated at a very low density they may experience a lag in cell growth, or if allowed to grow to a confluence of  $\geq 100\%$  the growth may plateau. The aim of this experiment was to investigate whether GRK5 expression varies at different phases of the growth cycle in HEK293 cells.

#### 4.5.4.1 Preparation of cDNA from HEK293 cells subjected to different culture conditions

HEK293 cells in their second passage (subcultured twice since they were thawed) were plated into individual 10cm<sup>2</sup> plates at a density of  $1.25 \times 10^5$  cells/plate. The cells were cultured for 1, 3, 5 or 7 days ( $\pm 1$  hour) without a medium change and then frozen for later RNA extraction. At the time of freezing the cells had reached a confluence of approximately 20, 65, 100 or >100%, respectively. RNA extraction and reverse transcription were performed at the same time for all samples to be analysed together.

#### 4.5.4.2 GRK5 expression in HEK293 cells in different culture conditions

The GRK5 expression in HEK293 cells frozen on days 1, 3, 5 and 7 was determined using qRT-PCR. The qPCR was performed as described in section 4.2.8 using either SYBR Green supermix (BioRad) or the “SYBR B1” mixture. The data for GRK5 was normalised to expression of 18S rRNA and  $\beta$ -actin, and expressed as a fold increase relative to results for cells frozen on day 3 (set as 1) which were assumed to be in the exponential growth phase. The results represent the data from two qPCR runs with each reaction performed in duplicate (Figure 4.19). The two qPCR runs were performed using different cDNA samples generated from RNA extracted from different cell cultures (biological replicates).

A problem with this experiment was that the qPCR data was often poor for cDNA samples from cells frozen on days 1 and 3. Dissociation curves showed that a non-specific product with a melting temperature of approximately 83°C was formed. This problem was most likely caused by very low GRK5 expression, which may have increased the tendency of the reaction to form non-specific products such as primer-dimers. Therefore, for this experiment only, the annealing temperature was increased to

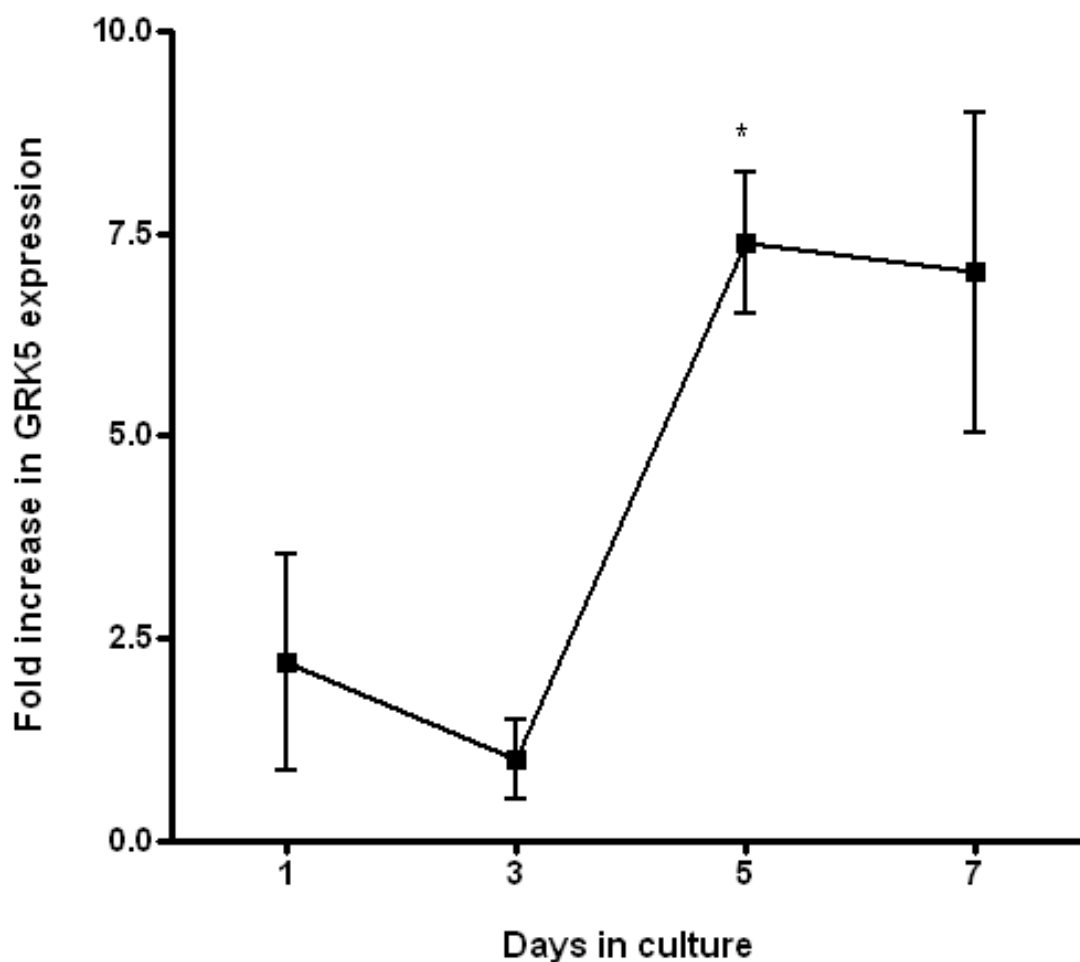


**Figure 4.19. GRK5 expression in HEK293 cells for different culture conditions (cell confluence).** The GRK5 expression in HEK293 cells at 20, 65, 100 and >100% confluence was investigated using qRT-PCR. Data were normalised using 18S rRNA and  $\beta$ -actin expression, and expressed as a fold increase relative to the results at 65% confluence. Data represent the mean  $\pm$  SEM and are the results of two qPCR runs, each performed in duplicate. (One-way AVOVA, \*  $P < 0.05$ ).

52°C to minimise non-specific product formation. Also, to avoid detection of any non-specific product an additional step was added to the 40 cycles of PCR. The reaction was heated to 86°C for 30 seconds following extension at 72°C for 45 seconds. The fluorescence was set to read during this step which meant that only the specific product (melting temperature of 86.3%) was detected.

The GRK5 expression tended to increase when the HEK293 cells were cultured for 5-7 days (grown to a confluence of  $\geq 100\%$ ) (Figure 4.19). For HEK293 cells frozen on day 5 (confluence  $\sim 100\%$ ),

the GRK5 expression was  $7.4 \pm 0.9$  fold greater than that for HEK293 cells frozen on day 3 (confluence ~65%). The result was only significant for cells cultured for 5 days, however a similar trend was observed for cells grown for 7 days. The GRK5 expression in cells cultured for 1 day (confluence ~20%) did not appear to differ from those frozen on day 3. These results suggest that when the HEK293 cells were allowed to become overconfluent ( $\geq 100\%$  confluent) GRK5 expression was up-regulated.

#### **4.5.5 EXPERIMENT 3: Comparison of GRK5 expression in different cell types**

There is evidence that the expression of GRK5 can vary quite considerably in disease paradigms, such as cancer. For example, GRK5 expression is decreased in differentiated thyroid carcinoma compared to normal thyroid tissue (Metaye et al., 2002). Therefore, to determine whether the qRT-PCR methods described here could be used to measure differences in GRK5 expression, its expression in three different human cancer cell lines was investigated. cDNA from the following human cell lines were provided as a kind gift from Dr Sarah Cunningham, Angiogenesis Research Group, Christchurch School of Medicine and Health Sciences: two breast cancer cell lines (T47D and MCF-7) and a prostate cancer cell line (Y79). It was hypothesised that the GRK5 expression in these different cell lines would vary quite considerably from that in HEK293.

The GRK5 expression in HEK293, T47D, MCF-7 and Y79 was determined using qRT-PCR. The qPCR was performed as described in section 4.2.8 using either FastStart SYBR Green Master (Roche) or the “SYBR B” (B1 or B2) mixture. The data for GRK5 was normalised to expression of 18S rRNA and  $\beta$ -actin, and expressed as a fold increase relative to results for MCF-7 (set as 1). The results represent the data from three qPCR runs with each reaction performed in duplicate (Figure 4.20). Of the three qPCR runs, two were performed using undiluted cDNA samples and one using 5-fold diluted cDNA (technical replicates).

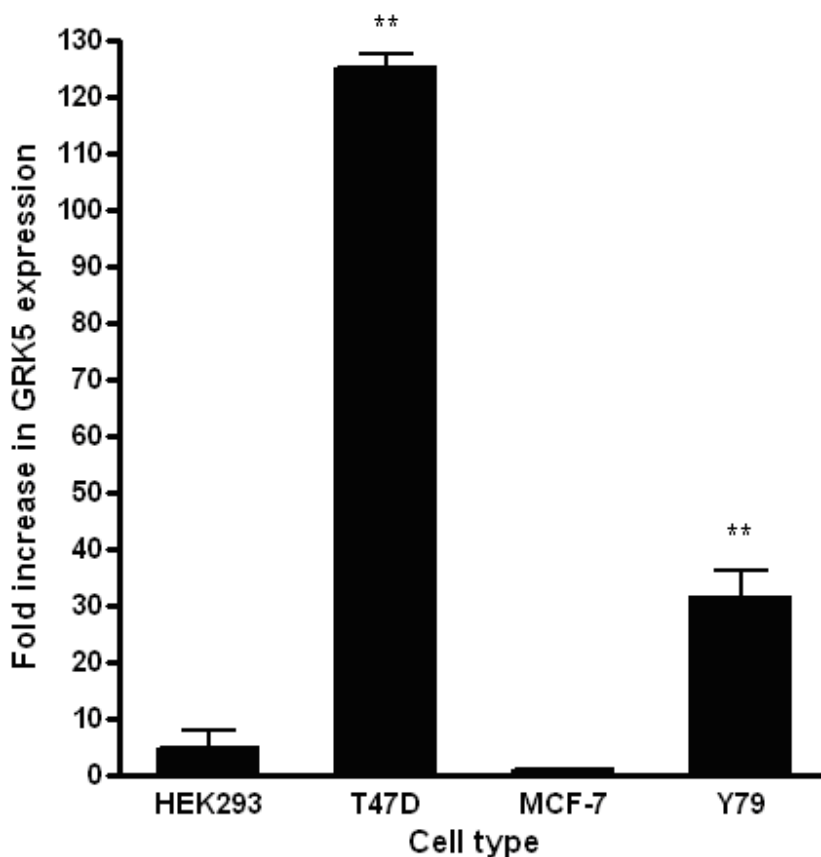


**Figure 4.20. GRK5 expression in HEK293 cells, and the following human cancer cell lines: T47D, MCF-7 and Y79.** The GRK5 expression in the different cell types was investigated using qRT-PCR. Data were normalised using 18S rRNA and  $\beta$ -actin expression, and expressed as a fold increase relative to the results for MCF-7. Data represent the mean  $\pm$  SEM and are the results of three qPCR runs, each performed in duplicate (One-way ANOVA, \*\*  $P < 0.01$ ).

The GRK5 expression in MCF-7 cells did not differ significantly from that in HEK293. Whereas, the GRK5 expression in T47D and Y79 cells was significantly different from HEK293 cells. The GRK5 expression was more than 100-fold greater in T47D cells, and 30-fold greater in Y79 cells, than in HEK293 cells. However, the expression of the 18S rRNA in T47D cells was low compared with all other cell types ( $C_t = 20$  for T47D whereas  $C_t = 16$  for all other cell types). Since the data were normalised using 18S rRNA, the final value for GRK5 expression data for T47D cells may have been an inaccurate representation of the actual relative expression. This highlighted the need for careful validation of the reference genes if comparing different cell types.



## 5

# DISCUSSION

### 5.1 SUMMARY

This study reported the development of a model cellular system that could be used to assess the effect of GRK5 knockdown on desensitisation of the pituitary vasopressin receptor (V1b-R). Desensitisation of the IP response to AVP was investigated using V1b-R-transfected HEK293 cells. These cells produced a marked response to stimulation with 100nM AVP for 15 minutes, whereas mock- and vector-transfected HEK293 cells did not produce a measurable IP response. Therefore, the response of V1b-R-transfected HEK293 was mediated by the V1b-R. Also, it appeared that the HEK293 cells do not express the V1b-R endogenously. Although De Keyzer and colleagues showed, using RT-PCR analysis, that the human V1b-R is expressed at very low levels in the human kidney (De Keyzer et al., 1994), HEK293 cells are thought to be neuronal in origin, rather than renal (Shaw et al., 2002). Data presented here indicated that if the V1b-R is expressed in HEK293 cells, the level of expression is too low to result in a detectable IP response in this experimental setup.

Significant desensitisation of the V1b-R was found to occur when the cells were exposed to a brief (5 minute) pre-treatment with a relatively low concentration of AVP (5nM). This concentration and duration is very close to that of endogenous AVP pulses measured in the pituitary portal circulation in both rats (~1.5nM AVP maximum) and sheep (~6nM AVP maximum) (reviewed in Mason et al., 2002). Therefore, the desensitisation observed may be physiologically relevant. This is consistent with previous studies of the V1b-R in our laboratory where a 5 minute exposure to

5nM AVP was sufficient to result in partial desensitisation of the V1b-R mediated ACTH response to AVP in ovine anterior pituitary cells (Hassan et al., 2003; Mason et al., 2002).

The rapidity of desensitisation suggested that the desensitisation process was most likely mediated by phosphorylation of the V1b-R, a common mechanism of desensitisation amongst the GPCR family (Ferguson, 2001). Phosphorylation and subsequent uncoupling of the receptor from its G protein is the most rapid means of attenuating GPCR responsiveness and occurs within seconds to minutes of agonist activation (Pitcher et al., 1998). Other mechanisms associated with GPCR desensitisation, such as internalisation of the receptor, occur too slowly to account for the desensitisation observed in this study. Therefore, this model system should allow the involvement of GRK5 in V1b-R desensitisation to be investigated using the RNAi.

When using RNAi it is essential to establish that the effects observed are the result of siRNA-specific degradation of the target mRNA (Dykxhoorn et al., 2003). Firstly, it is necessary to monitor any non-specific effects. Cell viability assays developed in this study could be used to monitor cytotoxic effects of the siRNA (Ciccarone et al., 1999; Jiang et al., 2008). It is also essential that both mRNA and protein levels of the target be assessed using quantitative methods. This demonstrates the mechanism by which the siRNA is acting, and also allows for an accurate estimate of the level of reduction of the target.

Quantitative reverse transcription PCR (qRT-PCR) was used to measure the expression of GRK5 at the mRNA level in HEK293 cells. Human GRK5 mRNA was amplified using both non-quantitative and qPCR techniques with GRK5 specific primers. Each of the three primer pairs tested amplified a single PCR product of the expected size (analysed using gel electrophoresis) and a single product specific melting temperature (dissociation curve analysis). The products were confirmed as the expected fragments of human GRK5 mRNA through sequencing. This provided confirmation that GRK5 is expressed endogenously in HEK293 cells, as expected based on previous studies using HEK293 cells (Kim et al., 2005; Ren et al., 2005).

GRK5 expression studies were carried out to evaluate whether the methods developed would be suitable to measure knockdown of GRK5 mRNA using RNAi. These experiments were also

designed to assess the impact of HEK293 cell culture methods on expression of GRK5. Based on the qPCR efficiency and primer specificity (assessed using qPCR data), a single GRK5 primer pair was selected for GRK5 expression studies. It was found that that expression of GRK5 did not vary with passages of the HEK293 cells (up to 26 passages). For the IP assay the HEK293 cells were used at 1-10 passages and the data presented here confirmed that GRK5 expression did not vary over this number of passages. It was also found that HEK293 cells that were maintained in culture for 5 days (grown to a confluence of approximately 100%) had a significantly greater GRK5 expression than cells cultured for only 1 or 3 days. This suggests that GRK5 expression was up-regulated when the HEK293 cells were allowed to reach, or exceed confluence ( $\geq 100\%$  confluent). This may be associated with the cells entering a plateau phase of growth (Freshney, 1987), however further investigation of HEK293 cell growth characteristics would be required to confirm that the cells were in this phase of growth. These results also demonstrated that a significant difference in GRK5 expression could be measured in HEK293 cells using qRT-PCR. Therefore the methods described in this study should be suitable to measure knockdown of GRK5 expression at the mRNA level following siRNA transfection.

## **5.2 GENERAL COMMENT ON THE METHODS USED**

### **5.2.1 Desensitisation of the inositol phosphate response to AVP using V1b-R-transfected HEK293 cells**

In this study desensitisation of the IP response to AVP was measured using V1b-R-transfected HEK293 cells. This system provides an effective tool for the examination of the effects of knockdown of the GRK5 expression using RNAi. Earlier work in our laboratory utilised ovine anterior pituitary cells to study desensitisation of the V1b-R (Mason et al., 2002), however carrying out experiments in primary cultures made the use of molecular techniques, such as RNAi, impractical. An additional advantage of using HEK 293 cells in this research is that the genetic sequence of human GRKs is known, and siRNAs for these GRKs have been designed and used to

specifically silence GRKs (Kim et al., 2005; Ren et al., 2005; Wei et al., 2003). However, the use of a cell line is not without its disadvantages. For instance, the regulation of GPCRs can vary depending on the cellular environment in which they are expressed (Ferguson, 2001). For example, IP responsiveness of PLC-coupled GPCRs can depend upon the size and/or rate of recycling of the PIP<sub>2</sub> pool in different cell types (Forrest-Owen et al., 1999). Because the cellular environment in the model system differs from that found in cells that endogenously express the V1b-R it is possible that there are differences in the regulation of the receptor in these two environments (Ferguson, 2001). Furthermore, recent evidence has shown that the level of GPCR expression can effect their regulation. For example, the thromboxane A<sub>2</sub> receptor becomes desensitised during agonist exposure at low receptor expression, but not at high receptor expression (Spurney 1998). Because the HEK293 cells were transiently transfected with the V1b-R, the level of receptor expression may have varied between assays. The variation observed in the absolute IP response is consistent with this notion. This variation may have been caused by variable transfection efficiency, which can be due to the number of passages the cell culture has undergone (Hawley-Nelson and Shih, 1995). Differences in the V1b-R expression may explain why the level of desensitisation varied somewhat between IP assays performed at different times.

While, the advantages of using RNAi are numerous and represent a significant improvement over alternative methods, there are some caveats that must be addressed. Foremost among these is the impossibility of complete silencing of the target in siRNA-transfected cells (Ahn et al., 2003). For example, in a recent study a 95% reduction in protein expression of GRK5 was achieved following transfection with GRK5 specific siRNA (Ren et al., 2005). Therefore, one might expect that if GRK5 is involved in desensitisation of the V1b-R-mediated response to AVP that cells in which GRK5 had been knocked down would be more resistant to desensitisation than the control cells, but not completely resistant. In this study, the IP response of 5nM pre-treated cells was reduced to approximately 60% of the non-pre-treated control. Therefore, knockdown of GRK5 should result in a reduction in IP response somewhere in the range of range 60-100%. Therefore, in order to be able to measure a significant reduction in desensitisation, the magnitude of desensitisation should ideally be as great as possible, and as reproducible as possible. However, as mentioned above there was some variability in the level of desensitisation seen with IP assays performed at different times. It may be possible to further optimise the methods to minimise this variation, for example

by developing a stably transfected cell line (see suggestions for further research in section 5.3). This would assist with the interpretation of the results of an RNAi experiment.

### **5.2.2 Assessment of human G protein-coupled receptor kinase 5 expression in HEK293 cells using qRT-PCR**

Quantitative reverse transcription PCR (qRT-PCR) is widely used for the quantification of mRNA levels. This method has a number of advantages over non-quantitative PCR. For example, it provides a more sensitive method of detection. The technology is not without its problems however. Reliable results depend on a number of conditions being met (for reviews see Bustin, 2002; Bustin and Nolan, 2004). For example, the template RNA must meet certain criteria (see chapter 4).

Despite attempts to optimise the qPCR for amplification of GRK5, variability in the results between qPCR runs persisted in this study. In real time PCR, the single most likely cause of data variation is variability introduced by the person carrying out the experiment (Bustin, 2002). In addition to duplicates of each reaction within a qPCR run, each run was performed at least twice for each experiment using different cDNAs. For example, technical replicates were obtained by generating new cDNA from the same RNA for experiment 1, and biological replicates (new RNA from different cells) were prepared for experiment 2. Since there are a large number of steps involved in going from a cell culture to a quantitative result, or even from RNA to a quantitative result, it is perhaps not surprising that variation occurred. A second potential source of variability was the reagents used. For example, two equivalent SYBR mixes made in our laboratory generated quite different Ct values for the same cDNA. There is also evidence that there is considerable variation between different batches of commercial SYBR mixes (Bustin, 2002). Based on this information and the results presented in this study, it is recommended for future GRK5 expression studies that only one type of SYBR mix be used for all qPCR runs.

It is also possible that the PCR primers used for amplification of GRK5 were not optimal. The qPCR reaction was optimised by testing different SYBR green reaction mixes. Although, all mixes performed well for the amplification of  $\beta$ -actin, the results were much more variable for amplification of GRK5. This suggested that the primers used for amplification of GRK5

(GRK5F2/R2) were highly dependent on the PCR conditions to function optimally. Therefore, very small variations in the qPCR reaction mixture could impact the quantitative result. One way to increase confidence in the data would be to demonstrate the same results using a different GRK5 specific primer pair, and this is recommended for future GRK5 expression studies.

### **5.3 SUGGESTIONS FOR FURTHER RESEARCH**

This study has shown that in V1b-R-transfected HEK293 cells the IP response to AVP undergoes rapid desensitisation. This model system can therefore be used to assess the role of GRK5 in this process. To do this, HEK293 cells can be transfected simultaneously with the V1b-R and either specific human GRK5 siRNA duplex or control siRNA (duplexes designed and published by Ren et al., 2005 can be used). The expression of GRK5 must then be quantified at both the mRNA and protein levels. Western blots have been used to quantitatively determine knockdown of GRK protein following transfection of HEK293 cells with siRNA (Kim et al., 2005; Ren et al., 2005; Violin et al., 2006). Western blots were not carried out in this study; however methods for this will need to be established and validated for the assessment of GRK protein knockdown in future RNAi experiments.

As discussed in section 5.2.1, there was some variability between IP assays performed at different times in this study. It is likely that this variability was due to differences in expression of the V1b-R. It is possible however to standardise the data by determining the expression levels of the V1b-R by radioligand binding assays using  $^3\text{H}$ AVP (Martin et al., 2003; Ren et al., 2005). Attempts were made to develop the methods needed to carry out ligand binding assays for use in this study. However, due to the high cost of radiolabelled AVP this was not a practical method for standardising all of the data. An alternative may be to co-transfect the V1b-R with a reporter, such as the luciferase reporter. The IP response could then be normalised to luciferase activity. However, perhaps the best way to address the issue of variable V1b-R expression is to develop a

cell line that stably expresses the receptor (for an example see Shenoy et al., 2006). It would still be necessary to assess the V1b-R expression using ligand binding assays alongside protein quantitation (Shenoy et al., 2006), however once a suitable stably transfected cell line was established and characterised this would avoid having to determine the receptor expression for every assay. In addition, this should minimise the variation in IP production.

It was hypothesised that GRK5 may be involved in the desensitisation of the V1b-R based on a recent study where the physical association of V1b-R with different GRKs was investigated (Berrada et al., 2000). Following stimulation with AVP, only GRK5 was detected in immune complexes with the V1b-R, suggesting a possible role for GRK5 in mediating V1b-R-signalling (Berrada et al., 2000). However, GRK5 is only one of 4 members of the GRK family that could potentially be involved. Ultimately, it would be useful to investigate the role of the other candidate GRKs (GRK2, 3 and 6) in V1b-R desensitisation. To do this, the work described in this study could be used as a template for establishing the methods needed to assess the involvement of other GRKs in V1b-R desensitisation.

## **ACKNOWLEDGEMENTS**

I am deeply grateful to my supervisor, Dr. Drusilla Mason, for all her encouragement and support. Her assistance and guidance in all areas of my research have been invaluable. Many thanks are also due to my associate supervisor, Dr. Jason Song, for all his advice regarding the quantitative PCR work and for his help designing primers for PCR. Thanks also to my other associate supervisors, Dr. Frank Sin and Dr. Ashley Garrill, for their ideas and suggestions.

I would like to thank the technical staff of the University of Canterbury, especially Linda Morris and Jackie Healy for their technical support. Thanks are also due to other staff of the University of Canterbury; thanks to Dr. Harry Taylor for advice and assistance regarding scintillation counting, and to Dr. Maxine Bryant for her advice regarding optimisation of PCR.

I would like to thank several staff from the Christchurch School of Medicine and Health Sciences for their contributions to this research. I would like to acknowledge Dr Anna Pilbrow for supplying a sample of her pooled reference RNA. I would also like to acknowledge Dr Sarah Cunningham for supplying cDNA from two breast cancer cell lines (T47D and MCF-7) and a prostate cancer cell line (Y79). Thanks to Leigh Elmers for her advice regarding primer design. Thanks also to Dr. Vicky Cameron who directed me to others within the school that could provide help.

Thankyou to Dr Ali Hassan (former student of University of Canterbury) and Dr Aaron Jeffs (University of Otago) for their advice regarding RNAi experiments and quantitative PCR.

I acknowledge Dr. Greti Aquilera of the NIH for supplying the prV1b-R and pALTER-MAX plasmids.

I acknowledge receipt of a Masters Scholarship from the University of Canterbury for financial support during part of this research.

Lastly, I would like to thank my family and friends for their support.



## REFERENCES

- Abd-Elsalam, K. A.** (2003). Bioinformatic tools and guideline for PCR primer design. *African Journal of Biotechnology* **2**, 91-95.
- Aguilera, G.** (1994). Regulation of pituitary ACTH secretion during chronic stress. *Frontiers in Neuroendocrinology* **15**, 321-350.
- Aguilera, G., Pham, Q. and Rabadan-Diehl, C.** (1994). Regulation of pituitary vasopressin receptors during chronic stress: relationship to corticotroph responsiveness. *Journal of Neuroendocrinology* **6**, 299-304.
- Aguilera, G. and Rabadan-Diehl, C.** (2000). Regulation of vasopressin V-1b receptors in the anterior pituitary gland of the rat. *Experimental Physiology* **85**, 19S-26S.
- Aguilera, G., Volpi, S. and RabadanDiehl, C.** (2003). G protein coupled receptor signalling in neuroendocrine systems: Transcriptional and post-transcriptional mechanisms regulating the rat pituitary vasopressin receptor gene. *Journal of Molecular Endocrinology* **30**, 99-108.
- Ahn, S., Nelson, C. D., Garrison, T. R., Miller, W. E. and Lefkowitz, R. J.** (2003). Desensitisation, internalisation, and signaling functions of B-arrestins demonstrated by RNA interference. *Proceedings of the National Academy of Sciences USA* **100**, 1740-1744.
- Antoni, F. A.** (1993). Vasopressinergic control of pituitary adrenocorticotropin secretion comes of age. *Frontiers in Neuroendocrinology* **14**, 76-122.
- Avison, M. B.** (2007). Measuring gene expression. New York: Taylor and Francis group.
- Bandaa, M., Bomminenia, A., Thomasa, R. A., Luckinbilla, L. S. and Tucker, J. D.** (2008). Evaluation and validation of housekeeping genes in response to ionizing radiation and chemical exposure for normalizing RNA expression in real-time PCR. *Mutation Research/Genetic Toxicology and Environmental Mutagenesis* **649**, 126-134.
- Barberis, C., Moullaic, B. and Durroux, T.** (1998). Structural bases of vasopressin/oxytocin receptor function. *Journal of Endocrinology* **156**.
- Basarkar, A., Devineni, D., Palaniappan, R. and Singh, J.** (2007). Preparation, characterisation, cytotoxicity and transfection efficiency of poly(DL-lactide-co-glycolide) and poly (DL-lactic acid) cationic nanoparticles for controlled delivery of plasmid DNA. *International Journal of Pharmaceutics* **343**, 247-254.
- Benovic, J., Pike, L., Cerione, R., Staniszewski, C., Yoshimasa, T., Codina, J., Caron, M. and Lefkowitz, R.** (1985). Phosphorylation of the mammalian beta-adrenergic receptor by cyclic AMP-dependent protein kinase. Regulation of the rate of receptor phosphorylation and

dephosphorylation by agonist occupancy and effects on coupling of the receptor to the stimulatory guanine nucleotide regulatory protein. *Journal of Biological Chemistry* **11**, 7094-7101.

**Benovic, J. L., Kuhn, H., Weyand, I., Codina, J., Caron, M. G. and Lefkowitz, R. J.** (1987). Functional desensitization of the isolated beta-adrenergic-receptor by the beta-adrenergic-receptor kinase - potential role of an analog of the retinal protein arrestin (48-Kda protein). *Proceedings of the National Academy of Sciences USA* **84**, 8879-8882.

**Benovic, J. L., Strasser, R. H., Caron, M. G. and Lefkowitz, R. J.** (1986). Beta-adrenergic receptor kinase: identification of a novel protein kinase that phosphorylates the agonist-occupied form of the receptor. *Proceedings of the National Academy of Sciences USA* **83**, 2797-2801.

**Berg, K. A., Stout, B. D., Maayani, S. and Clarke, W. P.** (2001). Differences in rapid desensitization of 5-hydroxytryptamine(2A) and 5-hydroxytryptamine(2C) receptor-mediated phospholipase C activation. *Journal of Pharmacology and Experimental Therapeutics* **299**, 593-602.

**Berrada, K., Plesnicher, C. L., Luo, X. and Thibonnier, M.** (2000). Dynamic interaction of human vasopressin/oxytocin receptor subtypes with G protein-coupled receptor kinases and protein kinase C after agonist stimulation. *Journal of Biological Chemistry* **275**, 27229-27237.

**Berridge, M. J., Dawson, R. M. C., Downes, C. P., Heslop, J. P. and Irvine, R. F.** (1983). Changes in the levels of inositol phosphates after agonist-dependent hydrolysis of membrane phosphoinositides. *Biochemical Journal* **212**, 473-482.

**Berridge, M. J., Downes, C. P. and Hanley, M. R.** (1982). Lithium amplifies agonist-dependent phosphatidylinositol responses in brain and salivary glands. *Biochemical Journal* **206**, 587-595.

**Birnbaumer, M.** (2000). Vasopressin receptors. *Trends in Endocrinology and Metabolism* **11**, 406-410.

**Buckingham, J., Cowell, A., Gillies, G., Herbison, A. and Steel, J.** (1997). Stress, Stress Hormones and the Immune System: John Wiley and Sons, Ltd.

**Burg, M. B., Ferraris, J. D. and Dmitrieva, N. I.** (2007). Cellular response to hyperosmotic stress. *Physiological Reviews* **87**, 1441-1474.

**Bustin, S. A.** (2002). Quantification of mRNA using real-time reverse transcription PCR (RT-PCR): trends and problems. *Journal of Molecular Endocrinology* **29**, 23-39.

**Bustin, S. A. and Nolan, T.** (2004). Pitfalls of quantitative real-time reverse-transcription polymerase chain reaction. *Journal of Biomolecular techniques* **15**, 155-166.

**Ciccarone, V., Chu, Y., Schifferli, K., Pichet, J.-P., Hawley-Nelson, P., Evans, K., Roy, L. and Bennett, S.** (1999). Lipofectamine Reagent for Rapid, Efficient Transfection of Eukaryotic Cells. *Focus* **21**, 54-55.

**Cortez, D. M., Feldman, M. D., Mummidi, S., Valente, A. J., Steffensen, B., Vincenti, M., Barnes, J. L. and Chandrasekar, B.** (2007). IL-17 stimulates MMP-1 expression in primary human cardiac fibroblasts p38 MAPK- and ERK1/2- dependent C/EBP-B, NFkB, and AP-1 activation. *American Journal of Physiology Heart and Circulatory Physiology* **293**, 3356-3365.

**Cupo, D.** (1999). Cationic lipid reagent selection. *Focus* **21**, 61.

**Dale, L. B., Bhattacharya, M., Anborgh, P. H., Murdoch, B., Bhatia, M., Nakanishi, S. and Ferguson, S. S. G.** (2000). G protein coupled receptor kinase-mediated desensitization of metabotropic glutamate receptor 1A protects against cell death. *Journal of Biological Chemistry* **275**, 38213-38220.

**Dautzenberg, F. M., Braun, S. and Hauger, R. L.** (2001). GRK3 mediates desensitization of CRF1 receptors: a potential mechanism regulating stress adaptation. *American Journal of Physiology Regulatory, Integrative and Comparative Physiology* **280**, 935-946.

**De Keyser, Y., Auzan, C., Lenne, F., Cherif, B., Thibonnier, M., Bertagna, X. and Clauser, E.** (1994). Cloning and characterisation of the human V3 vasopresin receptor. *FEBS letters* **256**, 215-220.

**Dhami, K., Anborgh, P. H., Dale, L. B., Sterne-Marr, R. and Ferguson, S. S. G.** (2002). Phosphorylation-independent regulation of metabotropic glutamate receptor signaling by G protein-coupled receptor kinase 2. *Journal of Biological Chemistry* **277**, 25266-25272.

**Downes, C. P. and Macphee, C. H.** (1990). myo-Inositol metabolites as cellular signals. *European Journal of Biochemistry* **193**, 1-18.

**Downes, C. P. and Michell, R. H.** (1981). The polyphosphoinositide phosphodiesterase of erythrocyte-membranes. *Biochemical Journal* **198**, 133-140.

**Dykxhoorn, D. M., Novina, C. D. and Sharp, P. A.** (2003). Killing the messenger: short RNAs that silence gene expression. *Nature Reviews Molecular Cell Biology* **4**, 457-467.

**Editorial.** (2003). Whither RNAi? *Nature Cell Biology* **5**, 489-490.

**Elbashir, S. M., Harborth, J., Lendeckel, W., Yalcin, A., Weber, K. and Tuschl, T.** (2001). Duplexes of 21-nucleotide RNAs mediate RNA interference in cultured mammalian cells. *Nature* **411**, 494-498.

**Felder, C. C., Kanterman, R. Y., Ma, A. L. and Axelrod, J.** (1989). A transfected M1 muscarinic acetylcholine-receptor stimulates adenylate-cyclase via phosphatidylinositol hydrolysis. *Journal of Biological Chemistry* **264**, 20356-20362.

**Ferguson, S. S. G.** (2001). Evolving concepts in G protein-coupled receptor endocytosis: The role in receptor desensitisation and signalling. *Pharmacological reviews* **53**, 1-24.

**Ferguson, S. S. G. and Caron, M. G.** (1998). G protein-coupled receptor adaptation mechanisms. *Cell and Developmental Biology* **9**, 119-127.

**Fire, A., Xu, S., Montgomery, M. K., Kostas, S. A., Driver, S. E. and Mello, C. C.** (1998). Potent and specific genetic interference by double-stranded RNA in *Caenorhabditis elegans*. *Nature* **391**, 806-811.

**Forrest-Owen, W., Willars, G. B., Nahorski, S. R., Assefa, D., Davidson, J. S., Hislop, J. and McArdle, C. A.** (1999). The lack of gonadotrophin-releasing hormone (GnRH) receptor desensitisation in alpha T3-1 cells is not due to GnRH receptor reserve or phosphatidylinositol 4,5-bis-phosphate pool size. *Molecular and Cellular Endocrinology* **147**, 161-173.

**Franca, L. P., Pacheco, N. A. S., Correa, S. A. A., Han, S. W., Nakaie, C. R., Paiva, A. C. M. and Shimuta, S. I.** (2003). Angiotensin II-mediated cellular responses: a role for the 3'-untranslated region of the angiotensin AT(1) receptor. *European Journal of Pharmacology* **476**, 25-30.

**Freedman, N. J., Ament, A. S., Oppermann, M., Stoffel, R. H., Exum, S. T. and Lefkowitz, R. J.** (1997). Phosphorylation and desensitization of human endothelin A and B receptors - Evidence for G protein-coupled receptor kinase specificity. *Journal of Biological Chemistry* **272**, 17734-17743.

**Freshney, R. I.** (1987). *Culture of Animal Cells: A Manual of Basic Technique*. New York: Wiley-Liss, Inc.

**Gaudreau, R., Gouill, C. L., Venne, M.-H. and Stankova, J.** (2002). Threonine 308 within a putative casein kinase 2 site of the cytoplasmic tail of the leukotriene B4 receptor (BLT1) is crucial for ligand-induced, G-protein-coupled receptor-specific kinase-6 mediated desensitisation. *The Journal of Biological Chemistry* **277**, 31567-31578.

**Gaudreau, R., Le Gouill, G., Metaoui, S., Lemire, S., Stankova, J. and Rola-Pleszczynski, M.** (1998). Signalling through the leukotriene B-4 receptor involves both alpha(i) and alpha(16), but not alpha(q) or alpha(11) G-protein subunits. *Biochemical Journal* **335**, 15-18.

**Gillies, G., Linton, E. A. and Lowry, P. J.** (1982). Corticotropin releasing activity of the new CRF is potentiated several times by vasopressin. *Nature* **299**, 355-357.

**Hasbi, A., Polastron, J., Allouche, S., Stanasila, L., Massoute, D. and Jauzac, P.** (1998). Desensitization of the delta-opioid receptor correlates with its phosphorylation in SK-N-BE cells: involvement of a G protein-coupled receptor kinase. *Journal of Neurochemistry* **70**, 2129-2138.

**Hassan, A.** (2001). Desensitisation of the adrenocorticotropin response to arginine vasopressin. In *School of Biological Sciences*, vol. PhD thesis. Christchurch: University of Canterbury.

**Hassan, A., Chacko, S. and Mason, D.** (2003). Desensitization of the adrenocorticotropin response to arginine vasopressin and corticotropin-releasing hormone in ovine anterior pituitary cells. *Journal of Endocrinology* **178**, 491-501.

- Hassan, A. and Mason, D.** (2005). Mechanisms of desensitization of the adrenocorticotropin response to arginine vasopressin in ovine anterior pituitary cells. *Journal of Endocrinology* **184**, 29-40.
- Hawley-Nelson, P. and Shih, P.-J.** (1995). Sensitivity of transfection efficiency to culture age. *Focus* **17**, 60-61.
- Hermans, E. and Maloteaux, J. M.** (1996). Desensitization of neurotensin-induced phosphoinositide hydrolysis in transfected CHO cells. *Biochemical Pharmacology* **51**, 1749-1752.
- Higashijima, T., Uzu, S., Nakajima, T. and Ross, E. M.** (1988). Mastoparan, a peptide toxin from wasp venom, mimics receptors by activating GTP-binding regulatory proteins (G proteins). *Journal of Biological Chemistry* **263**, 6491-6494.
- Holmes, C. L., Landry, D. W. and Granton, J. T.** (2003). Science Review: Vasopressin and the cardiovascular system - part 1 - receptor physiology. *Critical Care* **7**, 427-434.
- Iwata, K., Luo, J., Penn, R. B. and Benovic, J. L.** (2005). Bimodal regulation of the human histamine receptor by G protein-coupled receptor kinase 2. *Journal of Biological Chemistry* **280**, 2197-2204.
- Jiang, G., Park, K., Kim, J., Kim, K. S., Oh, E. J., Kang, H., Han, S.-E., Oh, Y. K., Park, T. G. and Hahn, S. K.** (2008). Hyaluronic acid: Polyethyleneimine conjugate for target specific intracellular delivery of siRNA. *Biopolymers* **89**, 635-642.
- Johnson, A. J.** (1992). The role of G proteins in ACTH secretion from ovine corticotrophs. In *School of Biological Sciences*, vol. Masters thesis. Christchurch: University of Canterbury.
- Kelly, E., Bailey, C. P. and Henderson, G.** (2008). Agonist-selective mechanisms of GPCR desensitization. *British Journal of Pharmacology* **152**, 379-388.
- Kim, J., Ahn, S., Ren, X. R., Whalen, E. J., Reiter, E., Wei, H. J. and Lefkowitz, R. J.** (2005). Functional antagonism of different G protein-coupled receptor kinases for beta-arrestin-mediated angiotensin II receptor signaling. *Proceedings of the National Academy of Sciences USA* **102**, 1442-1447.
- King, M. S. and Baertschi, A. J.** (1990). The role of intracellular messengers in adrenocorticotropin secretion in vivo. *Experientia* **46**, 26-40.
- Kobayashi, S., Kitzawa, T., Somlyo, A. V. and Somlyo, A. P.** (1989). Cytosolic heparin inhibits muscarinic and alpha-adrenergic Ca<sup>2+</sup> release in smooth muscle. Physiological role of inositol 1,4,5-triphosphate in pharmacomechanical coupling. *Journal Biological Chemistry* **264**.
- Kunapuli, P. and Benovic, J. L.** (1993). Cloning and expression of GRK5: A member of the G protein-coupled receptor kinase family *Proceedings of the National Academy of Sciences USA* **90**, 5588-5592.

**LeBeau, A. P.** (1998). Interaction between arginine vasopressin- and raised extracellular potassium-stimulated pathways in adrenocorticotropin secretion. *Life Science* **63**, 2233-2242.

**Li, J., Liu, Y. and Ru, B.** (2005). Effect of metallothionein on cell viability and its interactions with cadmium and zinc in HEK923 cells. *Cell Biology International* **29**, 843-848.

**Li, S. R., Dorudi, S. and Bustin, S. A.** (2000). Elevated levels of RanBP7 mRNA in colorectal carcinoma are associated with increased proliferation and are similar to the transcription pattern of the proto-oncogene c-myc. *Biochemical and biophysical research* **271**, 322-329.

**Liu, J. and Wess, J.** (1996). Different single receptor domains determine the distinct G protein coupling profiles of members of the vasopressin receptor family. *Journal of Biological Chemistry* **271**, 8772-8778.

**Livak, K. J. and Schmittgen, T. D.** (2001). Analysis of relative gene expression data using real-time quantitative PCR and the 2-(Delta Delta C(T)) method. *Methods* **25**, 402-408.

**Lohse, M. J.** (1993). Molecular mechanisms of membrane-receptor desensitization. *Biochimica Et Biophysica Acta* **1179**, 171-188.

**Lolait, S. J., Ocarroll, A. M., Mahan, L. C., Felder, C. C., Button, D. C., Young, W. S., Mezey, E. and Brownstein, M. J.** (1995). Extrahypothalamic expression of the rat V1b vasopressin receptor gene. *Proceedings of the National Academy of Sciences USA* **92**, 6783-6787.

**Mao, Z., Ma, L., Yan, J., Yan, M., Gao, C. and Shen, J.** (2007). The gene transfection efficiency of thermoresponsive N,N,N-trimethyl chitosan chloride-g-poly(N-isopropylacrylamide) copolymer. *Biomaterials* **28**, 4488-4500.

**Martin, N. P., Lefkowitz, R. J. and Shenoy, S. K.** (2003). Regulation of V2 vasopressin receptor degradation by agonist-promoted ubiquitination. *Journal of Biological Chemistry* **278**, 45954-45959.

**Martini, L. and Morpugo, C.** (1955). Neurohormonal control of the release of adrenocorticotrophic hormone. *Nature* **175**, 1127-1128.

**Mason, D., Arora, K. K., Mertz, L. M. and Catt, K. J.** (1994). Homologous down-regulation of gonadotropin-releasing hormone receptor sites and messenger ribonucleic acid transcripts in aT3-1 cells. *Endocrinology* **135**, 1165-1170.

**Mason, D., Hassan, A., Chacko, S. and Thompson, P.** (2002). Acute and chronic regulation of pituitary receptors for vasopressin and corticotropin releasing hormone. *Archives of Physiology and Biochemistry* **110**, 74-89.

**Metaye, T., Menet, E., Guilhot, J. and Kraimps, J.-L.** (2002). Expression and activity of G protein-coupled receptor kinases in differentiated thyroid carcinoma. *The journal of clinical endocrinology and metabolism* **87**, 3279-3286.

**Miao, G.-Y., Lu, Q.-M. and Zhang, X.-L.** (2007). Down-regulation of survivin by RNAi inhibits growth of human gastric carcinoma cells. *World Journal of Gastroenterology* **13**, 1170-1174.

**Munck, A., Guyre, P. and Holbrook, N. J.** (1984). Physiological function of glucocorticoids in stress and their relation to pharmacological actions. *Endocrine Reviews* **5**, 25-44.

**Nagayama, Y., Tanaka, K., Hara, T., Namba, H., Yamashita, S., Taniyama, K. and Niwa, M.** (1996). Involvement of G protein-coupled receptor kinase 5 in homologous desensitization of the thyrotropin receptor. *Journal of Biological Chemistry* **271**, 10143-10148.

**Neill, J. D., Duck, L. W., Musgrove, L. C. and Sellers, J. C.** (1998). Potential regulatory roles for G protein-coupled receptor kinases and beta-arrestins in gonadotropin-releasing hormone receptor signaling. *Endocrinology* **139**, 1781-1788.

**Nolan, T., Hands, R. E. and Bustin, S. A.** (2006). Quantification of mRNA using real-time PCR. *Nature Protocols*, 1559-1582.

**O'Connor, T. M., O'Halloran, D. J. and Shanahan, F.** (2000). The stress response and the hypothalamic-pituitary-adrenal axis: from molecule to melancholia. *Quarterly Journal of Medicine*, 323-333.

**Oppermann, M., Freedman, N. J., Alexander, R. W. and Lefkowitz, R. J.** (1996). Phosphorylation of the type 1A angiotensin II receptor by G protein-coupled receptor kinases and protein kinase C. *Journal of Biological Chemistry* **271**, 13266-13272.

**Park, M. T., Lee, M. S., Kim, S. H., Jo, E.-C. and Lee, G. M.** (2004). Influence of culture passages on growth kinetics and adenovirus vector production for gene therapy in monolayer and suspension cultures of HEK293 cells. *Applied Microbiology and Biotechnology* **65**, 553-558.

**Pichet, J.-P. and Ciccarone, V.** (1999a). Lipofectamine 2000 Reagent for Rapid, Efficient Transfection of Eukaryotic Cells. *Focus* **21**, 58-60.

**Pichet, J.-P. and Ciccarone, V.** (1999b). Transfection of Mammalian Cells in 96-Well Plates with LIPOFECTAMINE 2000 Reagent. *Focus* **21**, 57-63.

**Pitcher, J. A., Freedman, N. J. and Lefkowitz, R. J.** (1998). G protein-coupled receptor kinases *Annual Review of Biochemistry* **67**, 653-693.

**Plotsky, P. M., Bruhn, T. O. and Vale, W.** (1985). Hypophysiotropic regulation of adrenocorticotropin secretion in response to insulin-induced hypoglycemia. *Endocrinology* **117**, 323-329.

**Premont, R. T., Koch, R. J., Inglese, J. and Lefkowitz, R. J.** (1994). Identification, purification, and characterization of GRK5, a member of the family of G protein-coupled receptor kinases. *Journal of Biological Chemistry* **269**, 6832-6841.

- Rasmussen, R. P.** (2001). Quantification on the LightCycler. Heidelberg: Springer Press.
- Ren, X. R., Reiter, E., Ahn, S., Kim, J., Chen, W. and Lefkowitz, R. J.** (2005). Different G protein-coupled receptor kinases govern G protein and beta-arrestin-mediated signaling of V2 vasopressin receptor. *Proceedings of the National Academy of Sciences USA* **102**, 1448-1453.
- Reynolds, A., Anderson, E. M., Vermeulen, A., Fedorov, Y., Robinson, K., Leake, D., Karpilow, J., Marshall, W. S. and Khvorova, A.** (2006). Induction of the interferon response by siRNA is cell type- and duplex length-dependent. *RNA* **12**, 988-993.
- Reynolds, A., Leake, D., Boese, Q., Scaringe, S., Marshall, W. S. and Khvorova, A.** (2004). Rational siRNA design for RNA interference. *Nature Biotechnology* **22**, 326-330.
- Robbins, A. K. and Horlick, R. A.** (1998). Macrophage scavenger receptor confers an adherent phenotype to cells in culture. *Biotechniques* **15**, 240-244.
- Rosseau-Merck, M. F., Rene, P., Derre, J., Bienvenu, T., Berger, R. and De Keyzer, Y.** (1995). Chromosomal localisation of the human V3 pituitary vasopressin receptor (AVPR3) to 1q32. *Genomics* **30**, 405-406.
- Roy, R., Cates, S., Schifferli, K., Pitchet, J.-P., Ciccarone, V., Bennett, S. and Hawley-Nelson, P.** (1999). High transfection efficiency of cloned cell lines. *Focus* **21**, 62-65.
- Rozen, S. and Skaletsky, H. J.** (2000). Primer3 on the WWW for general users and for biologist programmers. New Jersey: Humana Press.
- Saitou, N. and Nei, M.** (1987). The neighbour-joining method: a new method for reconstructing phylogenetic trees. *Molecular Biology and Evolution* **4**, 406-425.
- Sambrook, J., Fritsch, E. F. and Maniatis, T.** (1989). Molecular Cloning: A Laboratory Manual: Cold Spring Harbor Laboratory Press.
- Scott, L. V. and Dinan, T. G.** (1998). Vasopressin and the regulation of hypothalamic-pituitary-adrenal axis function: implications for the pathophysiology of depression. *Life Science* **62**, 1985-1998.
- Shacham, S., Cheifetz, M. N., Fridkin, M., Pawson, A. J., Millar, R. P. and Naor, Z.** (2005). Identification of Ser(153) in ICL2 of the gonadotropin-releasing hormone (GnRH) receptor as a phosphorylation-independent site for inhibition of G(q) coupling. *Journal of Biological Chemistry* **280**, 28981-28988.
- Shaw, G., Morse, S., Ararat, M. and Graham, F. L.** (2002). Preferential transformation of human neuronal cells by human adenoviruses and the origin of HEK293 cells. *The FASEB journal*, 1-19.
- Shenoy, S. K., Drake, M. T., Nelson, C. D., Houtz, D. A., Xiao, K., Madabushi, S., Reiter, E., Premont, R. T., Lichtarge, O. and Lefkowitz, R. J.** (2006). B-arrestin-dependent, G



protein-independent ERK1/2 activation by the B2 adrenergic receptor. *Journal of Biological Chemistry* **281**, 1261-1273.

**Sledz, C. A., Holko, M., de Veer, M. J. and Williams, B. R.** (2003). Activation of the interferon system by short-interfering RNAs. *Nature Cell Biology* **5**, 834-839.

**Smith, P. K., Krohn, R. I., Hermanson, G. T., Mallia, A. K., Gartner, F. H., Provenzano, M. D., Fujimoto, E. K., Goeke, N. M., Olson, B. J. and Klenk, D. C.** (1985). Measurement of protein using bicinchoninic acid. *Analytical Biochemistry* **150**, 76-85.

**Smyth, E. M., Austin, S. C., Reilly, M. P. and FitzGerald, G. A.** (2000). Internalisation and sequestration of the human prostacyclin receptor. *Journal of Biological Chemistry* **275**, 32037-32045.

**Sugimoto, T., Saito, M., Mochizuki, S., Watanabe, Y., Hashimoto, S. and Kawashima, H.** (1994). Molecular cloning and functional expression of a cDNA encoding the human V1b vasopressin receptor. *Journal of Biological Chemistry* **269**, 27088-27092.

**Tang, H., Guo, D. F., Porter, J. P., Wanaka, Y. and Inagami, T.** (1998). Role of cytoplasmic tail of the type 1A angiotensin II receptor in agonist- and phorbol ester-induced sensitization. *Circulation Research* **82**, 523-531.

**Thibonnier, M., Berti-Mattera, L. N., Dulin, N., Conarty, D. M. and Mattera, R.** (1998). Signal transduction pathways of the human V1-vascular, V2-renal and V3 pituitary vasopressin and oxytocin receptors. *Progress in Brain Research* **118**, 147-161.

**Thompson, J. D., Gibson, T. J., Plewniak, F., Jeanmougin, F. and Higgins, D. G.** (1997). The ClustalX windows interface: flexible strategies for multiple sequence alignment aided by quality analysis tools. *Nucleic acids research* **22**, 4673-4680.

**Tobin, A. B.** (1997). Phosphorylation of phospholipase C-coupled receptors. *Pharmacology & Therapeutics* **75**, 135-151.

**van de Loosdrecht, A. A.** (1994). A tetrazolium-based colorimetric MTT assay to quantitate human monocyte mediated cytotoxicity against leukemic cells from cell lines and patients with acute myeloid leukemia. *Journal of Immunological Methods* **174**, 311-320.

**Vancha, A. R., Govindaraju, S., Parsa, K. V. L. and Jasti, M.** (2004). Use of polyethyleneimine polymer in cell culture as attachment factor and lipofectin enhancer. *BMC Biotechnology* **4**, 1472-1483.

**Ventura, M. A., Rene, P., De Keyser, Y., Bertagna, X. and Clauser, E.** (1999). Gene and cDNA cloning and characterisation of the mouse V3/V1b pituitary vasopressin receptor. *Journal of Molecular Endocrinology* **22**, 251-260.

**Violin, J. D., Ren, X. R. and Lefkowitz, R. J.** (2006). G-protein-coupled receptor kinase specificity for beta-arrestin recruitment to the beta(2)-adrenergic receptor revealed by fluorescence resonance energy transfer. *Journal of Biological Chemistry* **281**, 20577-20588.

**von Ahsen, N., Schutz, E., Armstrong, V. W. and Oellerich, M.** (1999). Rapid detection of prothrombotic mutations of prothrombin (G20210A), factor V (G1691A), and methylenetetrahydrofolate reductase (C677T) by real-time fluorescence PCR with the LightCycler. *Clinical Chemistry* **45**, 694-696.

**Wei, H. J., Ahn, S., Shenoy, S. K., Karnik, S. S., Hunyady, L., Luttrell, L. M. and Lefkowitz, R. J.** (2003). Independent beta-arrestin 2 and G protein-mediated pathways for angiotensin II activation of extracellular signal-regulated kinases 1 and 2. *Proceedings of the National Academy of Sciences USA* **100**, 10782-10787.

**Wojcikiewicz, R. J. H., Tobin, A. B. and Nahorski, S. R.** (1993). Desensitization of cell signalling mediated by phosphoinositidase C. *Trends in Pharmacological Sciences* **14**, 279-285.

**Wong, M. L. and Medrano, J. F.** (2005). Real-time PCR for mRNA quantitation. *Biotechniques* **39**, 1-11.

**Yang, W. and Xia, S.-H.** (2006). Mechanisms of regulation and function of G-protein-coupled receptor kinases. *World Journal of Gastroenterology* **12**, 7753-7757.

## APPENDIX A

### MATERIALS

AG1-X8 anion-exchange resin	BioRad
Agarose	Gibco, Invitrogen Corporation
Ammonium formate	Sigma-Aldrich Company
Ampicillin	Invitrogen
Arginine vasopressin (AVP)	Sigma-Aldrich Company
BCA protein assay kit	Pierce
BCP	Molecular Research Centre, Inc
Boric acid	BDH
Bovine serum albumin	Gibco, Invitrogen Corporation
Bromophenol blue	Sigma-Aldrich Company
Buffer for Reverse Transcriptase (5x)	Roche
Buffer for Taq Polymerase (10x)	Roche
Cell freezing medium	Gibco, Invitrogen Corporation
Chinese Hamster Ovary cell line	ATCC
Chloramphenicol	Sigma-Aldrich Company
dNTP primer	Invitrogen
DTT	Roche
Dulbecco's modified Eagle's medium (- inositol)	MP Biomedical
Ethanol (100%)	BDH
Expand Reverse Transcriptase (50U/ $\mu$ L)	Roche
FastStart SYBR Green Master	Roche
Foetal Bovine Serum (FBS)	Gibco, Invitrogen Corporation
Formic acid	Sigma-Aldrich Company
Glacial acetic acid	BDH
Glucose	BDH
Glycerol	BDH
High DNA mass ladder	Gibco, Invitrogen Corporation
Heat Inactivated Horse Serum (HIHS)	Gibco, Invitrogen Corporation
Human Embryonic Kidney cell line	ATCC
Hydrochloric acid	BDH
Hyperladder I	Bioline
KH <sub>2</sub> PO <sub>4</sub>	BDH
L-glutamine	Gibco, Invitrogen Corporation
Lipofectamine <sup>TM</sup> 2000 transfection reagent	Gibco, Invitrogen Corporation
Lithium chloride (LiCl)	Sigma-Aldrich Company
Magnesium Chloride	Promega
Minimal Essential Alpha Medium (AMEM)	Gibco, Invitrogen Corporation
Minimal Essential Medium (MEM)	Gibco, Invitrogen Corporation
Minimal Essential Medium (MEM) (-phenol red)	Gibco, Invitrogen Corporation

MTT reagent	Sigma-Aldrich Company
<i>myo</i> -[ <sup>3</sup> H]inositol	Amersham Biosciences
Neomycin	Sigma-Aldrich Company
Na <sub>2</sub> EDTA.2H <sub>2</sub> O	BDH
Na <sub>2</sub> HPO <sub>4</sub>	BDH
Oligo (dT) primers	Roche
OptiMEM	Gibco, Invitrogen Corporation
Penicillin/Streptomycin	Gibco, Invitrogen Corporation
Poly-L-lysine	Sigma-Aldrich Company
Poly-D-lysine	Becton Dickinson Biosciences
Poly-D-lysine coated 24-well plates	Becton Dickinson Biosciences
Polyprep® chromatography columns	BioRad
Potassium acetate	BDH
Potassium hydroxide	Sigma-Aldrich Company
pUC19 plasmid	Invitrogen
Restriction enzyme specific buffer	Gibco, Invitrogen Corporation
RPMI media (-phenol red)	Sigma-Aldrich Company
RNase	Gibco, Invitrogen Corporation
RNase-away	Invitrogen
RNAsecure	Ambion
RNasezap	Ambion
Scintillation cocktail (NBCS104)	Sigma-Aldrich Company
SDS	Sigma-Aldrich Company
Sodium chloride	BDH
Sodium formate	Sigma-Aldrich Company
Sodium hydroxide	BDH
Sodium pyruvate	Gibco, Invitrogen Corporation
SYBR green supermix	BioRad
SYBRsafe dye	Invitrogen
Taq Polymerase (5U/μl)	Roche
Tris base	BDH
Tric.HCl	Sigma-Aldrich Company
TRI reagent	Molecular Research Centre, Inc
Triton-X	Sigma-Aldrich Company
Trypan Blue	Sigma-Aldrich Company
Trypsin/EDTA (TE)	Gibco, Invitrogen Corporation
Ultra Clean DNA purification kit	MO BIO Laboratories, Inc
XhoI restriction enzyme	Gibco, Invitrogen Corporation
Xylene cyanol	Sigma-Aldrich Company

## **APPENDIX B**

### **SOLUTIONS AND MEDIA**

#### **B.1 CELL CULTURE**

##### **B.1.1 Minimal Essential Medium (MEM)**

One packet of commercially prepared powdered MEM was dissolved into ddH<sub>2</sub>O, and 1.5g of sodium Bicarbonate (NaHCO<sub>3</sub>) was added. The solution was made up to 1L with ddH<sub>2</sub>O, adjusted to pH 7.1 and sterilised by negative pressure filtration through a 0.45µm membrane filter. The medium was stored at 4°C, for up to 2 months. For culturing HEK293 cells this medium was supplemented with 10% heat-inactivated horse serum (HIHS), 1% sodium pyruvate and 1% penicillin/streptomycin.

##### **B.1.2 Minimal Essential Alpha Medium (AMEM)**

One packet of commercially prepared powdered AMEM was dissolved into ddH<sub>2</sub>O, and 2.2g of sodium bicarbonate (NaHCO<sub>3</sub>) was added. The solution was made up to 1L with ddH<sub>2</sub>O, adjusted to pH 7.1 and sterilised by negative pressure filtration through a 0.45µm membrane filter. The medium was stored at 4°C, for up to 2 months. For culturing CHO-V1b cells this medium was supplemented with 10% foetal bovine serum and 1% penicillin/streptomycin.

#### **B.2 CELL VIABILITY ASSAYS**

##### **B.2.1 MTT solution**

A 5mg/mL MTT solution was prepared. 50mg of MTT was dissolved into 10mL of RPMI media (-phenol red). The solution was sterilized by aseptic filtration through a 0.2µm filter. The solution was prepared in a laminar flow hood with the light switched off as the MTT is light sensitive. The solution was stored at -20°C.

### **B.2.2 Phosphate buffered saline (PBS)**

The reagents listed below were dissolved into ddH<sub>2</sub>O to make a stock solution of 5 x the working concentration. The solution was made up to 1L with ddH<sub>2</sub>O and adjusted to pH 7.2. The solution was stored at room temperature.

Na <sub>2</sub> HPO <sub>4</sub> (anhydrous)	40.47g
KH <sub>2</sub> PO <sub>4</sub>	12.24g
NaCl	22.5g

### **B.2.3 SDS (10% in HCl)**

5g of SDS was dissolved into 50mL of 0.01M HCl. The solution was stored at 4°C.

### **B.2.4 Trypan Blue: stock solution**

A stock solution of 0.2% trypan blue was made by dissolving 0.02g of trypan blue into 10mL of ddH<sub>2</sub>O. This was filtered into a clean glass vial through a 0.2µm filter. The solution was stored at 4°C.

### **B.2.5 Trypan Blue: working solution**

200µL of trypan blue stock solution was combined with 50µL of 5xPBS to create a working solution of trypan blue. This was made fresh as required for cell counts.

## **B.3 PLASMID PREPARATION**

### **B.3.1 0.8% Agarose/1xTBE gel**

0.4g of agarose was added to 50mL of 1 x TBE in a glass flask. The solution was heated in microwave until all agarose was dissolved. The gel was allowed to cool to approximately 50°C. The gel was then poured and allowed to set (approximately 30 minutes).

### **B.3.2 Alkali lysis preparation of plasmid: Solution I**

The chemicals listed below were dissolved into 10mL ddH<sub>2</sub>O. The solution was autoclaved and then stored at 4°C.

50mM glucose  
25mM Tric.HCl  
10mM EDTA

### **B.3.3 Alkali lysis preparation of plasmid: Solution II**

A single pellet of NaOH was weighed, then dissolved in an appropriate volume of ddH<sub>2</sub>O to give 0.2M NaOH. 10% SDS was then added as required to make give 1% SDS. The solution was made fresh on the day of the plasmid preparation.

### **B.3.4 Alkali lysis preparation of plasmid: Solution III**

The chemicals listed below were made up to 25mL with ddH<sub>2</sub>O. The solution was stored at room temperature.

Glacial acetic acid	7mL
Potassium acetate	15mL

### **B.3.5 Gel loading dye**

The chemicals listed below were made up to 12mL with ddH<sub>2</sub>O. The solution was aliquoted into several tubes and stored at 4°C.

0.25% bromophenol blue  
0.25% xylene cyanol  
30% (w/v) glycerol

### **B.3.6 LB agar plates**

The chemicals listed below were made up to 500mL with ddH<sub>2</sub>O.

Bacto-tryptone	5g
Bacto-yeast extract	2.5g
NaCl	2.5g

1M NaOH

0.5mL

Bacteriological agar (7.5g) was added and the solution was autoclaved. After autoclave the solution was allowed to cool to approximately 50°C. Antibiotics were then added as required at the following concentrations: 20µg/mL for chloramphenicol; 100µg/mL for ampicillin. The plates were poured immediately, using a pipette to measure 25mL/plate. The plates were allowed to set in a laminar flow hood (takes approximately 5 hours). The plates were stored at 4°C and used within 24 hours of being made.

### **B.3.7 LB broth**

The chemicals listed below were made up to 1L with ddH<sub>2</sub>O. The solution was adjusted to pH7.5 with NaOH and then sterilised by autoclaving. LB broth was stored at 4°C.

Bacto-tryptone	10g
Bacto-yeast extract	5g
NaCl	10g

Chloramphenicol was added to the LB broth at 20µg/mL for selective media, and once antibiotic was added the media was used within 24 hours.

### **B.3.8 Tris Borate EDTA (TBE)**

The chemicals listed below were dissolved into 1L ddH<sub>2</sub>O to make a stock solution of 5 x the working concentration. The solution was stored at 4°C.

Tris base	54g
Boric acid	27.5g
0.5M EDTA	20mL

### **B.3.9 Tris EDTA pH8 (TE8)**

The chemicals listed below were made up to 100mL with ddH<sub>2</sub>O. The solution was adjusted to pH8 then sterilised by autoclaving. TE8 was stored at room temperature.

10mM Tris.HCl (pH 8)
1mM EDTA



## **B.4 PROTEIN QUANTITATION**

### **B.4.1 Working Reagent (WR)**

Mix 50 parts reagent A (sodium carbonate/bicarbonate buffer, bicinchonic acid, sodium tartrate in 0.1M NaOH) with 1 part reagent B (4% CuSO<sub>4</sub>·5H<sub>2</sub>O). Both reagents were supplied in the Pierce® BCA protein assay kit. The WR was prepared fresh on the day of the assay.

## **B.5 INOSITOL PHOSPHATE ASSAY**

### **B.5.1 Elution buffer II**

The reagents listed below were dissolved into 100mL of ddH<sub>2</sub>O. This was made fresh on the day of inositol phosphate separation.

Sodium borate	0.191g
Sodium formate	0.408g

### **B.5.2 Elution buffer VI**

The reagents listed below were dissolved into 100mL of ddH<sub>2</sub>O. This was made fresh on the day of inositol phosphate separation.

Formic acid	436μL
Ammonium formate	12.612g

### **B.5.3 Inositol-free culture medium**

Inositol-free culture medium was prepared as required for labeling of cells with *myo*-[<sup>3</sup>H]inositol. The following reagents were combined to make 10mL of the medium. This was stored at 4°C until required, and then pre-warmed to 37°C before use. 25μL of *myo*-[<sup>3</sup>H]inositol was added just prior to labeling of the cells to make a final volume of 10mL.

Dulbecco's modified Eagle's medium (- inositol)	8.775mL
Heat-inactivated horse serum (HIHS)	1mL

L-glutamine	100µL
Penicillin/streptomycin	100µL

#### **B.5.4 Lithium chloride (LiCl) 1M**

4.24g of LiCl was dissolved into 100mL of ddH<sub>2</sub>O to make a 1M stock solution. This was filtered into a clean glass vial through a 0.2µm filter and then stored at 4°C.

#### **B.5.5 MEM/AMEM + 0.1 % BSA (± 10mM LiCl)**

0.1g of BSA powder was sprinkled over 100mL of either MEM (for HEK293) or AMEM (for CHO-V1b) in a large glass beaker. The BSA was then dissolved by gentle mixing of the medium using a magnetic stirrer. The resulting solution was sterilised by filtration through a 0.2µm filter into a sterile schott bottle and then stored at 4°C.

LiCl was added to the MEM/AMEM + BSA as required on the day of inositol phosphate collection. 100µL of 1M LiCl stock solution was added per 10mL of medium to give a final LiCl concentration of 10mM.

#### **B.5.6 “Neutralisation” solution**

37.5mL of 37% hydrochloric acid was added to 462.5mL of ddH<sub>2</sub>O to make a 7.5% HCl solution. 5mL of this solution was then combined with 5mL of “stop” solution and 5mL of inositol-free culture medium, and the acidity of the “neutralisation” solution was adjusted by addition of ddH<sub>2</sub>O to ensure the neutrality of the mixture. The final solution was stored at 4°C.

#### **B.5.7 Regeneration solution**

The reagents listed below were dissolved into 100mL of ddH<sub>2</sub>O. This was made fresh on the day of inositol phosphate separation.

Formic acid	436µL
Ammonium formate	18.920g

#### **B.5.8 “Stop” solution**

The following reagents were dissolved into approximately 450mL of ddH<sub>2</sub>O in the order listed below. The solution was made up to 500mL with ddH<sub>2</sub>O and then stored at 4°C.

## **B.6 QUANTITATIVE PCR AND ASSOCIATED METHODS**

### **B.6.1 1% Agarose/1xTAE gel**

0.3g of agarose was added to 30mL of 1 x TAE in a schott bottle. The solution was heated in microwave until all agarose was dissolved. 2 $\mu$ L of SYBRsafe DNA dye was added to the gel. The gel was allowed to cool to approximately 50°C, then poured and allowed to set (approximately 15 minutes).

### **B.6.2 Gel loading dye (6x)**

The reagents listed below (RNase-free) were dissolved into RNase-free ddH<sub>2</sub>O to make a stock solution of 6x the working concentration. This solution was stored at 4°C for a couple of weeks, or at -20°C for longer durations.

60% glycerol  
60mM EDTA  
10mM Tris-HCl  
0.03% xylene cyanol  
0.03% bromophenol blue

### **B.6.3 Reverse transcription mixture**

The reagents listed below were combined and then made up to 10 $\mu$ L with ddH<sub>2</sub>O. This mixture was prepared as required for reverse transcription.

5 x Expand reverse transcriptase buffer	4 $\mu$ L
DTT	2 $\mu$ L
RNAsecure	0.8 $\mu$ L
dNTPs	1 $\mu$ L
50U/L Expand reverse transcriptase	1 $\mu$ L

### **B.6.4 Tris Acetate EDTA (TAE)**

The chemicals listed below were dissolved into 1L RNase-free ddH<sub>2</sub>O to make a stock solution of 50 x the working concentration. The stock solution was stored at 4°C, and diluted with RNase-free ddH<sub>2</sub>O to give 1 x TAE as required for gel electrophoresis.

Tris base	242g
Glacial acetic acid	57.1mL
EDTA	18.6g

#### **B.6.5 Tris EDTA pH8 (TE8)**

The chemicals listed below were made up to 100mL with ddH<sub>2</sub>O. The solution was adjusted to pH8 then sterilised by autoclaving. TE8 was stored at -20°C.

10mM Tris.HCl (pH 8)  
1mM EDTA